



MATTHIEU GASQUET

SOLAR ORBITER: THERMAL ANALYSIS AND DESIGN OF
AN EXTREME ULTRA VIOLET SPECTROMETER

SCHOOL OF ENGINEERING

MSC IN ASTRONAUTICS AND SPACE ENGINEERING
RESEARCH THESIS REPORT



SCHOOL OF ENGINEERING

MSc in Astronautics and Space Engineering
Research Thesis Report

2002

MATTHIEU GASQUET

SOLAR ORBITER: Thermal Analysis and Design of an Extreme
Ultra Violet Spectrometer

Supervisors:

Ms. Sam Heys

Mr. Eric Sawyer

Mr. Tom Bowling

Presented: September 2002

*This thesis is submitted in partial fulfilment of the requirements for the Degree of MSc
in Astronautics and Space Engineering*

© Cranfield University 2002. All rights reserved. No part of this publication may be
reproduced without the written permission of the copyright owner.

Abstract

The Solar Orbiter, project funded by the European Space Agency, will be the first spacecraft to go as close as 0.2 Astronomical Units from the Sun. It will allow scientists to have a better understanding of the sun and in particular of its dynamics. The Rutherford Appleton Laboratory led a consortium to build an Extreme Ultra-Violet spectrometer which will be embedded on the solar probe. This instrument will provide information on plasma density, temperature, element/ion abundances, flow speeds and the structure and evolution of atmospheric phenomena.

Because of the very severe thermal environment the probe will have to withstand, the thermal design of this instrument has to be studied very carefully in order to control accurately the temperature on board. The work described in this report is a pre-analysis and design of some components of the spectrometer.

The goal of this task is mainly to study the thermal environment of the spacecraft and to find the main keys of the thermal control strategy which will allow each device to stay within its temperature requirements.

After a description of the available technological solutions to control the temperature in a satellite and a definition of the temperature requirements, a preliminary thermal analysis has been done on Excel in order to have a first idea of the radiator area dedicated to the instrument when the heat load is maximum. Then many simulations have been done on I-Deas and ESARAD/ESATAN, some thermal analysis software. The aim of the strategy developed is to minimise heat transfer by radiation, increase as much as possible the reflectivity of the spectrometer mirrors, and insulate the spectrometer from the rest of the spacecraft by minimising the conductive heat transfer between the spectrometer casing and the spacecraft. For mass and reliability reasons, this strategy is based on passive control systems such as Multi-Layers Insulation or thermal coatings.

With this strategy, it seems possible to keep the temperatures within allowable limits, but those temperatures are still oscillating a lot. That could be a problem for the thermal stability of the structure. One possibility to solve it would be to use some more complex thermal control devices such as thermal switches, variable conductance heat pipes, or louvers.

Contents

Abstract	i
Contents	ii
List of Figures	v
List of Tables	vii
Nomenclature	ix
1. INTRODUCTION	1
1.1 Mission Description	1
1.2 The work project	5
1.2.1 Presentation	5
1.2.2 Objectives of the thermal analysis	5
1.2.3 Scope of the thesis	6
1.2.4 Work planning	6
2. The Extreme Ultra-Violet Spectrometer	8
2.1 Scientific objectives of the instrument	8
2.2 Technical requirements	8
2.2.1 Mass budget	9
2.2.2 Miscellaneous	9
2.2.3 Particle environment	10
2.2.4 Contamination problems	10
2.2.5 Materials	10
2.2.6 Thermal requirements	13
2.3 Optical design possibilities	13
2.3.1 Optical designs	13
2.3.1.1 The off axis telescope	14
2.3.1.2 The grazing incidence telescope	15
2.3.2 Applied coatings	17
2.4 Review of thermal control systems and devices	18
2.4.1 Passive thermal control devices	19
2.4.1.1 Multi Layers Insulation (MLI)	19
2.4.1.2 Radiators	20
2.4.1.3 Thermal control coatings	21
2.4.1.4 Conductive tapes and joints	21
2.4.1.5 Phase Change Materials (PCM)	22
2.4.1.6 Thermal doublers	23
2.4.2 Active Thermal control devices	23

2.4.2.1	Louvers	23
2.4.2.2	Heat pipes	24
2.4.2.3	Heaters	25
2.4.2.4	Thermal switches	26
2.4.2.5	Pumped-loop systems	26
2.4.2.6	Heat exchangers	27
2.4.2.7	Cold plate	27
3.	Preliminary thermal analysis.....	28
3.1	Assumptions and description of the model.....	28
3.2	Excel calculation process	28
3.2.1	Grazing incidence option	28
3.2.2	Off axis option	32
3.2.3	Formulae	34
3.3	Results, analysis, feasibility, model precision	35
4.	Transient thermal analysis	39
4.1	The thermal environment.....	39
4.2	Presentation of the softwares	43
4.2.1	ESARAD / ESATAN.....	43
4.2.1.1	ESARAD Overview.....	43
4.2.1.2	ESATAN Overview	44
4.3	I-Deas simulations	45
4.3.1	Description of the thermal model	46
4.3.1.1	Geometry	46
4.3.1.2	Finite element mesh	48
4.3.1.3	Materials	48
4.3.2	Heat loads	49
4.3.3	Correlation of the thermal model with preliminary analysis	50
4.3.4	Transient results	52
4.4	ESARAD/ESATAN simulations	58
4.4.1	Description of the thermal model	58
4.4.1.1	Geometry	59
4.4.1.2	Finite element mesh	61
4.4.1.3	Materials	62
4.4.2	Heat loads	63
4.4.2.1	The radiative case	63
4.4.2.2	ESATAN computation.....	64
4.4.3	Transient results	65
4.4.3.1	Sensitivity of the model to the insulation of the heat shield	67

4.4.3.2	Sensibility of the model to the conductance between the satellite casing and the heat shield	68
4.4.3.3	Sensibility of the model to the conductance between the satellite casing and the telescope casing	69
4.4.3.4	M1 temperature with specific radiators attached to the heat shield....	71
4.4.3.5	Influence of M1 absorptivity	72
5.	Conclusion	74
5.1	Further work	74
5.2	Conclusion	75
6.	Bibliography	76
Appendix A : Thermo-Optical properties of some thermal control coatings		78
Appendix B : Excel calculation spreadsheets and results of the preliminary thermal analysis		85
Appendix C : Maple program giving the Sun heat load as a function of time		90
Appendix D : ESARAD program		92
Appendix E : ESATAN program		105

List of Figures

Figure 1-1: Artistic view of the Solar Orbiter (solar orbiter website)	3
Figure 1-2: perihelion as a function of time (solar orbiter website)	3
Figure 1-3: solar latitude as a function of time (solar orbiter website).....	4
Figure 1-4:Elliptic projection of the Solar Orbiter's trajectory (solar orbiter website)	4
Figure 1-5: Work planning of the Thesis	7
Figure 2-1: layout of the different elements in the Off-Axis design telescope.....	15
Figure 2-3: A typical MLI layer covered with a gold paint.....	20
Figure 2-4: The external face of the Cassini space probe almost entirely covered with MLI	20
Figure 2-5: Conductive joint (courtesy of COMERICS)	22
Figure 2-6: – Conductive tapes (Courtesy of CHOMERICS)	22
Figure 2-7: A venitian blind louver. On the picture, the blades are fully open.	24
Figure 2-8: A typical heat pipe with its different constituent parts.	25
Figure 2-9: Different types of heaters (courtesy of MINCO Inc.).....	26
Figure 2-10: A typical pumped looped system.....	27
Figure 3-1 : Calculation process for the different heat flow on the mirrors for the grazing incidence telescope	30
Figure 3-2 : M1 radiator area calculation process for the grazing incidence telescope when there is no heat path between the sun and the radiator.....	31
Figure 3-3 : M1 radiator area calculation process for the grazing incidence telescope when there is a heat path between the sun and the radiator	31
Figure 3-4 : Calculation process for the different heat flow on the mirrors for the off axis telescope	33
Figure 4-1 : calculation process of the incident sun heat load as a function of time	41
Figure 4-2 : Incoming heat load on the solar orbiter VS orbit days. The period of the orbit is around 150 days and the first day of the orbit corresponds tp the perihelion	42
Figure 4-3: Comparaision of maximum Solar heat loads for diffrent missions (from <i>Solar Orbiter Assessment Study</i> , Solar Orbiter Website)	43
Figure 4-4 : Wireframe view of the I-DEAS model.	47
Figure 4-5 : Three dimensional view of the I-DEAS model.....	47
Figure 4-6 : temperature variation for the Primary Mirror with a high emissive coating, without a radiator and with the IDEAS-TMG software.....	52

Figure 4-7 : M1 temperature with a conductance of 0.5 W/°C between the radiator and M1, a high emissive coating and M1 either lowly or highly absorptive.....	53
Figure 4-8 : M1 temperature with a low emissive coating on the heat shield, M1 lowly absorptive, and a conductance of 50 W/°C.....	54
Figure 4-9 : M1 temperature with a high emissive coating (MLI) on the telescope, M1 either lowly or highly absorptive, and a conductance of 50 W/°C	55
Figure 4-10 : M1 temperature with a thermal switch between the mirror and the radiator	57
Figure 4-11 : Conductance law applied to the thermal switch.....	57
Figure 4-12 : Temperature gradients on the primary mirror.....	58
Figure 4-13: A view of the ESARAD geometrical model with the different devices	61
Figure 4-14 : M1 temperature variations for different values of the heat shield conductivity.	68
Figure 4-15 : M1 temperature variations with different values of the contact conductance between the heat shield and the satellite casing.....	69
Figure 4-16 : M1 temperature variations with different values of the contact conductance between the telescope casing and the satellite casing.....	70
Figure 4-17 : M1 temperature variations with different values of the conductivity between the heat shield and its radiators.....	71
Figure 4-18 : Influence of M1 absorptivity on M1 temperature.....	72

List of Tables

Table 2-1: Mass budget of the EUV spectrometer (made by Eric Sawyer, Rutherford Appleton Laboratory).....	9
Table 2-2: general information about the telescope.....	10
Table 2-3: particle density and particle threats that the Solar Orbiter could have to encounter.....	10
Table 2-4 : Thermo-mechanical properties of some of the most used materials for the design of mirrors and telescope devices embedded in space. The values in bold correspond to the best ones.	12
Table 2-5: Thermal requirements of the EUV telescope	13
Table 2-6 : general dimensions of the Off-Axis design telescope	14
Table 2-7 : general dimensions of the Grazing Incidence telescope	17
Table 2-8: Thermo optical properties of some multilayer coatings which could be applied on the telescope mirrors	18
Table 3-1: Incident sun heat load on the telescope (hot case) for each design.....	36
Table 3-2: Steady State simulation results for the grazing incidence design.	37
Table 3-3: Steady State simulation results for the off axis design.....	37
Table 4-1: Typical value of the sun heat load for different points of the orbit.....	39
Table 4-2 : Geometrical dimensions of the different elements of the I-DEAS model ...	46
Table 4-3 : Physical properties of the different materials used in the I-DEAS model ...	49
Table 4-4 : Thermo-optical properties of the different coatings applied on the EUV Spectrometer	49
Table 4-5 : Maximum temperature for the Primary mirror with a high emissive coating, without radiator and with the preliminary thermal analysis spreadsheet.....	51
Table 4-6 : Nodes definition of the ESARAD model. There is one node per device and per face in order to implement any radiative heat transfer.	60
Table 4-7 : thermo-optical properties of the different materials and coatings applied on the model developed under ESARAD/ESATAN	62
Table 4-8 : List of materials applied on each part of the telescope.	62
Table 4-9 : values of the different parameters used in ESARAD or ESATAN to obtain different simulations	63
Table 4-10 : summary of the different simulations done with ESARAD/ESATAN. Those in bold and italic stopped before the end because one of the temperature device (generally the heat shield) could'nt converge. The parameters which has been modified for each simulation is underlined.....	66

Table 4-11 : M1 temperature extremums as a function of its absorptivity.....	73
--	----

Nomenclature

α	Absorptivity
ε	Emissivity
τ	Transmittivity
U.V	Ultra – Violet
A.U	Astronomical Unit ($\approx 1.5 \times 10^8$ km)
Gs	Solar constant (1367 W/m^2 at 1 A.U)
MLI	Multi Layers Insulation

1. INTRODUCTION

1.1 Mission Description

The mission description comes from the *Solar Orbiter Assessment Report* (available on the Solar Orbiter website).

The Sun's atmosphere and the heliosphere represent uniquely accessible domains of space, where fundamental physical processes common to solar, astrophysical and laboratory plasmas can be studied in detail and under conditions impossible to reproduce on Earth or to study from astronomical distances.

The results from missions such as Helios, Ulysses, Yohkoh, SOHO, and TRACE have enormously advanced our understanding of the solar corona, the associated solar wind and the three-dimensional heliosphere. However, we have reached the point where further in-situ measurements, now much closer to the Sun, together with high-resolution imaging and spectroscopy from a near-Sun and out-of-ecliptic perspective, promise to bring about major breakthroughs in solar and heliospheric physics.

The Solar Orbiter will, through a novel orbital design and its state-of-the-art instruments, provide exactly the required observations.

The Solar Orbiter will for the first time

- Explore the uncharted innermost regions of our solar system,
- Study the Sun from close-up (45 solar radii, or 0.21 AU),
- Fly by the Sun, tuned to its rotation and examine the solar surface and the space above from a co-rotating vantage point,
- Provide images of the Sun's polar regions from heliographic latitudes as high as 38 degrees.

The scientific goals of the Solar Orbiter are

- To determine in-situ the properties and dynamics of plasma, fields and particles in the near-Sun heliosphere,
- To investigate the fine-scale structure and dynamics of the Sun's magnetised atmosphere, using close-up, high-resolution remote sensing,
- To identify the links between activity on the Sun's surface and the resulting evolution of the corona and inner heliosphere, using solar co-rotation passes,

- To observe and fully characterise the Sun's polar regions and equatorial corona from high latitudes.

The near-Sun interplanetary measurements together with simultaneous remote sensing observations of the Sun will permit to disentangle spatial and temporal variations during the co-rotational phases. They will allow understanding the characteristics of the solar wind and energetic particles in close linkage with the plasma conditions in their source regions on the Sun. By approaching as close as 45 solar radii, the Solar Orbiter will view the solar atmosphere with unprecedented spatial resolution. Over extended periods the Solar Orbiter will deliver images and data of the Polar Regions and the side of the Sun not visible from Earth.

The Solar Orbiter will achieve its wide-ranging aims with a suite of sophisticated instruments. Due to the Orbiter's proximity to the Sun, the instruments can be fairly small, compared to instrumentation required at the Earth's orbit.

The payload includes two instrument packages, optimised to meet the solar and heliospheric science objectives:

- **Heliospheric in-situ instruments:** solar wind analyser, radio and plasma wave analyser, magnetometer, energetic particle detectors, interplanetary dust detector, neutral particle detector, solar neutron detector.
- **Solar remote sensing instruments:** EUV full-Sun and high resolution imager, high-resolution EUV spectrometer, high-resolution visible-light telescope and magnetograph, EUV and visible-light coronagraph, radiometer

.

The spacecraft will be 3-axis stabilised and always Sun-pointed. Figure 1-1 gives a view of the solar orbiter with the observations solar panel deployed.

The Solar Orbiter spacecraft benefits from technology developed for the Mercury Cornerstone mission. Using solar electric propulsion (SEP) in conjunction with multiple planetary swing-by manoeuvres, it will take the Solar Orbiter only two years to reach a perihelion of 45 solar radii at an orbital period of 150 days. Within the nominal 5 year mission phase, the Solar Orbiter will perform several swing-by manoeuvres at Venus, in order to increase the inclination of the orbital plane to 30° with respect to the solar equator. During an extended mission phase of about two years the inclination will be further increased to 38°. Figures 1-2 and 1-3 gives the perihelion and latitude evolution

with respect to the time. Figure 1-4 shows the trajectory of the solar probe during its different phases.

The total mass of the Solar Orbiter is compatible with a Soyuz-Fregat launch from Baikonur.

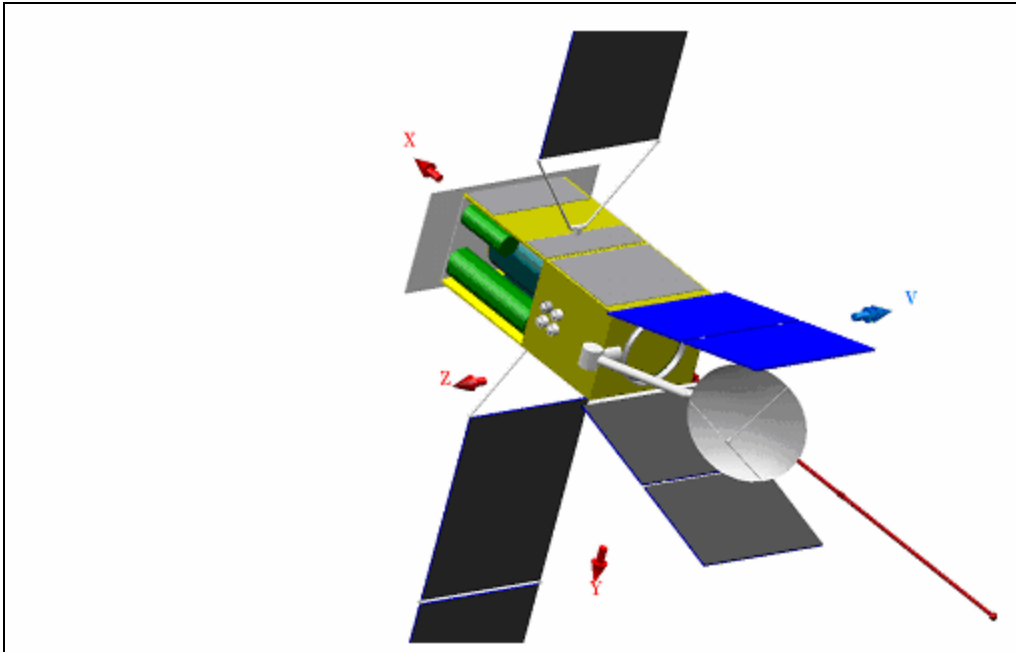


Figure 1-1: Artistic view of the Solar Orbiter (solar orbiter website)

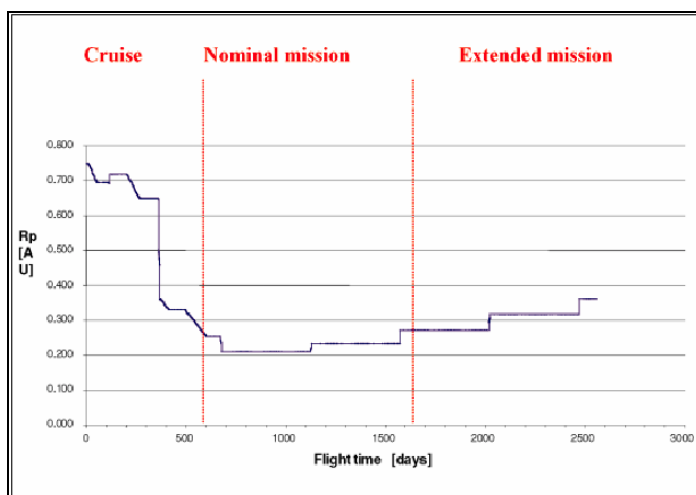


Figure 1-2: perihelion as a function of time (solar orbiter website)

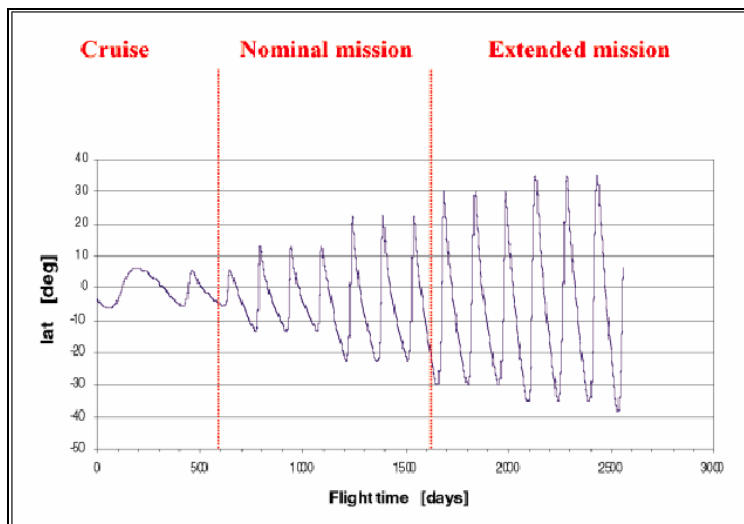


Figure 1-3: solar latitude as a function of time (solar orbiter website)

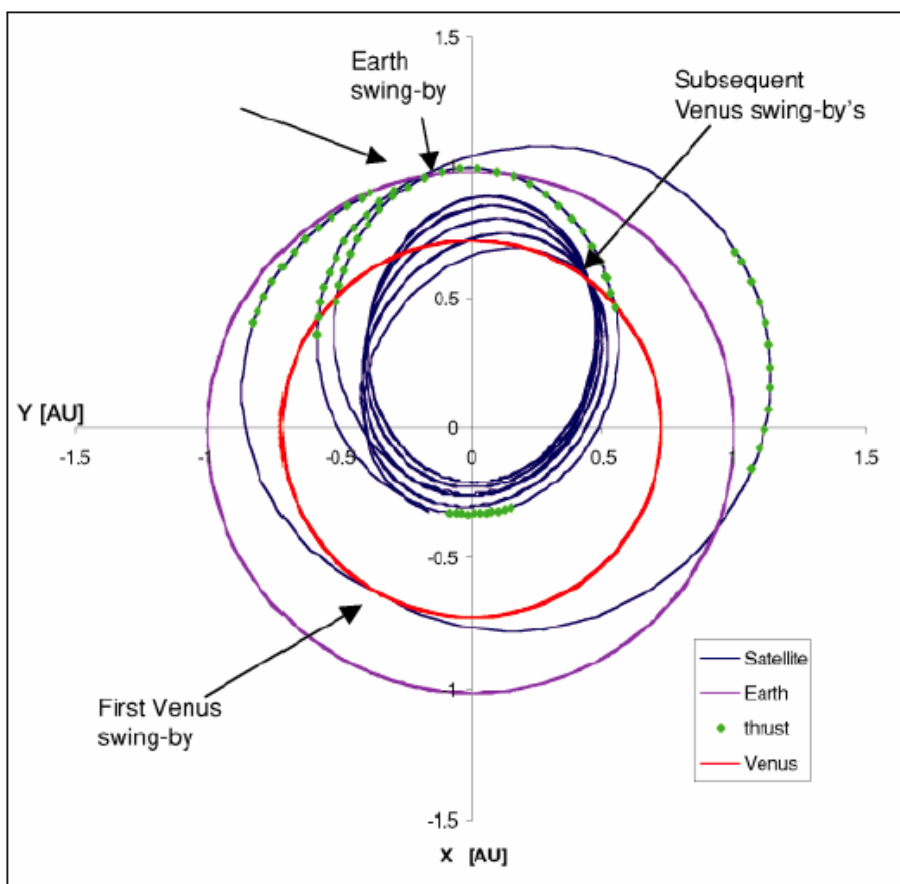


Figure 1-4: Elliptic projection of the Solar Orbiter's trajectory (solar orbiter website)

1.2 The work project

1.2.1 *Presentation*

The MSc Thesis research has been done under the supervision of Sam Heys and Eric Sawyer from the Rutherford Appleton Laboratory (RAL) in Oxford, and Tom Bowling from Cranfield University.

The RAL is leading a consortium to build the high-resolution Ultra-Violet spectrometer/imager of the solar orbiter. This instrument is going to be used to have a better understanding of the sun atmosphere.

The Thesis research began in April and finished at the end of August.

1.2.2 *Objectives of the thermal analysis*

The aim of the thermal analysis and design is to determine with a good accuracy the temperature mapping of any parts of the EUV spectrometer and then develop a thermal strategy to maintain all components within their allowable temperature limits for all operating modes.

The following is a list of requirements for the thermal control system:

- All components to be kept within allowable limits
- The total mass of the instrument should not exceed 22 kg with 3.5 kg for the thermal system
- The power requirement, including any active thermal control system, should not exceed 25 W
- The design must be predictable by thermal analysis and verifiable by ground tests.

Because there are a lot of doubts on the materials and designs used for this instrument at the moment, the temperature limits are not really fixed and can be very different whether some coatings are applied on surfaces or not.

For instance, if some multilayer coatings are applied on the mirrors, the surface temperature should be between -60°C and 100°C . (The coating could be vaporized if the temperature is higher, and if the temperature is lower, there will be some contraction in the material ...). On the other hand, it could be possible to extend this range by using other technologies, such as a polished Silicon-Carbide mirror.

1.2.3 Scope of the thesis

The following is a guideline as how this thesis is organised.

Chapter 2 presents the Extreme Ultra-Violet Spectrometer, gives some technical requirements which can be useful for the thermal design and shows the two possible optical design which could be applied to the instrument. At the end of the chapter, a paragraph presents the different control thermal system which could be applied in order to maintain the instrument in the allowable temperature range.

Chapter 3 presents a preliminary thermal analysis of the instrument cooled with radiators. Several thermal strategies are tried.

Chapter 4 describes the transient thermal analysis. After a presentation of the thermal environment, the different models which have been developed are presented. In this chapter thermal control strategies are assessed to determine the most appropriate scheme for the Solar Orbiter.

1.2.4 Work planning

Figure 1.5 presents the Thesis work planning which has been created at the beginning of the study.

This planning has been respected for every task, except the mechanical and optical components research which has been reduced a lot. Because we are in a very early phase of the project, it is not really useful to look in details for the design of the instrument.

The thermal components research has been developed a little bit more because it can be useful for the thermal analysis to know which system can be applied and to know its characteristics.

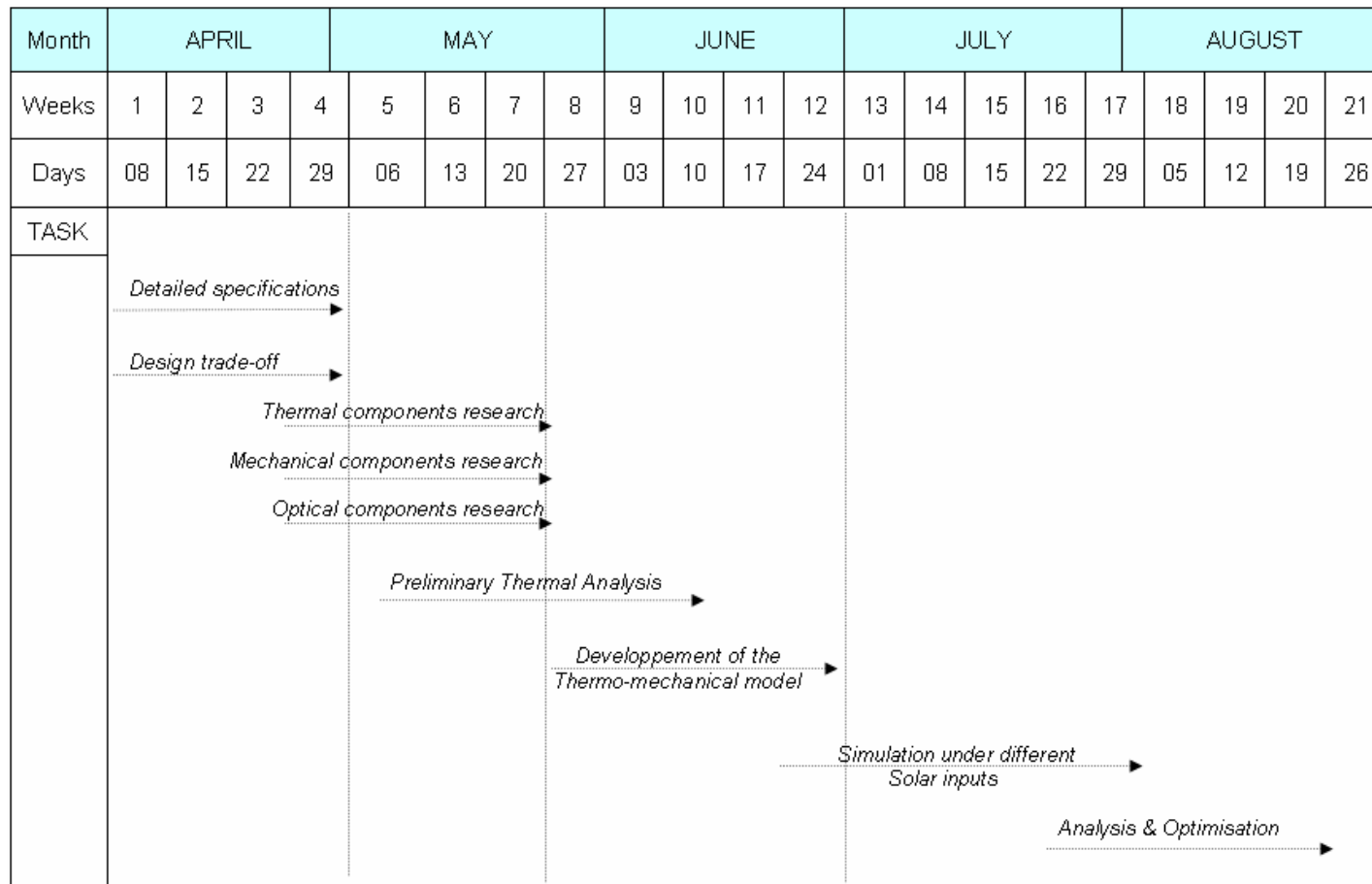


Figure 1-5: Work planning of the Thesis

2. The Extreme Ultra-Violet Spectrometer

2.1 Scientific objectives of the instrument

Observations of the UV/EUV spectral range are critical for the determination of plasma diagnostics in the solar atmosphere across the broad temperature range from tens of thousands to several million K.

Analysis of the emission lines, mainly from trace elements in the Sun's atmosphere, provides information on plasma density, temperature, element/ion abundances, flow speeds and the structure and evolution of atmospheric phenomena. Such information provides a foundation for understanding the physics behind a large range of solar phenomena.

Current spacecraft instrumentation (SOHO) provides EUV spatial and spectral resolving elements of order 2-3 arcsec and 0.01 nm, respectively, and UV resolutions of 1 arcsec and 0.002 nm. There are no plans for EUV or UV spectroscopic measurements from the NASA STEREO mission (2004 launch), the NASA Solar Dynamics Observatory (~2005 launch) and the Solar Probe (~2007 launch). The only planned EUV spectrometer for a future mission is the EIS instrument on Solar-B with 1 arcsec (750 km on the Sun) and 0.001 nm resolving elements. However, this instrument is tuned to active region observations with almost no transition region capability.

The European solar physics community has a well established expertise in solar EUV/UV spectroscopy as illustrated by the successful CDS and SUMER instruments on SOHO.

2.2 Technical requirements

This section presents the different technical requirements which could have an incidence on the thermal design of the spacecraft.

2.2.1 Mass budget

This mass budget, detailed in table 2-1, is just an estimation of the mass of each component of the EUV spectrometer. However, even if the optical design changes, the new mass budget should not be very different from this one.

Maximum total mass	30 kg	
Detailled Mass Budget (kg)	Primary mirror	0.5
	Mirror support	0.3
	Secondary mirror	0.1
	Mirror scan mechanism	0.6
	Slit assembly	0.3
	Grating assembly	0.6
	OPS (Offset Pointing System, ie Actuator)	1.5
	Detector	1
	Detector electronics	1.5
	Baffles	0.5
	Structure	5.4
	Thermal subsystem	3.5
	Harness	1.2
	Margin	2
	Total instrument	17
	Main electronics including PSU	6
	GRAND TOTAL	25

Table 2-1: Mass budget of the EUV spectrometer (made by Eric Sawyer, Rutherford Appleton Laboratory)

2.2.2 Miscellaneous

This table presents some very general information about the telescope.

Total power	30 W max
Electrical power dedicated to the thermal control system	Around 5W
Spatial resolving element	0.5 arcsec (75 km on Sun at 0.2 A.U.)
Spectral resolving element	0.001 nm/pixel (5km/s)

Detector type	Active Pixel Sensor
Maximum exposure time	Usually around 10 s
Wavelength operation	170-650 Å to 170-1200 Å
Lifetime	8 years
Instrument size	Max length 2.5 m

Table 2-2: general information about the telescope

2.2.3 Particle environment

Because of the close distance to the sun, the solar orbiter will have to withstand a much more severe particle environment than previous solar missions.

Solar background proton	1 AU: 9 cm^{-3} (300 km/s and 3.5 eV) 0.2 AU: 225 cm^{-3}
Solar events	Storms
Solar neutrons	100 cm^{-3} at 0.2 AU (neutron half-life : 15.5 min)
Cosmic rays	Around 30 particle hits of 1 GeV protons/ cm^2s

Table 2-3: particle density and particle threats that the Solar Orbiter could have to encounter

2.2.4 Contamination problems

Under high radiation, any contaminant deposited on an optical surface polymerizes, so the reflectivity of the surface drastically decreases.

Because of the dust which could have been deposited during the assembly, there is a risk of serious rapid degradation of the reflectivity at this orbit

2.2.5 Materials

Different materials can be used for the optics and the structure of the spectrometer. However, because of the very severe thermal environment, those materials should either have a very low thermal expansion to avoid any compression or expansion in the

spectrometer structure or a very high conductivity in order to ensure a homogeneous temperature almost without thermal inertia.

Table 2-4 presents some materials which are used to build telescope in space or on earth.

Many properties are used to assess the material:

- The *Young modulus* E is the ratio between the elongation and the stress
- The *microyield stress* μ is equal to the stress that produces a relative elongation equal to 10^{-6}
- The *expansion coefficient* is the relative elongation per °C
- The *Diffusivity* D represents the heat propagation into the material
- The *specific heat* C is the energy necessary to increase the temperature of 1 °K
- The *conductivity* K represents the capacity to transfer heat power.
- The *specific stiffness* represents the flexion of a device made with this material under its weight.
- The *first order thermal distortion* corresponds to the buckling under a temperature gradient
- The *thermal distortion* represents the buckling under transient heat load
- The *dimensional change* represents the inflation under an heat flux

N.B:

$$E = \frac{\sigma}{\frac{\Delta L}{L}} \text{ with } \frac{\Delta L}{L} = \text{relative distortion}$$

$$\alpha = \frac{\frac{\Delta L}{L}}{T}$$

*Beryllium has good mechanical and thermal properties but it is also **toxic** and so can not really be used.*

PROPERTIES	Aluminium	Beryllium	Silicon-Carbide	Al ₂ O ₃ (Sapphire)	Zerodur	Fused Silica	Silicon
Physical							
Density ρ (kg.m ⁻³)	2730	1850	3210	3750	2530	2201	2330
Mechanical							
Young Modulus E (GPa)	69	303	466	390	91	72.5	134
Microyield Stress (MPa)	98	35	??	??	10	10	10
Thermal							
CTE α (10 ⁻⁶ .K ⁻¹)	23.9	11.4	2.4	7.1	0.02	0.51	2.55
Diffusivity D (10 ⁻⁶ .m ² .s ⁻¹)	65.97	64.3	89.9	??	0.8	0.812	72
Specific Heat C (J.kg ⁻¹ .K ⁻¹)	960	1820	700	1088	821	772	720
Conductivity K (W.m ⁻¹ .K ⁻¹)	237	220	202	26	1.64	1.38	149
FIGURES OF MERIT							
Structural (Higher is better)							
Specific Stiffness E/ ρ	25.3	163.8	145.2	104.0	36.0	32.9	57.5
Thermal (Lower is better)							
1 st order distortion δ /K	0.101	0.052	0.012	0.273	0.012	0.369	0.017
Thermal distortion δ /D	0.362	0.177	0.027	??	0.025	0.628	0.035
Dimensional Change δ . ρ /K	0.275	0.096	0.038	1.024	0.031	0.813	0.040

Table 2-4 : Thermo-mechanical properties of some of the most used materials for the design of mirrors and telescope devices embedded in space. The values in bold correspond to the best ones.

2.2.6 Thermal requirements

Table 2-5 presents the general thermal requirements for the EUV spectrometer.

Thermal control system	Passive as much as possible
Maximum temperature for Solar Arrays	130 °C
Maximum temperature for multilayer coatings	100 °C
Maximum detector temperature for the detector	-80 °C
Maximum available area for all the EUV spectrometer radiator	The footprint of the instrument, i.e around 0.56 m ²
Maximum temperature gradient for a primary mirror to a secondary mirror separation tolerance of 3 µm and a distance of 400 mm between M1 and M2	SiC : 3 °C Invar or Zerodur: 120 °C Carbon/Carbon: 60 °C

Table 2-5: Thermal requirements of the EUV telescope

2.3 Optical design possibilities

2.3.1 Optical designs

Several different optical designs could be applied on the EUV telescope. Two of them seem to be particularly adapted for the Solar Orbiter:

- A grazing-incidence telescope feeding a normal-incidence VLS-grating spectrometer (**L. Poletto, G. Tondello** *Istituto Nazionale per la Fisica della Materia (INFN), Information Engineering Department - Padova (Italy)*)

- An off-axis design telescope feeding the spectrometer (**M. Caldwell**, *Rutherford Appleton Laboratory, Space Science and Technology Department – Oxford (UK)*)

For each design a steady state thermal analysis has been done, and only the grazing incidence telescope has been modelled in the transient analysis.

Those two configurations respect the same requirements:

- A spatial resolution of 0.5 arcsec pixel with a field of view of 34 arcmin
- A spectral resolution of 580-630 angstrom in 34 arcmin
- A collecting power of 4×10^{12} photons/(cm².sr.s)

2.3.1.1 The off axis telescope

This telescope is made with two mirrors and one heat stop. One of its advantages is that this design can be easily embedded in the telescope because of its relatively small length. Table 2-6 presents some specifications for this telescope.

Telescope	Richley-Chretien adaptation
<i>Field of view</i>	34 arcmin
<i>Entrance aperture</i>	circular
Diameter	135 mm
<i>Primary mirror</i>	
M1 diameter	120 mm
M1 incidence	7.5 °
<i>Secondary mirror</i>	
M2 diameter	20 mm
M2 incidence	8.5 °
Distance between M1 and M2	400 mm
<i>Focal length</i>	
Heat stop	rectangular
Heat stop size	460 mm x 180 mm
Heat stop incidence	??

Table 2-6 : general dimensions of the Off-Axis design telescope

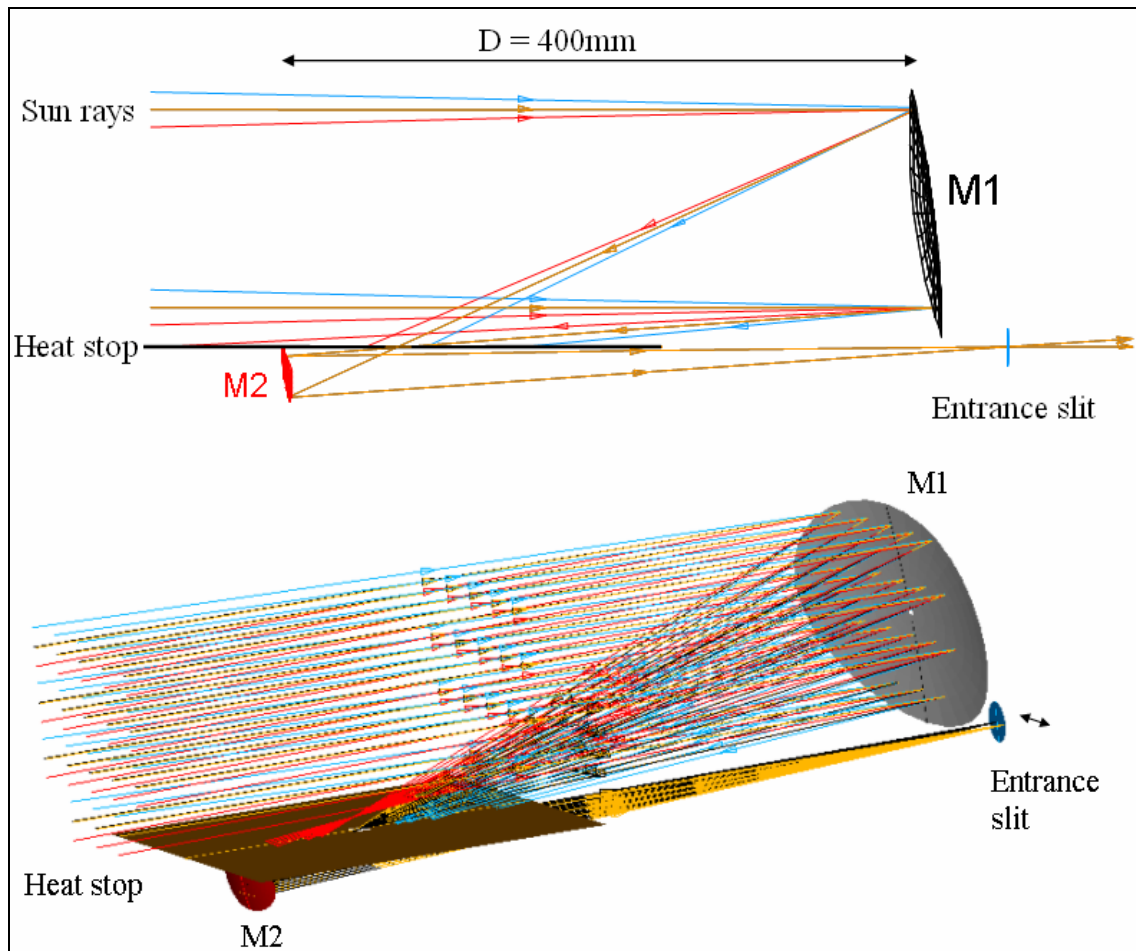


Figure 2-1: layout of the different elements in the Off-Axis design telescope

2.3.1.2 The grazing incidence telescope

Figure 2-2 and Table 2-7 present the main characteristics and architecture of this design. According to Mr Poletto:

“The advantages of using grazing incidence optics are mainly the reduction of the thermal load (because of the relatively small entrance aperture) and the increase in the reflectivity, at the expense of an additional reflective surface”.

An other advantage of this type of design is that the equivalent focal length of the telescope can exceed substantially the system length.

The primary and secondary mirrors of the Wolter II telescope are separated by 200 mm with a focal plane 1550 mm beyond the primary. The effective focal length is about 2.3 mm. An additional plane mirror for the rastering is inserted between the telescope and the slit.

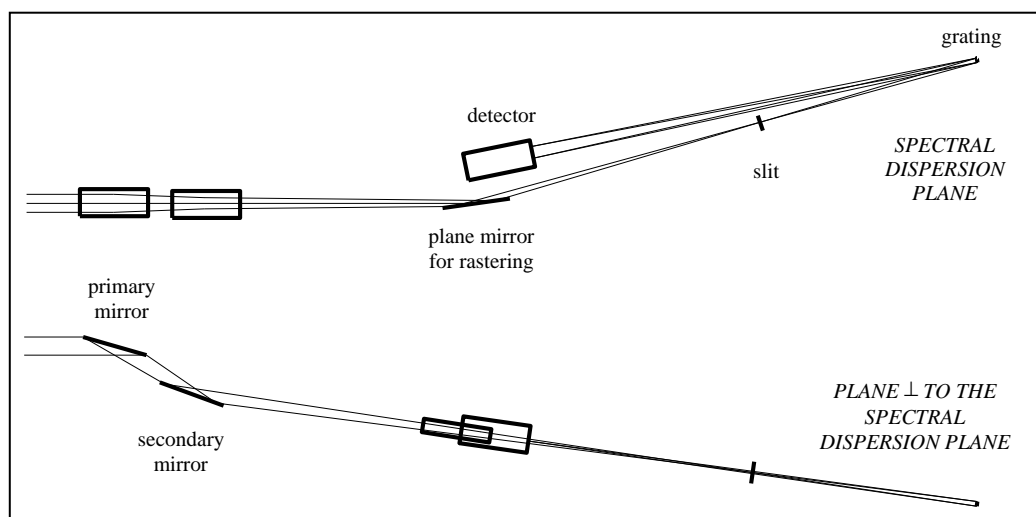


Figure 2-2 :layout of the different elements in the Grazing Incidence telescope

Telescope	Wolter II
<i>Field of View</i>	30 arcmin parallel and perpendicular to the slit
<i>Entrance aperture</i>	Square
Size	35 mm x 35 mm
<i>Primary mirror</i>	Paraboloid
Size	130 mm x 35 mm
Incidence Angle	74°
<i>Secondary mirror</i>	Hyperboloid
Distance from the primary	200 mm
Distance from the slit	1250 mm
Size	120 mm x 25 mm
Incidence Angle	78°

<i>Focal length</i>	2030 mm
Mirror for the rastering	Plane
Distance from the slit	650 mm
Size	130 mm x 25 mm
Incidence angle	81°
Slit	
Size	10 μm x 18 mm
Resolution perpendicular to the slit	1 arcsec
Grating	Spherical VLS
Central groove density	3600 lines/mm
Wavelength	580-630 Å
Entrance arm	500 mm
Exit Arm	1035
Incidence angle	8.5 °
Radius	670 mm
Size	20 mm x 35 mm
Detector	
Pixel size	10 μm x 20 μm
Format	1850 x 1800 pixel
Area	18.5 mm x 36 mm
Velocity resolution	13.5 km/s
Spatial resolution at 0.2 Å.U	150 km

Table 2-7 : general dimensions of the Grazing Incidence telescope

2.3.2 *Applied coatings*

In order to protect the APS detector, this one should not receive more than a couple of watts (in order of 2 watts or maybe more).

To do so, the mirrors will have either to absorb a large part of the incoming energy or to reject to space this energy. A way to play with the thermo-optical properties such as the emissivity or absorptivity is to put a coating on the mirror surface with specific thermo-optical values.

The only requirement is that the instrument has to reflect most of the incoming energy which is roughly situated in the following wavelength range: 17 nm to 150 nm. That range corresponds to the wavelengths which are going to be studied by the spectrometer.

Because of the Gaussian repartition of the energy on the solar spectrum, it appears that more than 93.3% of the incoming sun heat load is situated at a wavelength bigger than 300 nm.

That means that the EUV spectrum is not very energetic and so the thermal strategy which is going to be used can be pre-designed without taking into account any absorbed heat load coming from the EUV spectrum.

For those reasons, all the thermo-optical properties described and used in the thermal analysis are “grey” factor, which means that their values are independent of the wavelength.

The following table give some value of absorptivity and reflectivity of some Multilayers coatings which are specially designed for telescope mirrors:

Multilayers coatings	Absorptivity α	Reflectivity ρ (in the visible)
Silicon-Carbon/Gold 10 layers Si-Pt/Si/C (Silicon-Carbon 1)	0.1	0.9
Gold	0.2	0.8
Platinum/Iridium	0.4	0.6
Silicon-Carbon/Gold 10 layers Si-Pt/Pt (Silicon-Carbon 2)	0.8	0.2

Table 2-8: Thermo optical properties of some multilayer coatings which could be applied on the telescope mirrors

According to Mr Poletto (*Istituto Nazionale per la Fisica della Materia (INFN), Information Engineering Department - Padova (Italy)*), it could maybe not be possible to obtain an absorptivity less than 0.2 for the grazing incidence telescope.

2.4 Review of thermal control systems and devices

There are two different types of thermal control systems (TCS): passive or active.

A passive system relies on conductive and radiative heat paths (no convection in space) and has no moving parts and no electrical power inputs.

An active system is used in addition to the passive system when passive system is not adequate. They rely on pumps, thermostats, and heaters, use moving parts and need electrical power.

2.4.1 Passive thermal control devices

2.4.1.1 Multi Layers Insulation (MLI)

This is the most common thermal element to insulate the inside of the satellite from its external environment. It is used either to prevent excessive heat loss from a component or excessive heating.

A MLI is generally composed of multiple layers of aluminised Mylar® or Kapton® films alternated with a low conductance spacer (a Dacron mesh for instance).

Heat transfer in space through MLI is a combination of radiation and solid conduction. Solid-conduction heat transfer is minimised by keeping the density of the low conductance spacers between the reflective surfaces as low as possible and making the blanket “fluffy” to minimize contact between layers. Radiation heat transfer is minimised by interposing as many enclosing reflective surfaces (metallized sheets with high emissivity ϵ and low absorptivity α) as possible.

In order to evacuate the air trapped between blanket layers before launch, vent paths have to be provided. It is done by making all blanket layers from a material with small perforations.

The MLI has a degradation process in time, especially in LEO orbit. There is an interaction between the MLI and the atomic oxygen, which results in the oxidation of the polymers used in making thermal blanket.

Figures 2-3 and 2-4 show different MLI applied on satellites.



Figure 2-3: A typical MLI layer covered with a gold paint.



Figure 2-4: The external face of the Cassini space probe almost entirely covered with MLI

2.4.1.2 Radiators

The only way to reject heat into space for a satellite is to radiate it. The heat is rejected through radiators which can be a part of the structure (honeycomb panels, solar cells,) or not (body mounted radiators).

Sometimes, in order to improve the efficiency of such radiators, some heat pipes are included in the thickness of the radiator. By doing that it is possible to split the heat load on the whole radiator area and so to run the radiator with a better efficiency.

2.4.1.3 Thermal control coatings

Surface can either naturally or after treatment be made to absorb and emit radiant energy at specific rates corresponding to the spectrum of radiation. Thermal control coatings can be classified into three categories:

- Solar refelectors, which have a low solar absorptivity but high emissivity, are useful in a solar or earth albedo environment as they reflect much of the impinging energy while retaining the high Infra Red emissivity needed for efficient rejection of spacecraft waste heat. They include white paint ($\alpha = 0.06$ and $\epsilon = 0.88$ for the best ones) and optical solar reflector that work on the principle of the second surface mirror, where solar radiation penetrates a thin transparent high-emissivity material (Teflon or glass) then reflects off a metallic substrate effectively producing a low absorptivity and high emissivity surface ($\alpha = 0.08$ and $\epsilon = 0.78$ for a quartz mirror)
- Flat coatings, which reflect and absorb nearly equally in the solar and IR spectra, including black paint ($\alpha = 0.8-0.9$ and $\epsilon = 0.8-0.9$) and metallic paint ($\alpha = 0.23-0.5$ and $\epsilon = 0.25-0.5$). Black paints are widely used inside satellite canisters, including the exteriors of the electronic covers, to enhance heat sharing by radiation.
- Solar absorbers, which are seldom used on satellite surfaces.

As the MLI, thermal control coatings are degrading by the ultraviolet radiation, charge particles, and spacecraft debris. In the case of the Solar Orbiter, the degradation process has to be studied very carefully because of the very important heat load which is applied on the spacecraft.

Appendix A gives some value (emissivity, absorptivity ...) of different thermal coatings and materials which could be used on the solar orbiter.

2.4.1.4 Conductive tapes and joints

Those devices are very useful to ensure a good heat path between two devices or materials. It is commonly used between metallic boxes to improve the contact conductance between the box and its harness for instance.

They are generally made of silicon filled with silver or carbon particles in order to increase the conductivity of those flexible devices.

Figures 2-5 and 2-6 show different type of conductive joints.



Figure 2-5: Conductive joint (courtesy of COMERICS)



Figure 2-6: – Conductive tapes (Courtesy of CHOMERICS)

2.4.1.5 Phase Change Materials (PCM)

Phase change devices absorb thermal energy by changing from a solid to a liquid for the most common devices. As the temperature decreases, the material re-solidifies. It is especially useful for electrical equipment that experiences short power spikes.

The main disadvantage of phase change device is that they are unable to absorb any more heat after melting, which allows the temperature to increase.

An interesting application is to link a PCM to several heat pipes stuck to some electronic components or solar cells: the dissipative losses of energy from those components, which generally are treated as wasted energy, can be heat-piped to a central PCM Temperature Control System for later use in thermal control.

2.4.1.6 Thermal doublers

Thermal doublers are heat sink made of highly conductive material placed in thermal contact with a component. Heat is conducted to the sink during an increase in temperature and then dispersed by radiation or conduction.

The process also works in reverse and keeps the components from experiencing severe cooling. They can also be used to spread heat out over radiator surfaces, and are frequently used to control the temperature of electrical equipment that has high dissipation.

2.4.2 *Active Thermal control devices*

2.4.2.1 Louvers

Louvers are mechanical devices that, in effect, regulate the area of a radiator in response to its temperature. The regulation is preset to accommodate a wide range of heating within a relatively small change in temperature.

The most common louvers are the venetian blind type (figure 2-7). It is a framed array of highly reflective blades, with central shafts that fit tightly into the centre of bimetallic spring actuator calibrated to expand or contract to various angular positions at prescribed temperatures. As radiator heating increases, the rise in temperature warms up the actuators, which then generate thermal torques that rotate the blades and let radiators

expulsing heat into deep space. When the radiator temperature decreases, the actuators move the blades toward their closed positions.

This automatic opening and closing of blades compensates for changes in dissipation and environment heating and keep the temperature within a narrow band.



Figure 2-7: A venetian blind louver. On the picture, the blades are fully open.

2.4.2.2 Heat pipes

Heat pipes are lightweight devices used to transfer heat from one location to another. It is a hermetically sealed tube with a wicking device on the inside surface (figure 2-8) . A fluid inside the tube operates by changing phases during heating and cooling period. Heat applied at one end of the pipe causes evaporation of the liquid in the wick. The gas formed by the evaporation flow goes to the other end of the pipe. Then, it condenses, cooling back into a liquid and releasing the heat to a radiator. The liquid returns to the evaporator place by way of capillary wicks, thus completing a heat transfer loop.

Because of the high latent heat of evaporation of the heat pipe 's working fluid (ammonia, methanol or oxygen are the most used in space), this type of device allows high heat transfer, even with a low temperature gradient between each faces. Moreover, heat pipes can have a fixed conductance or variable conductance (with temperature) which can be a basic thermal control system.

Typically, a heat pipe can transport more than 100 W on 1 meter.

Sometimes, heat pipes are bonded into the satellite honeycomb panels or in radiators behind louvers. This technique allows a better and more efficient heat transfer through the devices and then limited any hot point on it.

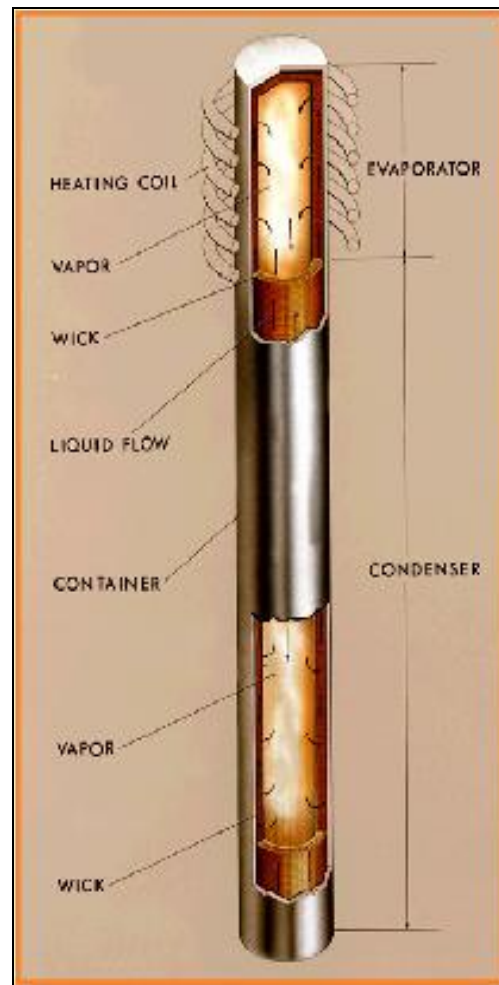


Figure 2-8: A typical heat pipe with its different constituent parts.

2.4.2.3 Heaters

Heaters are resistor elements that generate heat by Joule's effect when an electric current passes through them. They are used throughout the satellite to prevent fluids from freezing, maintain payloads at specific temperatures, and as shunts up to dump surplus heat.

They can be hard or flexible. Flexible heaters are the most common in the satellite because they can conform to various shapes (circular for a fuel tank, spiral for the fuel feeding lines). They consist of a thin electrical resistor between two polymeric sheets, such as polyimide, kapton®, or mylar® (figure 2-9) .

Typical heater power densities are on the order of less than 1W.cm^{-2} .

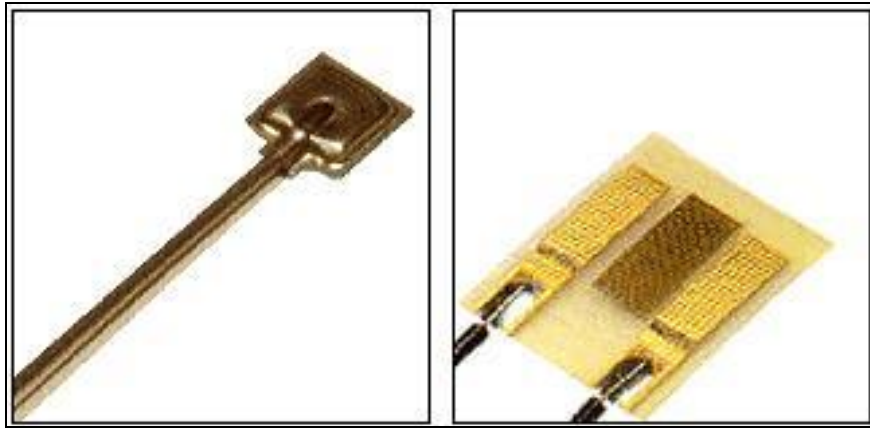


Figure 2-9: Different types of heaters (courtesy of MINCO Inc.).

2.4.2.4 Thermal switches

A thermal switch provides a direct conduction path between the heat source and the equipment mounting plate when the contacts are closed.

2.4.2.5 Pumped-loop systems

The pumped-loop systems works like heat pipes. In those systems, the gas path and the liquid path are not the same and the capillary structure which is present only in the evaporator drives all the system because of the pressure difference between the evaporator and the condenser (figure 2-10).

This system allows very large heat transfer (around 100 kW.m) but it is bigger, more complex and more expensive than simple heat pipes.

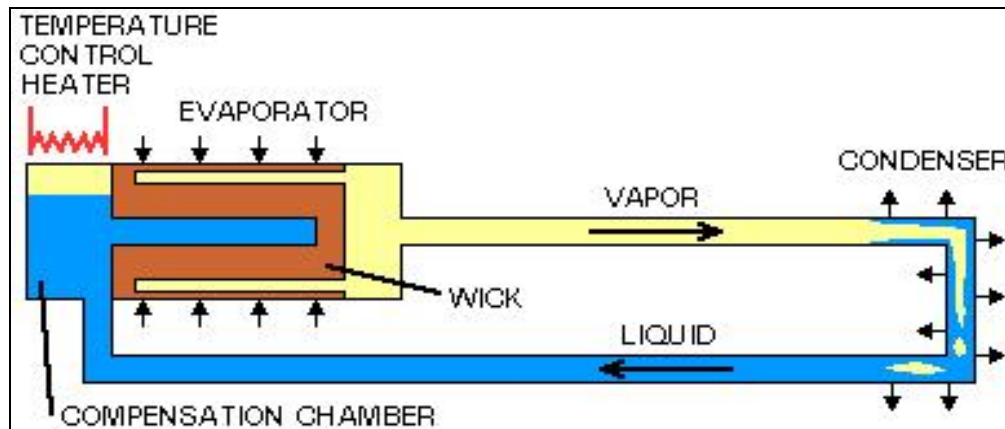


Figure 2-10: A typical pumped looped system

2.4.2.6 Heat exchangers

A heat exchanger is used to transfer thermal energy between two or more fluids at different temperatures.

They can use direct or indirect contact: In direct contact heat exchangers, the working fluids come in contact with each other, exchange heat and are separated. Indirect contact heat exchangers transfer heat through a wall or a baffle.

The most common heat exchangers can be classified into three categories:

- flat plate
- shell and tube
- crossflow : the two fluids flow at right angles to each other. The flow may be called mixed or unmixed within the crossflow arrangement.

2.4.2.7 Cold plate

A cold plate is used for mounting heat dissipating equipment. In this system, there are fluid passages within the plate itself. The fluid is then pumped to a radiator. All the energy absorbed by the fluid on the cold plate is then dissipated into the radiator.

This system is very efficient but it needs regular maintenance (pipes tend to be choked by the fluid) and is generally quite heavy.

3. Preliminary thermal analysis

3.1 Assumptions and description of the model

This preliminary thermal analysis has been done at the beginning of the project in order to have an idea of the temperature the spacecraft should have to withstand during an orbit. At this time, it seemed obvious that the worst conditions would be at the perihelion, at 0.2 A.U, when the heat load on the spacecraft is around 34000 W/m².

As we will see in the next chapter, not only the very high temperature is problems for this mission but also and above all the heat load gradient between the perihelion and aphelion.

However, for this steady-state simulation, only the hot case has been studied.

The other assumptions for this model are:

- The mirror temperatures are fixed to 61 °C.
- All radiators temperatures are fixed to 50 °C.
- There are no view factors between the heat shield and the radiators.

3.2 Excel calculation process

3.2.1 *Grazing incidence option*

The grazing incidence telescope is made with three mirrors:

- The primary mirror M1
- The secondary mirror M2
- The rastering mirror MR

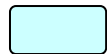
Then the heat load which is reflected by the rastering mirror goes to the slit which is used to protect the detector against any overload.

The computation method for this design is the following one:

- Figure 3-1 presents the general calculation process of the different heat flow on the mirrors
 - Figures 3-2 and 3-3 show the calculation process of the radiator area for each mirror. Because the process is exactly the same for each radiator, and because
-

those processes are totally independent from one to another, only the M1 radiator calculation method has been represented. The others can be obtained by substituting M1 by M2 or MR.

The colour code for those diagrams is the following:



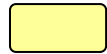
: « variable parameter 1 »



: « variable parameter 2 » which can be deduced from « variable parameter 1 »



: « fixed parameter »



: « result of a calculation »

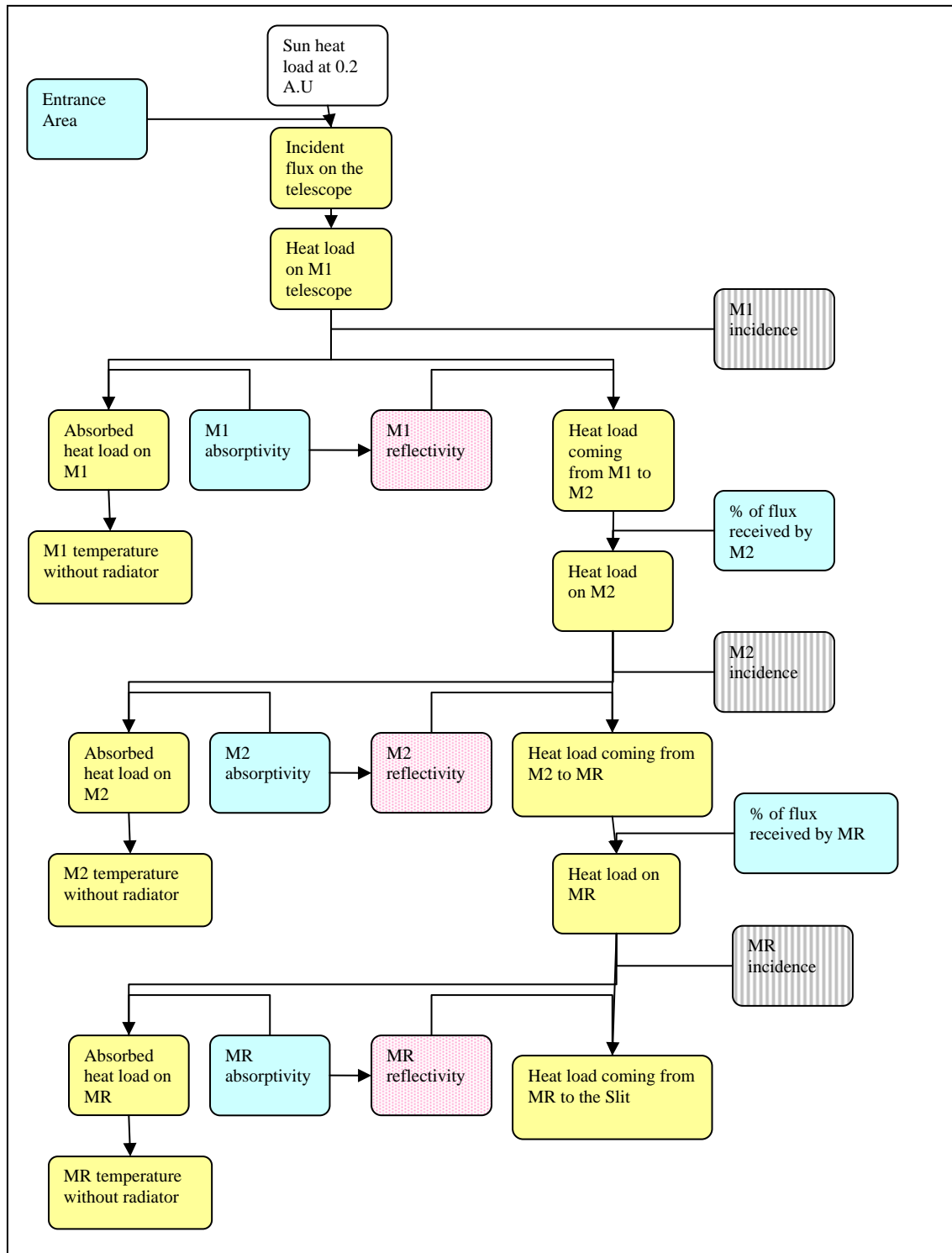


Figure 3-1 : Calculation process for the different heat flow on the mirrors for the grazing incidence telescope

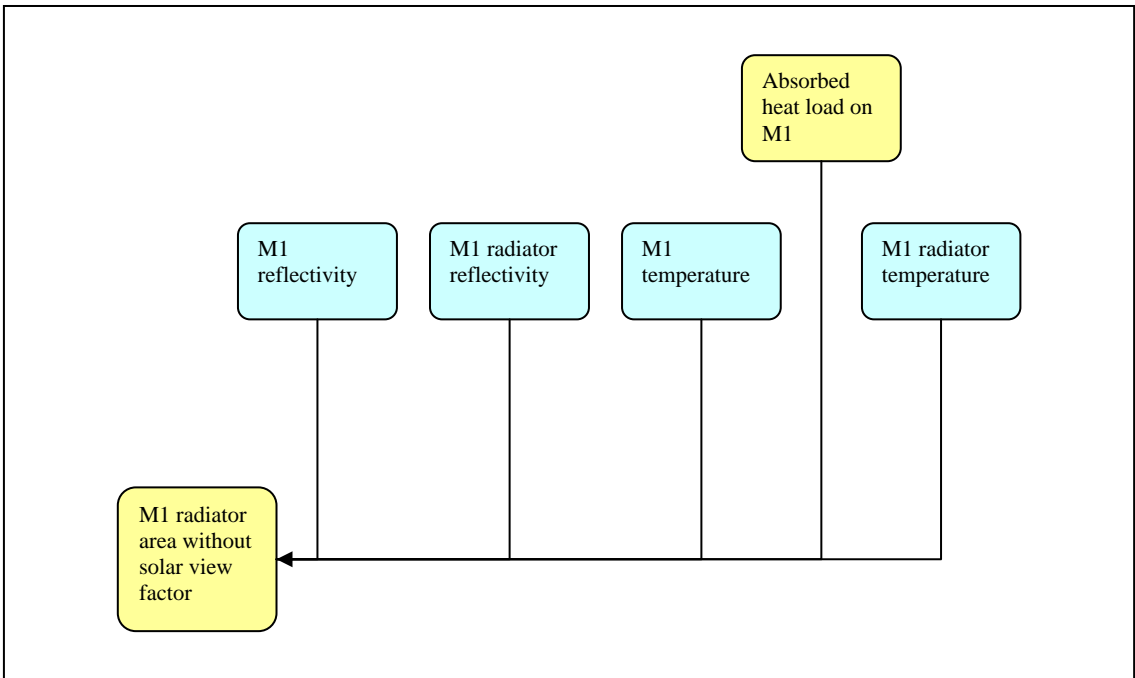


Figure 3-2 : M1 radiator area calculation process for the grazing incidence telescope when there is no heat path between the sun and the radiator

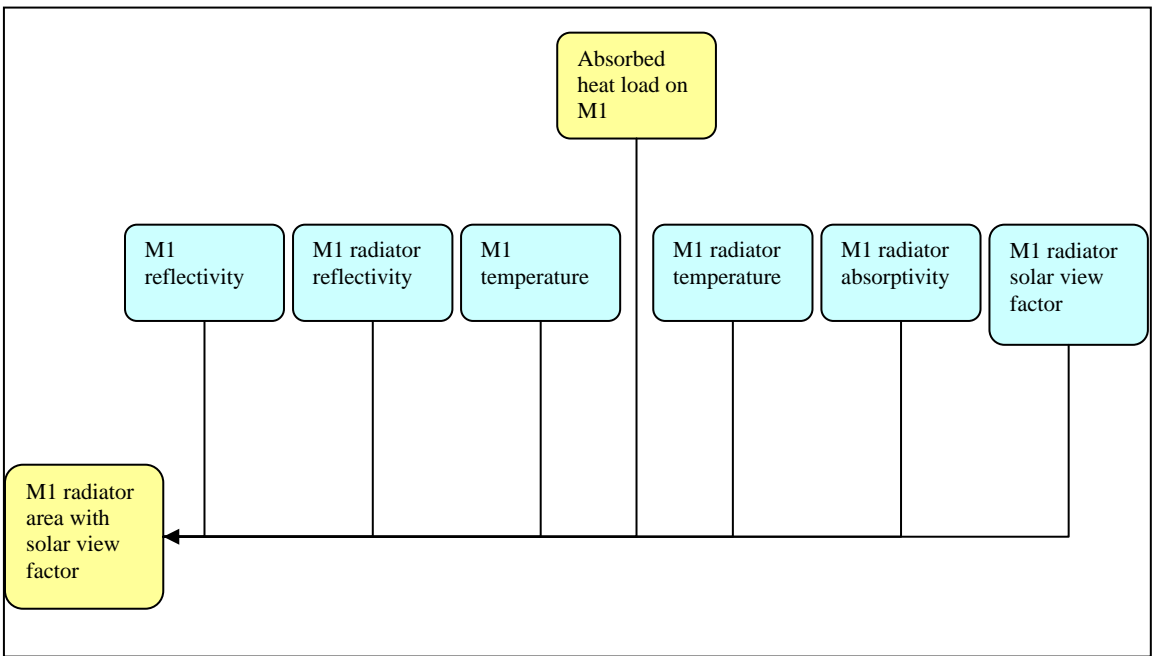


Figure 3-3 : M1 radiator area calculation process for the grazing incidence telescope when there is a heat path between the sun and the radiator

3.2.2 *Off axis option*

The off-axis telescope is made with:

- A primary mirror which sees the sun
- A heat stop which reflect a large part of the incident energy, absorb another part, and transmit the rest (absorptivity + reflectivity + transmittivity = 1).
- A secondary mirror which reflect the energy coming from the heat stop to the slit.

The computation method is almost the same than for the grazing-incidence telescope.

The only difference is coming from the heat stop which is a surface which is defined not only by its absorptivity and reflectivity, but also by its transmittivity.

As far as the calculation process is exactly the same for the radiator area, only the method for the heat flow determination has been detailed in the figure 3-4.

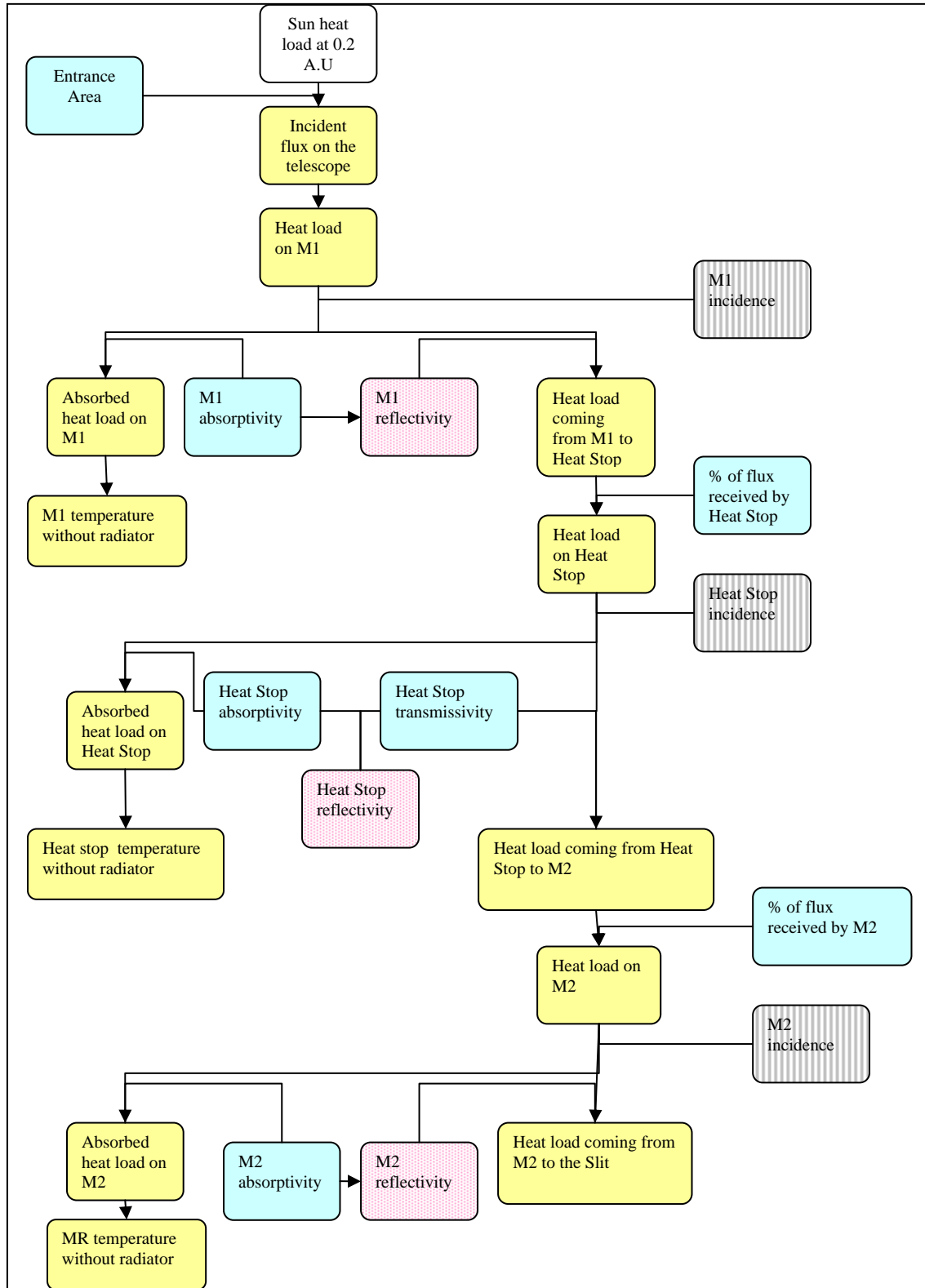


Figure 3-4 : Calculation process for the different heat flow on the mirrors for the off axis telescope

3.2.3 Formulae

Most of those formulae are obvious but are written here to facilitate the understanding of the calculations.

$$\text{Mirror effective area} = \text{Mirror inclined area} \cdot \cos(\phi)$$

$$\text{Heat load on a mirror} = G_s \cdot \text{Mirror effective area}$$

$$\text{Flux density on a mirror} = \frac{\text{heat load on the mirror}}{\text{mirror inclined area}}$$

$$\text{Absorbed flux density on a mirror} = \frac{\text{Flux density on the mirror}}{\text{absorptivity of the mirror}}$$

$$\text{Total heat absorption on the mirror} = \text{Absorbed flux density on the mirror} \times \text{mirror inclined area}$$

The following three formulas come from the energetic balance. Indeed, if the surface is at its equilibrium temperature, then all the energy absorbed is equal to the emitted energy.

$$\text{Mirror temperature without radiator} = \sqrt[4]{\frac{\alpha_M \cdot G_s}{\rho_M \cdot \sigma}}$$

$$\text{Mirror radiator area if no absorption} = \frac{G_s \cdot \alpha_M \cdot A_M - \epsilon_M \cdot \sigma \cdot A_M \cdot T_M^4}{\epsilon_R \cdot \sigma \cdot T_R^4}$$

$$\text{Mirror radiator area if absorption} = \frac{G_s \cdot \alpha_M \cdot A_M - \epsilon_M \cdot \sigma \cdot A_M \cdot T_M^4}{\epsilon_R \cdot \sigma \cdot T_R^4 - \alpha_R \cdot G_s \cdot V_F}$$

Those two last formulae are applicable if the mirror is seeing directly the sun (this is the reason why there is a term in $G_s \alpha_M A_M$). In the case of the secondary mirror, or the heat stop or the rastering mirror the term in $G_s \alpha_M A_M$ has to be replaced by the total heat load absorption on the device.

For instance, the radiator area of the secondary mirror is:

$$A_{R_{M_2}} = \frac{\text{total heat absorption on M2} - \epsilon_{M_2} \cdot \sigma \cdot A_{M_2} \cdot T_{M_2}^4}{\epsilon_{R_2} \cdot \sigma \cdot T_{R_2}^4}$$

To simplify the study the reflectivity of the mirrors and radiators are equal to their emissivity.

ϕ	= Mirror incidence
G_s	= Solar constant at 0.2 A.U = 33750 W/m ²
σ	= Stefan constant = 5.67 · 10 ⁻⁸ W · m ⁻² · K ⁻⁴
α_M	= Mirror absorptivity
ρ_M	= Mirror reflectivity
ϵ_M	= Mirror emissivity
A_M	= Mirror effective area
T_M	= Mirror temperature
α_R	= Radiator absorptivity
ρ_R	= Radiator reflectivity
ϵ_R	= Radiator emissivity
T_R	= Radiator Temperature

3.3 Results, analysis, feasibility, model precision

A copy of the spreadsheet used for each design is attached in Appendix B

Several simulations have been done for each design. In each simulation, the absorptivity of the mirror has been changed in order to find the best trade-off.

The only requirement was that the heat load coming to the slit was between 1.5 and 3 Watts.

Table 3-1 gives some very general characteristics of the incoming sun heat load on the telescope for each design.

Optical design	Grazing Incidence	Off Axis
Entrance area (cm ²)	12.25	143.13
Incident heat load on the telescope (W)	41.34	483.06
heat load on M1 (W)	41.18	379.45

Table 3-1: Incident sun heat load on the telescope (hot case) for each design

As we can see here the incoming heat load is not at all the same for each design and so it appears clearly here that the Grazing Incidence design should be much more better on a thermal point of view because the total energy to evacuate is only 41 W.

For the Off-axis design two problems appears:

- First of all, 379 W are coming to M1. So if M1 is highly absorptive, it will have to dissipate a large amount of power, which means that the radiator area has to be quite large and the heat path between M1 and its radiator has to be very efficient. If M1 is highly reflective, that means that the reflected heat load has to be either rejected to space or absorbed by the telescope casing, which would be a problem for the pointing accuracy of the telescope.
- Moreover, because 483 W are going through the telescope aperture and only 379 W reach the primary mirror, more than 100 W are going directly to the rear of the casing and have to be absorbed and dissipated by the structure, which would be once again a problem for its stability.

Table 3-2 and 3-3 present the radiator area which is necessary to cool the temperature of the mirrors at 61 °C (the temperature of the radiators is fixed at 50 °C). Only the results which meet the requirements are shown here. The Appendix B gives all the results of the different simulations. For the Grazing Incidence, there are some other possibilities by inverting coatings on M1 and M2.

Grazing Incidence Design					
M1 coating	Silicon-Carbon 1	Silicon-Carbon 1	Silicon-Carbon 1	Gold	Platinum
M2 coating	Silicon-Carbon 1	Gold	Platinum	Gold	Gold

M1 absorptivity	0.10	0.10	0.10	0.20	0.40
M2 absorptivity	0.10	0.20	0.40	0.20	0.20
rastering mirror absorptivity	0.20	0.20	0.20	0.20	0.20
total heat absorption on M1 (W)	4.12	4.12	4.12	8.24	16.47
total heat absorption on M2 (W)	3.52	7.04	14.08	6.26	4.69
total heat absorption on rastering mirror (W)	0.63	0.56	0.42	0.50	0.38
heat load coming from the rastering mirror to the slit (W)	2.53	2.25	1.69	2.00	1.50
Total radiator area (m2)	0.0123	0.0186	0.0311	0.0246	0.0367
Total radiator area (m2) if absorption	0.0313	0.0473	0.0794	0.0627	0.0935

Table 3-2: Steady State simulation results for the grazing incidence design.

<i>Off Axis Design</i>			
M1 coating	Silicon-Carbon 1	Gold	Platinum
M2 coating	Silicon-Carbon 2	Silicon-Carbon 2	Silicon-Carbon 2
M1 absorptivity	0.10	0.20	0.40
heat stop absorptivity	0.20	0.20	0.20
heat stop transmissivity	0.05	0.05	0.05
M2 absorptivity	0.80	0.80	0.80
total heat absorption on M1 (W)	37.95	75.89	151.78
total heat absorption on heat stop (W)	68.30	60.71	45.53
total heat absorption on M2 (W)	13.66023	12.14242	9.10682
heat load coming from M2 to the slit (W)	3.42	3.04	2.28
Total radiator area (m2)	0.1895	0.2429	0.3496
Total radiator area (m2) if absorption	0.5087	0.6446	0.9166

Table 3-3: Steady State simulation results for the off axis design

For the grazing incidence telescope, it seems easy to find a coating which can meet the temperature and radiator area requirements.

For the off axis telescope, it is clear that the coatings have to be chosen more carefully. If we only look at the radiator area without absorption, there is only one possibility which comply with the requirements because of the heat load coming to the slit. Nevertheless, if we increase the heat load requirement on the slit by 0.5 W, two other possibilities appear. If now, we are looking at the radiator area with absorption, there is just one possibility. Because of the different assumptions which have been made in the

model, this radiator area value should be closer to the reality (even if the radiator is not directly seeing the sun, it is seeing the heat shield which is going to run very hot. The radiator is then going to absorb a part of the energy coming from the heat shield.). Moreover, as we said before, the total radiator area is limited by the footprint of the instrument, which is around 0.56 m^2 . At the moment we have only calculated the radiator area for the three mirrors, but the detector and maybe other devices will need a radiator.

So, by considering that point, only one coating strategy seems to be really valid: if M1 is covered with the silicon-Carbon 1 coating and M2 with the Silicon-Carbon 2 coating, the total radiator area with absorption is 0.5087 m^2 .

In conclusion, it appears clearly here that the off axis design is really more challenging on a thermal point of view. So, only this design is going to be studied in the transient analysis (if it is possible to find and develop a thermal strategy for it, it is obviously feasible with the grazing incidence design).

4. Transient thermal analysis

The purpose of this chapter is to develop a thermal model which will simulate the Solar Orbiter during its nominal orbit. This model is developed using three specialised software called IDEAS-TMG, ESARAD, and ESATAN.

4.1 The thermal environment

The extreme environments encountered by the spacecraft throughout the whole mission drives the thermal design of the Solar Orbiter and its payloads.

The spacecraft is designed to get as close to the sun as the materials and engineering will allow (0.21 A.U). Solar radiation increases with decreasing distance from the Sun, and is, of course, the most challenging aspect of the present mission. The solar constant at a distance “r” (in Astronomical Unit [AU]) is given by:

$$C_s(r) = \frac{C_{s0}}{r^2}$$

Where C_{s0} is the solar constant measured at 1 AU, i.e. 1367 W/m².

Moreover, because the orbit of the Solar Orbiter is highly elliptic and because also of the different stage of its mission (cruise phase and nominal phase), its distance from the sun will vary from 0.21 to 1.21 A.U, which means that the satellite has to withstand those heat flow gradients and to adapt its thermal strategy to the incoming heat flux.

Table 4-1 gives the typical values of the heat load during the life time of the solar orbiter. In this study, only the nominal phase has been modelled.

Distance from Sun	Heat load
Cruise Phase	
0.25 A.U (37.5 10 ⁶ km)	21936 W/m ²
1.21 A.U (181.5 10 ⁶ km)	936 W/m ²
Nominal Phase	
0.8 A.U	2142 W/m ²
0.21 A.U	34275 W/m ²

Table 4-1: Typical value of the sun heat load for different points of the orbit

As the lector will notice later in the thesis, it is necessary to calculate numerically the heat load coming to the spacecraft at each point of the orbit and also and above all it is necessary to know the heat load as a function of time.

For the moment, it is possible to know the solar constant C_S as a function of the Sun-Satellite distance. Hopefully, because the orbit is an elliptic one, it is possible to express this distance “r” as a function of a polar angle “ θ ” :

$$r = \frac{p}{1 + e \cos(\theta)}$$

The eccentricity “e” of the ellipse and its parameter “p” are given by the following formulae:

$$2a = r_{Perihelion} + r_{Aphelion}$$

$$p = a(1 - e^2)$$

$$r_{Aphelion} = a(1 + e)$$

Here, $2a = 0.75 + 0.2 = 0.95$ A.U, and so $e = 0.578$ and $p = 0.3163$ A.U = $47.44 \cdot 10^6$ km.

So, the problem is now to link the polar angle “ θ ” to the time. By using the *Gauss equation* and then the *Kepler equation*, we can link “ θ ” to the eccentric anomaly “E” which is then linked to the time “t”

$$\text{Gauss Equation: } \tan\left(\frac{E}{2}\right) = \sqrt{\frac{1-e}{1+e}} \cdot \tan\left(\frac{\theta}{2}\right)$$

$$\text{Kepler Equation : } E - e \cdot \sin(E) = \frac{2\pi}{T} \cdot t$$

where T is the period of the orbit (150 days).

As you can notice, it is not possible to obtain the exact solution of the Kepler equation. Nevertheless, by using a mathematical software like Maple or Mathcad, it is possible to obtain a numerical expression with a very good accuracy. A copy of the program is in Appendix C.

So, for any time “t” we can know the radius “r” and then the solar constant C_S .

Figure 4-1 summarises the method used to compute the Sun heat load coming on the spacecraft as a function of time.

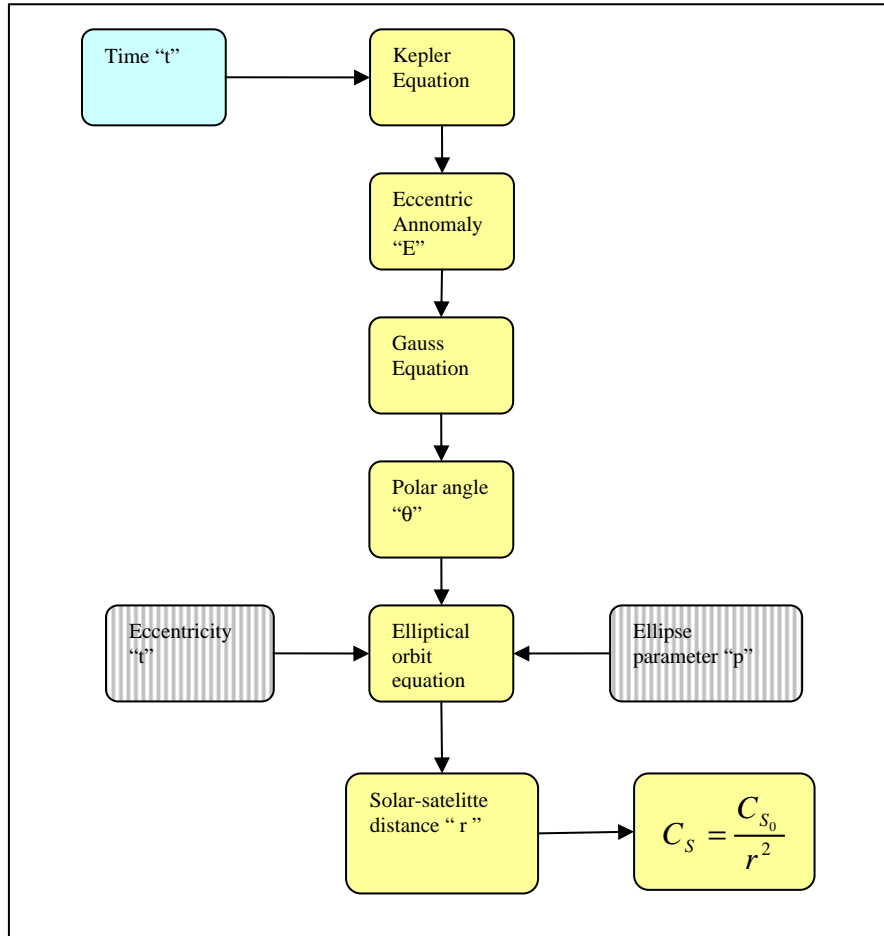


Figure 4-1 : calculation process of the incident sun heat load as a function of time

Figure 4-2 describes the evolution of the thermal heat load during a whole orbit in the nominal phase. Those values have been computed with the method described above. As we can notice there, the variation in time of this load is quite fast (it lost and gain around 50% of its value in less than 10 days), which means that the thermal mass of the spacecraft (which determines its thermal inertia) will play a very crucial role in the thermal strategy.

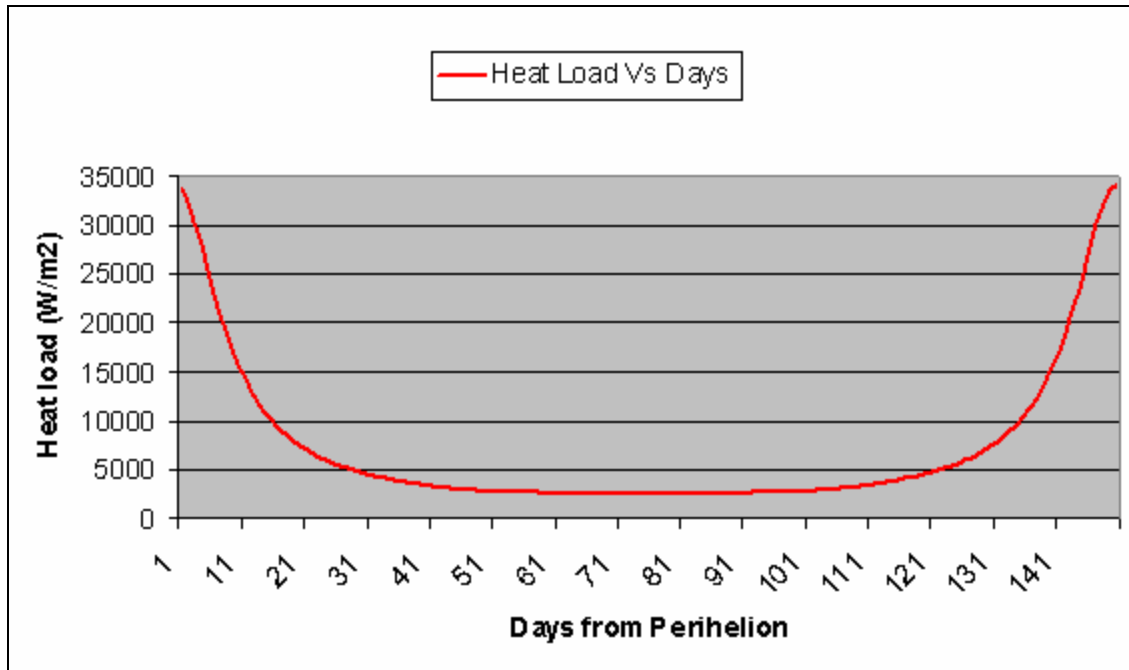


Figure 4-2 : Incoming heat load on the solar orbiter VS orbit days. The period of the orbit is around 150 days and the first day of the orbit corresponds tp the perihelion

Figure 4-3 compares the maximum heat load coming on different spacecrafts. It appears here that the solar orbiter is really challenging because of its very short distance to the sun.

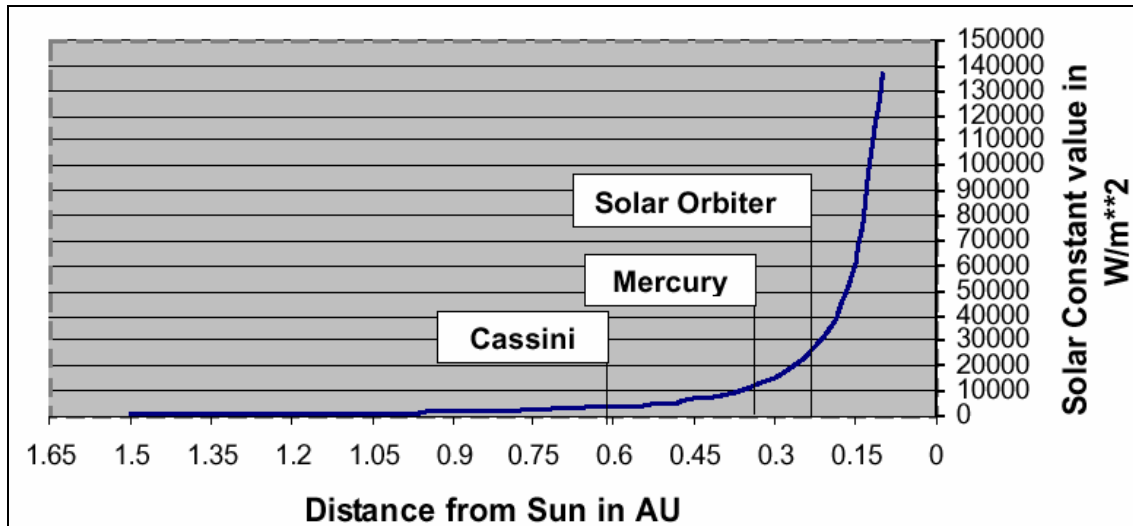


Figure 4-3: Comparaison of maximum Solar heat loads for diffrent missions (from *Solar Orbiter Assessment Study*, Solar Orbiter Website)

4.2 Presentation of the softwares

Two different software packages have been used in those transient simulations. The first one is I-Deas TMG, developed by Electronic Data System Inc (EDS). The second one is ESARAD / ESATAN developed by Alstom.

4.2.1 ESARAD / ESATAN

The Technology Centre has developed a suite of advanced analysis tools in co-operation with the European Space Agency.

ESARAD is a pre and post processor for ESATAN and provides a suite of integrated software tools for the analysis of surface to surface radiative heat exchange and the space thermal radiative environment.

ESATAN, is a comprehensive, flexible thermal and fluid flow software package, suitable for a wide range of applications

4.2.1.1 ESARAD Overview

ESARAD is a radiative analysis software package for analysing spacecraft in orbit.

ESARAD allows a user to calculate radiative couplings and output a thermal model for the spacecraft. The thermal model takes the form of an input file to the ESATAN thermal analysis program. After performing a thermal analysis, ESARAD will also allow the user to post-process his results.

The ESARAD user interface has four main workspaces which allow to complete the analysis. These workspaces are:

- Building the geometric model of the spacecraft
- Viewing the model
- Calculating the model's radiative characteristics
- Defining and creating the thermal model

Key features of ESARAD include:

- Complete pre-/post-processing capabilities for industry leading thermal analysis package such as ESATAN.
- Enhanced ray-tracing method for rapid analysis of surface to surface radiative heat exchange.
- Support for diffuse, specular and transmissive radiative heat transfer.
- Advanced 3D surface geometry modelling, including support for cutting operations and moving assemblies.
- Modern, easy to use interface with short learning curve.
- Powerful underlying language allowing enormous flexibility when needed.

4.2.1.2 ESATAN Overview

ESATAN is a software package for the prediction of temperature distributions in engineering components and systems using the thermal network analysis technique. It enables the user to specify his problem in the thermal network quantities of nodes, conductances and material properties, together with the sequences of solutions required to obtain the required steady-state or transient temperature distributions. It also has a batch edit facility which permits previously defined thermal/fluid networks model to be incorporated into a model and changes to be carried out if required.

It will accept models of components or systems presented to it in thermal network terms, together with instructions for their solution. All models are checked during input for self consistency and translated into a database which is held permanently on the computer storage system until the user chooses to remove it.

Either steady-state or transient analyses can be handled, for problems with any degree of dimensional complexity. Any mode of heat transfer can be accommodated: explicit facilities exist for conduction, radiation, and convective heat transfer, any of which may be non-linear with respect to temperature or time. Additional features permit the handling of phase-change phenomena such as boiling, condensation, melting, solidification, ablation and gas-solid transitions. Material properties, such as specific heat, may also vary with time, temperature or any other independent or dependent quantity.

It should be recognised that ESATAN does not derive network models from specified geometries: that task must be performed by the user. The role of ESATAN is to handle, check, and solve the network models that the user has devised to represent his problem.

Key features of ESATAN include:

- Steady-state and transient analysis.
- One, two and three dimensional models.
- True sub-modelling approach allowing logical break-down of complex systems.
- Fully linked solution of both the solid and fluid thermal system (with FHTS).
- Conductive, convective and radiative heat transfer.
- Modelling of arbitrarily complex thermal control behaviour.
- Time and/or temperature dependent conditions and properties.
- Combined analyses of thermal and electrical problems.
- Extremely powerful and flexible parametric analysis capabilities.
- Large, user extensible library of functions and routines.
- User definable library for re-useable models and families of similar designs.

4.3 I-Deas simulations

4.3.1 Description of the thermal model

4.3.1.1 Geometry

Once again, because we are in an early phase of the project, the detailed geometry of the spacecraft is not known with a very good accuracy, in particular the dimensions of the EUV spectrometer depend of the optical design (the length of the telescope can varies from 1.5 m to 2.5 m). In order to move forward in the thermal analysis, dimensions have been fixed to the one showed in table 4-2 . All dimensions are given in millimetres. Figures 4-4 and 4-5 presents the geometric model as it appears on I-Deas.

<i>Item</i>	<i>shape</i>	<i>Dimension 1</i>	<i>Dimension 2</i>	<i>Dimension 3</i>	<i>thickness</i>
Primary mirror M1	disk	Diameter: 100			2
Secondary mirror M2	disk	Diameter: 20			2
Heat stop	Parallelepiped	Length : 460	Height : 180		1
Heat shield	Parallelepiped	Length : 1200	Height : 2800		5
Heat shield aperture	hole	Diameter:135			Through the heat shield
Telescope casing	box	Length : 1000	Height : 200	Depth : 500	3

Table 4-2 : Geometrical dimensions of the different elements of the I-DEAS model

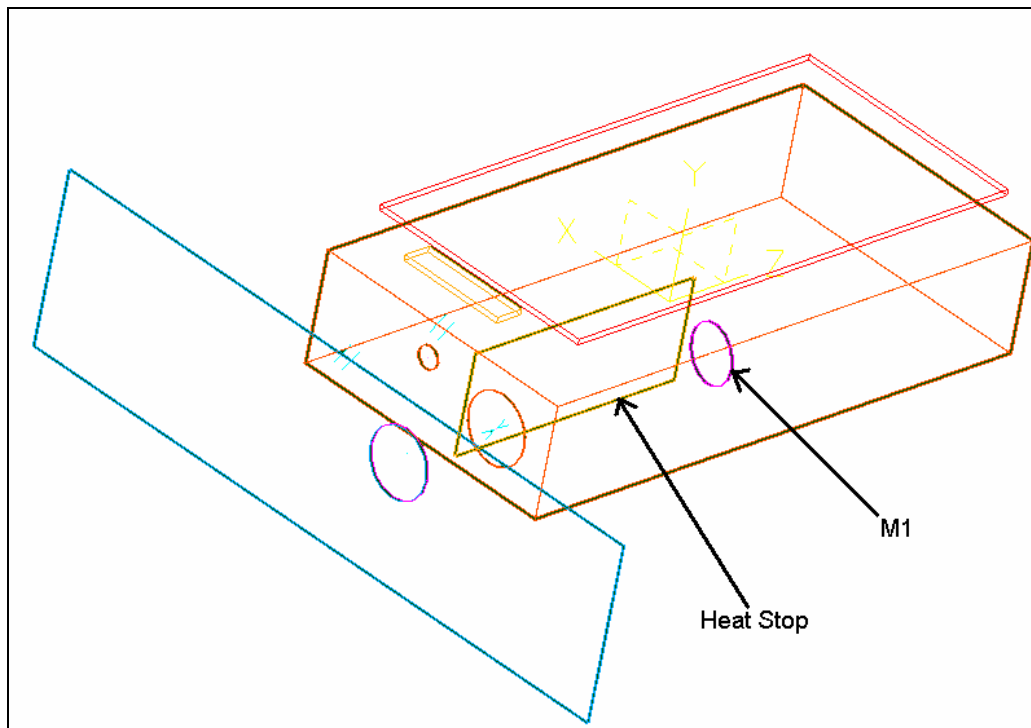


Figure 4-4 : Wireframe view of the I-DEAS model.

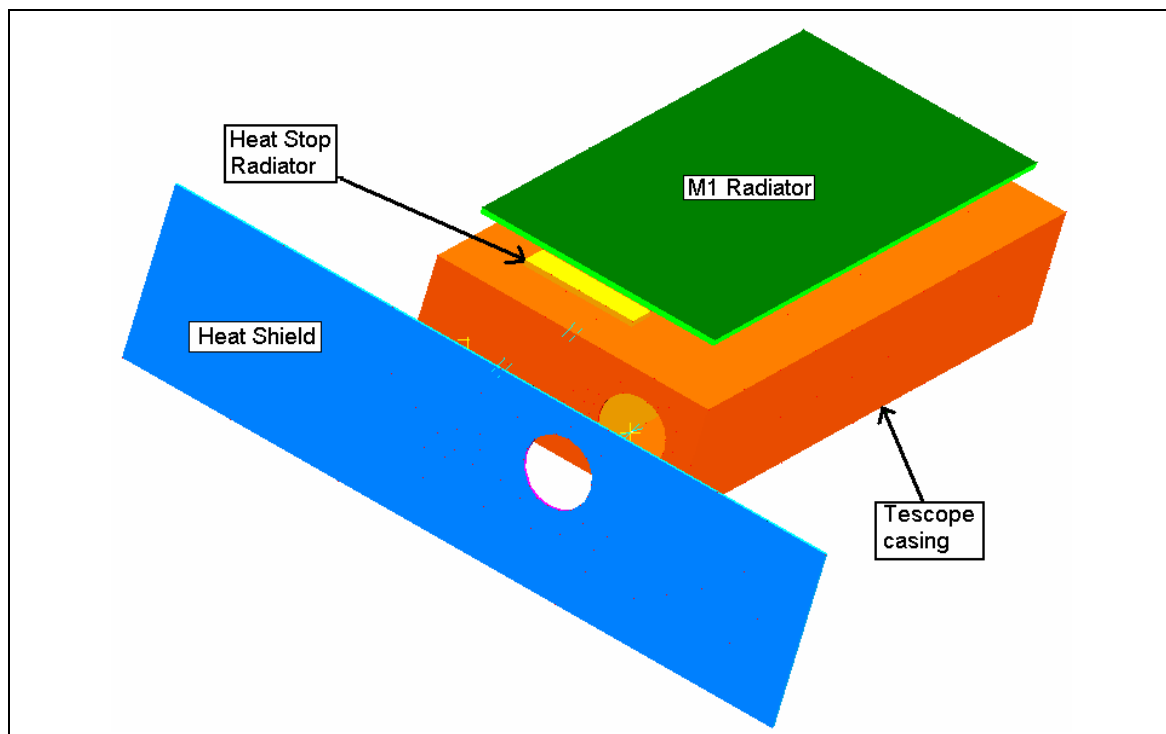


Figure 4-5 : Three dimensional view of the I-DEAS model

The dimension of the telescope casing, the heat shield and the heat stop may have to be changed in the future as they have been taken arbitrarily (there were no detailed information about those devices when the study has been done).

Moreover, the dimension of the primary mirror is no longer the good one. Following the last consortium meeting, the diameter of M1 is 120 mm, but because of a shortage in time, it has not been possible to modify it.

As the I-DEAS user will notice very quickly, it is not really easy to modify a parameter such as a dimension in a model (sometimes, such modification can create aberrations which make the model totally useless), and if several of those value have to be changed it could be better to redo the entire model. This is one of the weaknesses of this software which is both very powerful but difficult to use.

4.3.1.2 Finite element mesh

The IDEAS-TMG software uses a finite difference method to solve the temperature distribution in the model. For this to be implemented, the model has to be divided into a network of elements.

The elements chosen from the IDEAS-TMG library were quadrilateral thin shells. This type of element assumes a constant thickness. Because of the small thickness of all the elements described in the previous paragraph, those thin shells were the most appropriate element which could represent it without using an excessive number of elements.

The parameter governing the size of an element is the element length.

Four different elements were created. Each one has a different thickness.

4.3.1.3 Materials

In order to simulate the physical properties of each element, several materials have been created. Those one have particular properties, such as conductivity, emissivity, reflectivity ... (other physical properties like Young Modulus or microyeld stress can also be added but they are not used in the IDEAS-TMG thermal calculation)

Table 4-3 list the different materials and their associated properties.

<i>Device</i>	<i>Material</i>	<i>Density (kg/m³)</i>	<i>Thermal conductivity (W/m².°K)</i>	<i>Heat Capacity (J/kg.K)</i>
Mirrors (M1 and M2)	Silicon Carbide (SiC)	3170	190	700
Heat Stop	Aluminium	2700	237	903
Heat Shield	Aluminium	2700	237	903
Radiator	Carbon	3000	20	667
Telescope Casing	Carbon Fibre Reinforced Plastic (CFRP)	800	33	1000

Table 4-3 : Physical properties of the different materials used in the I-DEAS model

Different thermo-optical properties have been applied on those material to simulate different coatings. Table 4-4 gives the values of such coatings.

<i>Coating</i>	<i>Emissivity</i>	<i>Solar transmissivity</i>	<i>Solar reflectivity</i>	<i>Solar absorptivity</i>	<i>Infra-red reflectivity</i>	<i>Infra-red transmissivity</i>
Teflon	0.88	0	0.91	0.09	0.12	0
White paint	0.89	0	0.81	0.19	0.11	0
Gold	0.02	0	0.81	0.19	0.98	0
Black paint	0.874	0	0.025	0.975	0.126	0
M.L.I	0.8	0	0.8	0.2	0.2	0

Table 4-4 : Thermo-optical properties of the different coatings applied on the EUV Spectrometer

4.3.2 Heat loads

IDEAS-TMG has got an “orbital package” which can be used to simulate an orbit around a planet. Unfortunately, it can not be used to simulate an orbit around the sun!! Hopefully, as it has been mentioned in paragraph 4.1, the Sun heat load can be known at each point of the orbit by using the Kepler and Gauss equations.

So, to simulate the orbit, the heat load has been applied on the Heat Shield and the Primary mirror as a function of time (each day, a new value is applied and this value correspond to the figure 4-2). By doing that, the model should be quite similar to the reality. Nevertheless, it is not possible to simulate the heat load which is coming on the back of the telescope casing. As it has been explained in paragraph 3.3, because the hole on the heat shield is 135 mm diameter and the primary mirror only 120 mm diameter, a part of the incoming energy is not going to hit the mirror but will continue its path until it is reflected or absorbed by an physical surface (if there is nothing behind the mirror, it will be the rear of the telescope casing).

So, there are about 100 W ($483.06 - 379.45 = 103.61$ to be exact), which are going to reach the telescope casing. Obviously, those watts will have an impact on the thermal strategy of the Solar Orbiter but it was not possible to model it simply.

To ensure that heat can be transferred between one set of elements to another set at joints, a condition could be imposed and is known in IDEAS as “thermal coupling”. In this model, only one type of thermal coupling has been used: the Absolute one. It represent the absolute conductance (in W/ C) between two elements.

Thermal coupling was imposed at different areas in the model:

- between the primary mirror and its radiator
- between the heat stop and its radiator

In order to determine the sensibility and approximate value of the thermal coupling which could be both feasible and optimum, different values have been tried in the model. Those values are in a range of 0.05 W/C to 100 W/C (can be achieved with a very good heat pipe)

4.3.3 Correlation of the thermal model with preliminary analysis

As we have seen before, the steady-state solutions could be computed with analytical calculations. By comparing those value with the IDEAS one (with the same assumptions), it could determine the confidence with one could accept the temperature predictions given by the IDEAS-TMG package.

Table 4-5 presents the results obtained with the preliminary thermal analysis whereas figure 4-6 presents the results of the transient analysis obtained with IDEAS. The results have been computed on 2 orbits (300 days) in order to check the stability of the solution.

For both simulations, the absorptivity of the primary mirror has been fixed to 0.1.

M1 absorptivity	0.10
heat stop absorptivity	0.20
heat stop transmissivity	0.05
M2 absorptivity	0.20
total heat absorption on M1 (W)	37.95
total heat absorption on heat stop (W)	68.30
total heat absorption on M2 (W)	3.41506
heat load coming from M2 to the slit (W)	13.66
M1 temperature without radiator (°C)	507.12
Heat stop temperature without radiator (°C)	624.50
M2 temperature without radiator (°C)	701.69

Table 4-5 : Maximum temperature for the Primary mirror with a high emissive coating, without radiator and with the preliminary thermal analysis spreadsheet

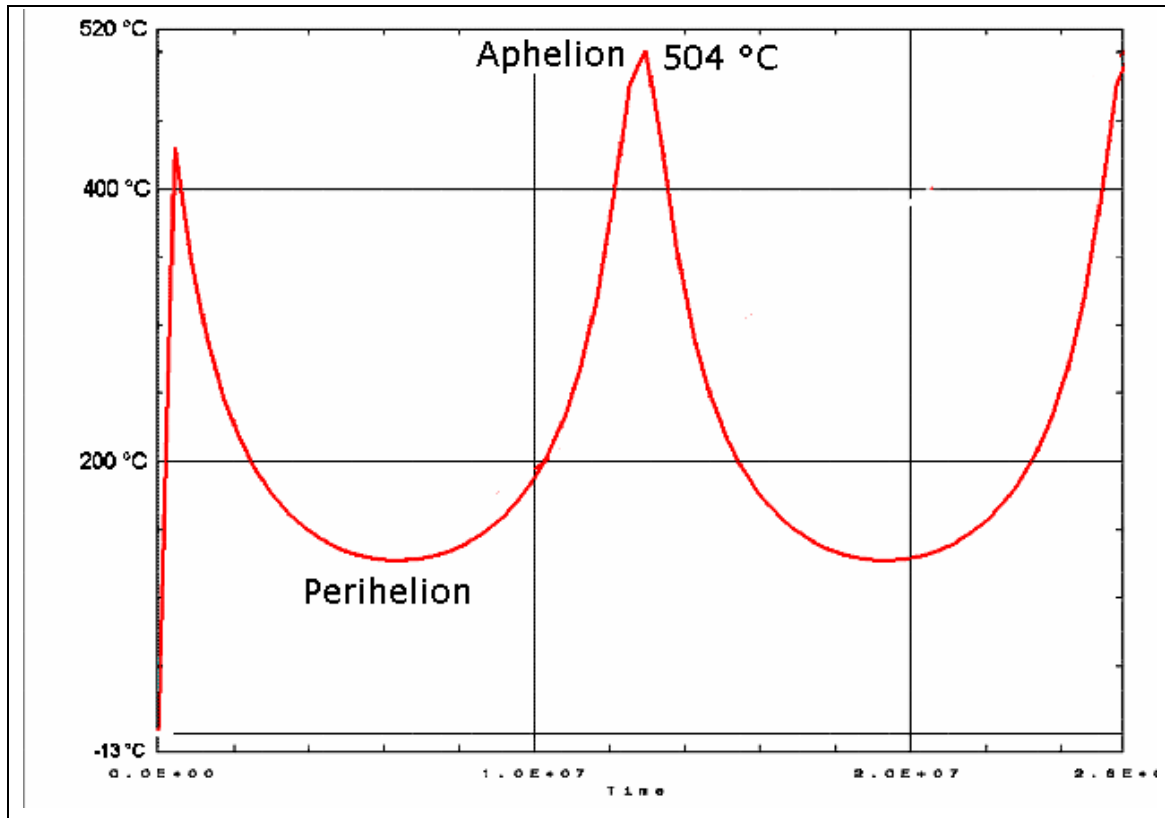


Figure 4-6 : temperature variation for the Primary Mirror with a high emissive coating, without a radiator and with the IDEAS-TMG software

As one can notice here, there is a difference of 3°C between the two models for the maximum temperature. Assuming the very high heat load and the approximations in the calculation (the preliminary one) that have been done, this difference is really small, and so it seems that the IDEAS model should give values which are quite realistic. That also means that for each value of the heat load (in the model the value of the heat load changes everyday), the time response of the system is quite fast.

4.3.4 Transient results

In order to determine the best strategy to apply to the spectrometer, many simulations have been done. Because, the system was quite complex, I focused my study on the primary mirror. This choice is also explained by the fact that M1 is the one which receives almost all the heat load and so if it is possible to control the temperature on M1, it should be feasible on the rest of the telescope. The heat stop will also receive a

large amount of heat but because of its size, the heat density (W/cm^2 on the surface of the element) is not as big as on M1. Moreover, the heat stop could be made with materials which resist better to the heat (even if there is a thermal distortion on the heat stop, it should not have the same impact than for M1 from an optical point of view).

Different parameters have been tested and studied:

- the emissivity of the telescope casing and heat shield
- The absolute conductance between M1 and its radiator
- The absorptivity of M1

Only four simulations will be presented here. They are the most relevant.

All the temperature variations of the primary mirror are taken on the central node of the mirror (the node which is the closest to the centre of the mirror)

The first three simulations (figures 4-7, 4-8 and 4-9) show the very high importance of two parameters:

- The heat shield coating
- The value of the conductance between the mirror and its radiator

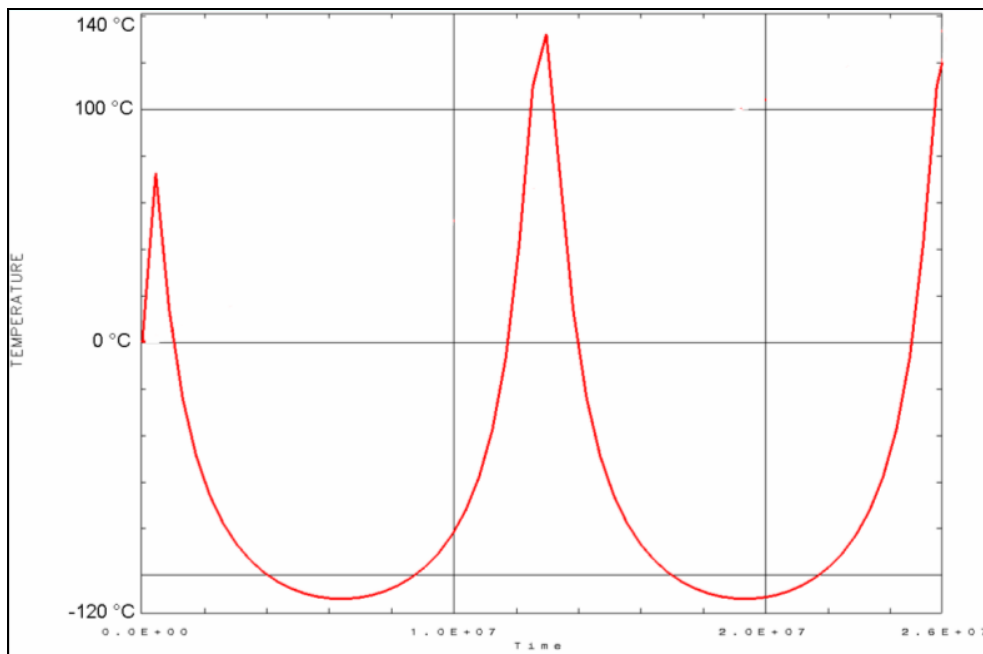


Figure 4-7 : M1 temperature with a conductance of 0.5 $\text{W}/^\circ\text{C}$ between the radiator and M1, a high emissive coating and M1 either lowly or highly absorptive

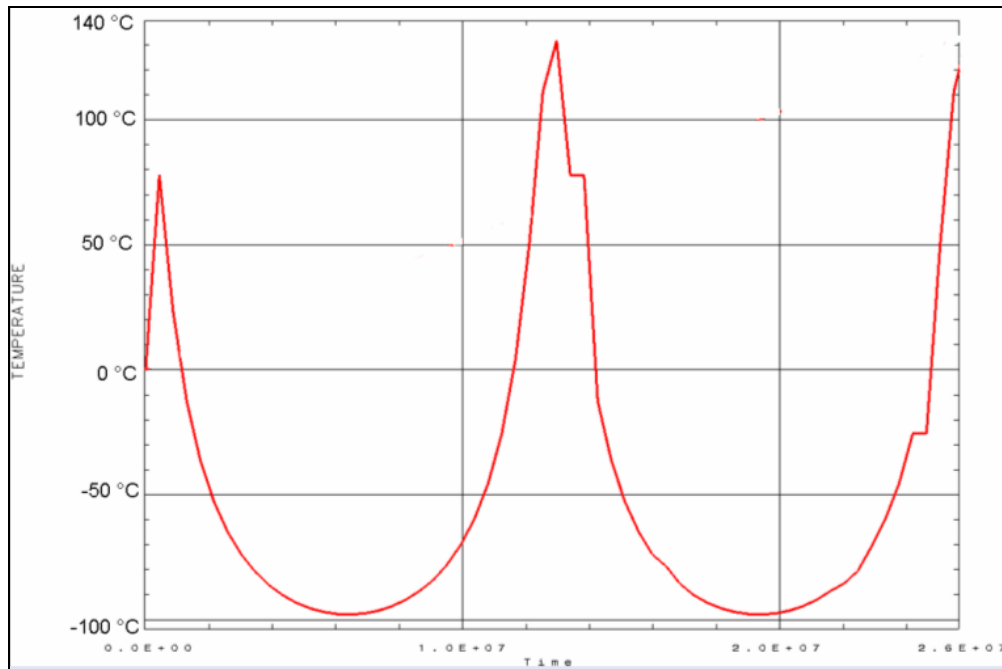


Figure 4-8 : M1 temperature with a low emissive coating on the heat shield, M1 lowly absorptive, and a conductance of 50 W/°C.

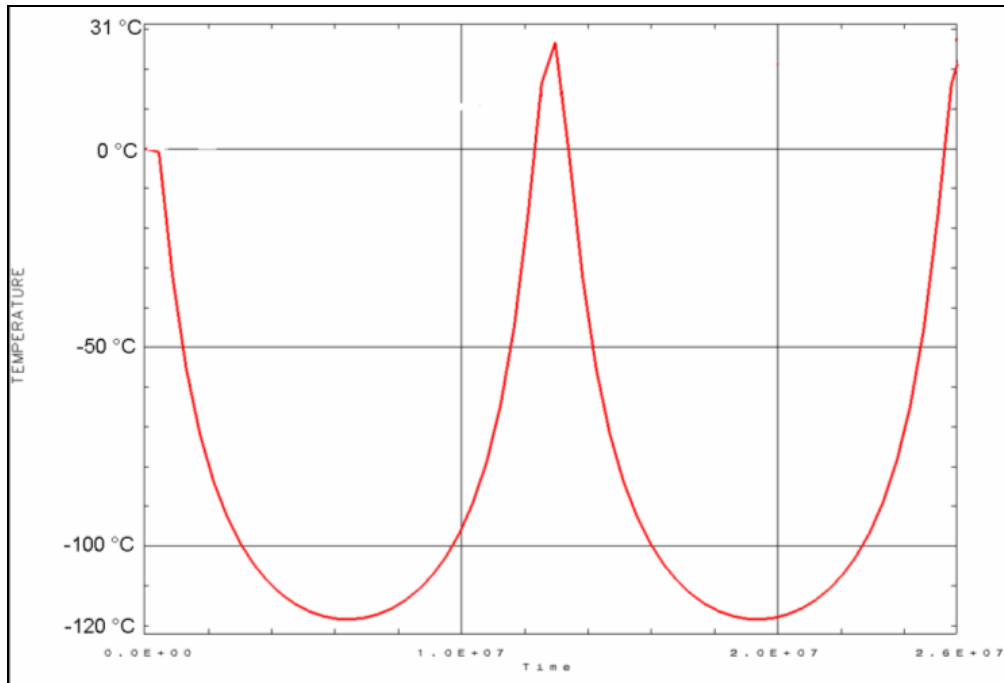


Figure 4-9 : M1 temperature with a high emissive coating (MLI) on the telescope, M1 either lowly or highly absorptive, and a conductance of 50 W/°C

The only way to really reduce the temperature variations on the mirror is to have a high emissive and reflecting coating such as white paint, Teflon ®, or a multilayer insulation (MLI) on the heat shield. It is even better to put MLI on it because of the very low conductivity it creates. With such a low conductivity, the temperature on the back face of the heat shield should not be too high, which is better for the efficiency of the radiators. (There is a view factor between the heat shield and the radiator and so a radiative heat path between those two devices).

Moreover, it is also very important to have a high conductance between the radiator and its mirror. Even if a heat pipe can achieve on a small distance a conductance of 50 W/°K, it is not sure that this conductance can be really achieved: all the problem is to have also very good thermal contact between the heat pipe and the mirror (and between the heat pipe and the radiator). A common solution to solve this problem is to put a conductive tape or joint (like the one developed by Chomerics, cf 2.4.1.4) to insure a very good heat path.

The figure 4-9 shows the temperature variation on the primary mirror if such conditions are applied.

Here, the temperature of M1 is within the temperature limits but this strategy still presents a problem: even if the temperature limits are validated, it is oscillating a lot,

and so it will be very difficult to maintain a constant and low temperature gradient between M1 and M2. As it has been showed in paragraph 2.2.6, if M1 is made with Silicon-Carbide (which is the case for the I-DEAS model), the temperature gradient between M1 and M2 should not exceed 3°C . This requirement is essential for the optical performances of the telescope.

During all those simulations, the impact of the mirror coatings has been quite small on the temperature variations (there is only a difference of about ten degrees in the maximum or minimum temperatures). It is difficult to explain this result which is inconsistent with the values given by the preliminary analysis. One hypothesis is that it is due to the oscillating shape of the heat load which reduce the thermal effect of the coating. Another hypothesis is that there is a problem in the model and so results are not really realistic. At this time, it is impossible to explain it.

So a solution to decrease drastically the temperature oscillation would be to put a thermal switch between the radiator and M1. Few simulations have been done with this assumption. As one can see on figure 4-10, it is possible with such solution to improve a little bit the temperature gradient of the mirror (-80°C to 50°C instead of -120°C to 31°C). Because of the very basic conductance law (figure 4-11) which has been applied, the results are oscillating a lot but it could be possible to stabilise those oscillations. Even if it is achieved with the I-DEAS model, the problem is to know if it is technically possible.

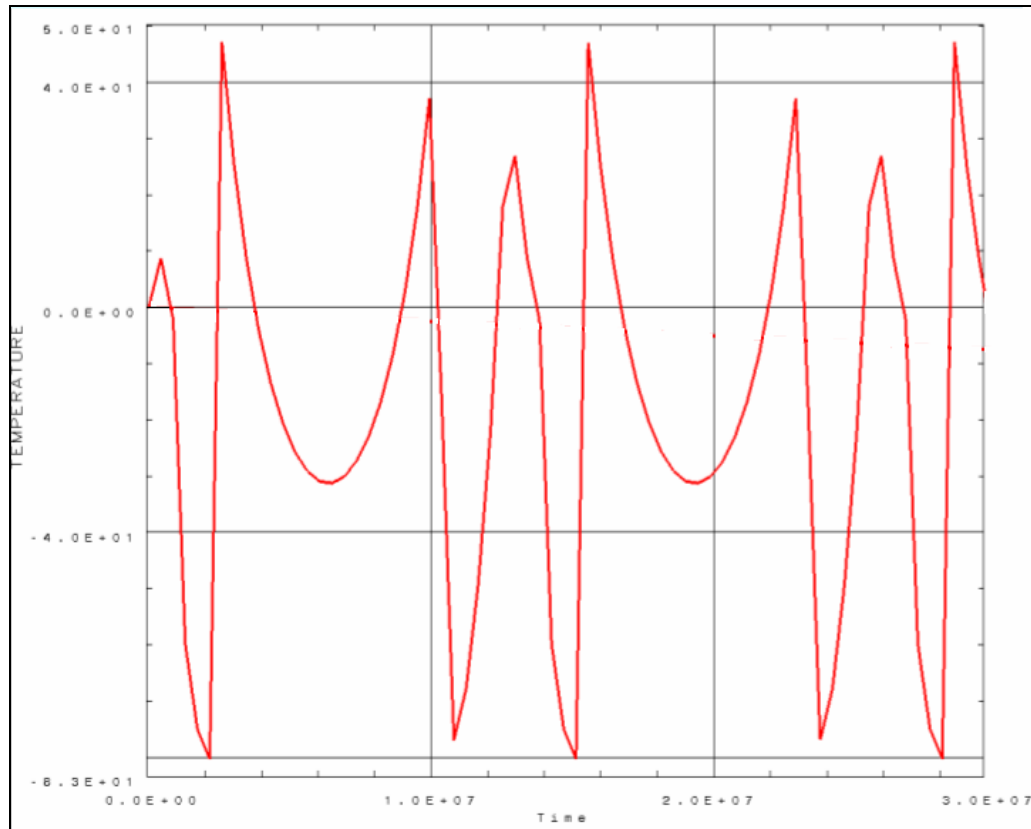


Figure 4-10 : M1 temperature with a thermal switch between the mirror and the radiator

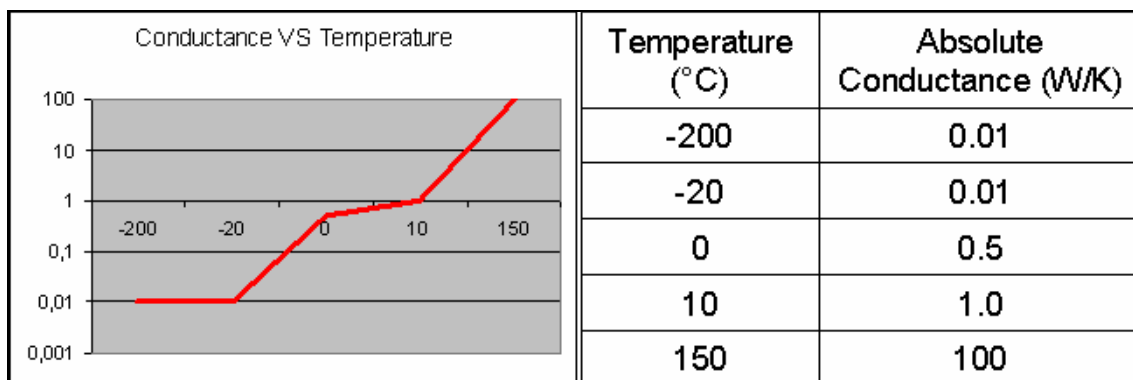


Figure 4-11 : Conductance law applied to the thermal switch.

Another problem that has been raised through those simulations is the temperature gradient which can occur between two points of the mirror. Figure 4-12 gives an example of this variation. In this example, the telescope casing is covered with MLI on its inner and

outer faces (that creates a lot of multi-reflexions and so encourages radiative heat paths and temperature gradients) . As one can see, there is a gradient of about one hundred degrees between each extremity (identified by A and B on the figure). The main reason for this gradient are the multi-reflexions that occur in the telescope casing (B is closer than A from the wall and so receive more energy from it). That shows that all the different parts of the telescope (structure, casing ...) have to be as much as possible lowly reflective in order to reduce any radiative heat transfer.

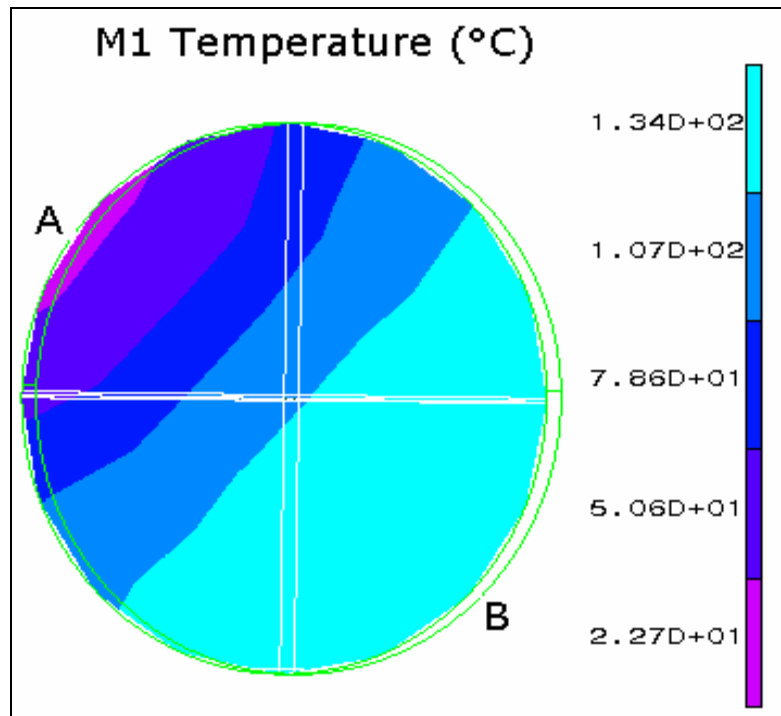


Figure 4-12 : Temperature gradients on the primary mirror

A solution to avoid those multireflexions is to paint in black any devices which could be painted like that. Because of its very low reflectivity and high absorptivity, it is a good way to limit radiative heat transfer.

4.4 ESARAD/ESATAN simulations

4.4.1 Description of the thermal model

4.4.1.1 Geometry

For each simulation on ESARAD, the geometric model is quite the same.

The geometrical model is composed by 12 parts, which can be grouped in 5 “super-parts”:

- The heat shield
- The satellite casing
- The telescope casing
 - The edge 1 telescope casing
 - The edge 2 telescope casing
 - The top telescope casing
 - The bottom telescope casing
 - The front telescope casing
 - The back telescope shield
- The radiators
 - The Heat Stop radiator
 - The Primary mirror radiator
 - The heat shield radiators
- The telescope itself
 - The primary mirror M1
 - The Heat stop

As a very first model, the number of node has been limited to its minimum. So each device is represented by one node on each face, except the satellite casing which is represented by one node on each side of the outer face (6 nodes in total).

So, there is a total of 32 nodes for the geometric model.

Each node is identified as follow:

<i>Device</i>	<i>Node number</i>	<i>Node position</i>
Heat Shield, Side 1	100	Telescope facing
Heat Shield, Side 2	150	Sun facing
Satellite Casing	200, 201, 202, 203, 204, 205	
Edge 2 telescope casing side 1	400	External face

Edge 2 telescope casing side 2	450	Internal face
Edge 1 telescope casing side 1	500	Internal face
Edge 1 telescope casing side 2	550	External face
Top telescope casing side 1	600	Internal face
Top telescope casing side 2	650	External face
Bottom telescope casing side 1	700	External face
Bottom telescope casing side 2	750	Internal face
Front telescope casing side 1	800	Internal face
Front telescope casing side 2	850	External face
Back telescope casing side 1	1000	External face
Back telescope casing side 2	1050	Internal face
Heat Stop radiator side 1	1100	Telescope casing facing
Heat Stop radiator side 2	1150	External face
M1 radiator side 1	1200	Telescope casing face
M1 radiator side 2	1250	External face
M1 side 1	1300	Rear telescope casing facing
M1 side 2	1350	Sun facing
Heat Stop side 1	1400	M1 facing
Heat Stop side 2	1450	Edge 2 telescope casing facing
Heat Shield radiator 1 side 1	1600	Satellite casing facing
Heat Shield radiator 1 side 2	1650	External face
Heat Shield radiator 2 side 1	1500	Satellite casing facing
Heat Shield radiator 2 side 2	1550	External face

Table 4-6 : Nodes definition of the ESARAD model. There is one node per device and per face in order to implement any radiative heat transfer.

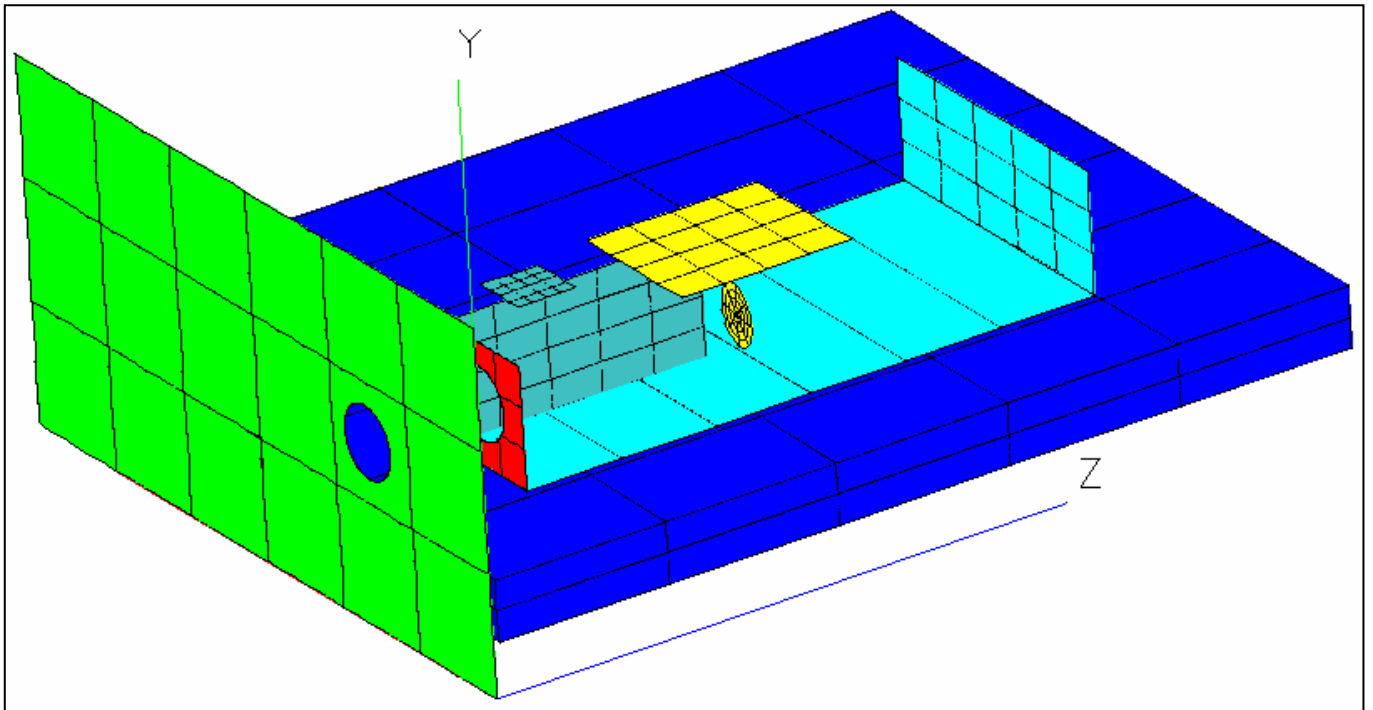


Figure 4-13: A view of the ESARAD geometrical model with the different devices

All the faces, except the inner satellite casing, have been activated to study the different impacts of coatings.

4.4.1.2 Finite element mesh

Like The IDEAS-TMG software, ESARAD/ESATAN uses a finite difference method to solve the temperature distribution in the model. For this to be implemented, the model has to be divided into a network of elements.

Nevertheless, the meshing technique is really simple with this software. Because ESARAD only computes the radiation exchange between the different surfaces, the mesh which is defined doesn't have any thickness and has a square shape. For each surface, the user defines the number of nodes in each direction. Because this model is a

basic one and because the radiative exchanges have generally the same value on each point of the same surface (any surface is less than 0.1 m^2), all the elements of a same surface have been merged into one “super-element”. By doing that, it is possible to decrease the computation time while having good results.

4.4.1.3 Materials

Thermo-optical properties:

Material	ε	ρ_{diffuse}	ρ_{specular}	τ	α	ρ_{diffuse}	ρ_{specular}	τ
MLI	0.012	0.0	0.988	0.0	0.2	0.0	0.8	0.0
Black paint	0.874	0.126	0.0	0.0	0.975	0.025	0.0	0.0
Gold coating	0.02	0.98	0.0	0.0	0.19	0.81	0.0	0.0
Heat shield coating	0.012	0.988	0.0	0.0	0.2	0.8	0.0	0.0
White paint	0.89	0.11	0.0	0.0	0.19	0.81	0.0	0.0
Teflon	0.88	0.0	0.12	0.0	0.09	0.0	0.91	0.0
Aluminium	0.26	0.69	0.0	0.05	0.8	0.15	0.0	0.05
M1_coating	0.8	0.2	0.0	0.0	0.1	0.9	0.0	0.0

Table 4-7 : Thermo-optical properties of the different materials and coatings applied on the model developed under ESARAD/ESATAN

Materials applied on the devices:

<i>device</i>	<i>Side 1</i>	<i>Side 2</i>
Heat shield	Heat shield coating	Heat shield coating
Radiator M1	Black paint	Teflon coating
Radiator Heat stop	Black paint	Teflon coating
Satellite Casing	MLI	
M1	M1_coating	M1_coating
Heat Stop	Aluminium	Aluminium
Telescope Casing	MLI	Black paint
Back telescope casing	White paint	Black paint

Table 4-8 : List of materials applied on each part of the telescope.

Other physical properties:

Parameter	Parameter name	value
Orbit period	PERIOD	1.296E+007 s (=150 days)
CFRP conductivity	kCfrp	50 W/(m.K)
Heat stop – Heat stop radiator metric conductance	kRad2	0.5 to 5000 W.m/K
M1 – M1 radiator metric conductance	kRad3	0.5 to 5000 W.m/K
Radiator conductivity	kRad1	20 W/(m.K)
M1 conductivity	kMir	190 W/(m.K)
Heat stop conductivity	kHstop	190 W/(m.K)
Heat shield conductivity		0.5 to 5000 W/(m.K)
Contact conductance between each side of the telescope casing	kContact1	10000 W/(m2.K)
Contact conductance between the heat shield and the satellite casing	kContact2	0.5 to 5000 W/(m2.K)
M1 radiator area		0.39 m ²
Heat Stop radiator area		0.01 m ²
Heat shield radiator area (only after simulation S303)		1.92 m ²

Table 4-9 : Values of the different parameters used in ESARAD or ESATAN to obtain different simulations

4.4.2 Heat loads

4.4.2.1 The radiative case

Usually, the radiative case is used to describe the radiative heat loads applied on the object either in steady-state or transient case.

Because it is not possible to compute, with the version of ESARAD (V5), an orbit which is both sun-centered and sun oriented, the radiative case developed here does not represent the heat load variation on the spacecraft but just a way to calculate view factors and radiative conductance in the model.

During the entire orbit, SOLO will be a sun-oriented spacecraft. That means that, at any time, the view factor between the sun and each elements (and also between elements) of the satellite are exactly the same. So, ESARAD has been used to compute at one known position the different view factors and the radiative links between those elements.

The heat load in a sun centered and sun-oriented elliptic orbit is only a function of time. By using the Kepler's equation the heat load can be calculated for each day and then applied to the heat shield and the mirror. This heat load is exactly the same than the one applied on the I-DEAS model (cf figure 4-2)

This model is quite close to the reality. The main error is due to the difference of diameter between the hole in the heat shield and the diameter of the primary mirror. Because M1 has a diameter of 120 mm and the hole is a 135 mm diameter one, that supposed that the back of the telescope casing has a non-null view factor with the sun. So, the back of the spacecraft should receive a little bit of the sun power, which is not the case in the model.

Appendix D gives the full listing of the program.

4.4.2.2 ESATAN computation

As we mentioned before, the ESARAD simulation gives the radiative link between each element and the Sun heat load on each element for an incoming heat load of 1000 W/m² on the satellite.

Then, those two arrays will be copied in the ESATAN input file and completed with the following information:

- Conductive link between different elements
- Conductive link between the two sides of a same element
- Solar factor arrays.

Appendix E gives the detailed structure of this program.

4.4.3 *Transient results*

Several simulations have been done to study the impact of different parameters:

- The insulation of the heat shield.
- The conductive heat path between the satellite casing and the telescope casing
- The conductive heat path between the heat shield and the satellite casing.
- The thermo optical properties of the primary mirror.

Table 4-10 presents the different simulations and the evolution of each parameter for those simulations.

Simulation #	Internal heat shield conductance	Conductance between the heat shield and the satellite casing	Conductance between the satellite casing and the telescope casing	Heat shield connected to the M1 radiator	Heat shield connected to specific radiators	M1 absorptivity
S50	0.5	5000	5000	NO	NO	0.1
S51	<u>5</u>	5000	5000	NO	NO	0.1
S52	<u>50</u>	5000	5000	NO	NO	0.1
S53	<u>500</u>	5000	5000	NO	NO	0.1
S54	<u>5000</u>	5000	5000	NO	NO	0.1
S100 = S50	<u>0.5</u>	5000	5000	NO	NO	0.1
S101	0.5	<u>500</u>	5000	NO	NO	0.1
S102	<u>5</u>	500	5000	NO	NO	0.1
S103	<u>0.5</u>	<u>50</u>	5000	NO	NO	0.1
S104	<u>5</u>	50	5000	NO	NO	0.1
<i>S105</i>	5	<u>0.5</u>	5000	NO	NO	0.1
S106	5	<u>5</u>	5000	NO	NO	0.1
S150 = S101	<u>0.5</u>	<u>500</u>	5000	NO	NO	0.1
<i>S151</i>	0.5	500	<u>500</u>	NO	NO	0.1
S152	<u>5</u>	500	500	NO	NO	0.1
S153	<u>0.5</u>	500	500	<u>50W/K</u>	NO	0.1
S154	0.5	500	<u>5</u>	<u>50W/K</u>	NO	0.1
S303	0.5	<u>5000</u>	<u>5000</u>	<u>NO</u>	<u>250W/K</u>	0.1
S304	0.5	5000	5000	NO	<u>50W/K</u>	0.1
S305	0.5	5000	<u>500</u>	NO	50W/K	0.1
S306	0.5	<u>500</u>	500	NO	50W/K	0.1
S307	<u>5</u>	500	<u>500</u>	NO	50W/K	0.1
S308	5	500	<u>0.5</u>	NO	50W/K	0.1
S1000 = S306	<u>0.5</u>	500	500	NO	50W/K	0.1
S1001(model6)	0.5	500	500	NO	50W/K	<u>0.4</u>
S1002	0.5	500	500	NO	50W/K	<u>0.8</u>

Table 4-10 : summary of the different simulations done with ESARAD/ESATAN. Those in bold and italic stopped before the end because one of the temperature device (generally the heat shield) could'nt converge. The parameters which has been modified for each simulation is underlined.

It appears that the results are not exactly the same than for the I-DEAS simulations. However, they are not very far and they are also consistent with it. They are different because the heat paths are not the same (there is no conductive heat path between the heat shield and the telescope casing and also between the telescope casing and the satellite casing in the I-DEAS model) and the geometry of the model are not also exactly the same (there are no satellite casing in the I-DEAS model and so the bottom space of the telescope casing is like a radiator, which could explain the low temperature obtained sometimes).

4.4.3.1 Sensitivity of the model to the insulation of the heat shield

Because the heat shield is directly seeing the sun it will have to withstand the sun heat load during all the life of the probe. Moreover, because there is a view factor between the heat shield and the rest of the spacecraft (in particularly the telescope casing and the mirror radiator), the temperature of the shield has a direct impact on the temperature of the mirror.

Even with a very high reflective coating (such as a Multi Layer Insulation), it is running very hot. What has been tried in the following simulation is to insulate the face facing the satellite from the face facing the sun. By doing that, it should be possible to decrease the temperature of the internal face of the heat shield and so decrease the radiative conductance between the heat shield and the radiator.

In simulations S50 to S54, the conductivity between each face has been increase progressively to study the impact on M1. Figure 4-14 shows the results of those simulations. S53 and S54 have not been drawn because their results were the same than S52.

As one can see, the effect of insulating one face to another on the heat shield has a really big impact on M1 temperature. It seems obvious that the insulation on the heat shield has to be as efficient as possible. Nevertheless, this insulation has also an impact on the temperature of the heat shield. On those simulations, it is not linked to any radiators, and so its temperature can be very hot (more than 1200 °C for the face facing the sun and 500 °C for the other side during simulation S50).

So, it seems reasonable to reduce as much as possible the conductance through the thickness of the heat shield, but this fact suppose that the heat shield can be cooled through specific radiators.

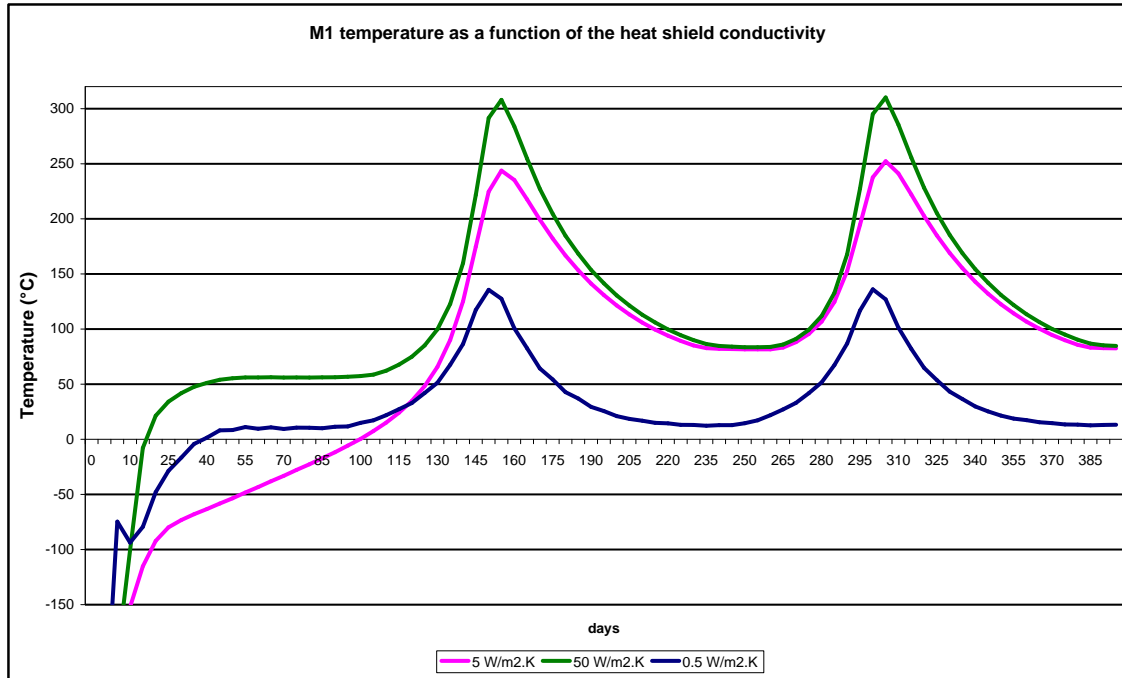


Figure 4-14 : M1 temperature variations for different values of the heat shield conductivity.

4.4.3.2 Sensibility of the model to the conductance between the satellite casing and the heat shield

As we said in the previous paragraph, the heat shield has to be cooled by any way in order to decrease its temperature. One way would be to insure a good heat path between the satellite casing and the heat shield. Nevertheless, because of the very severe thermal condition, this conductance could be seriously damaged in the time. Figure 4-15 presents the results of M1 temperature with respect to the conductance between the heat shield and the satellite casing (the conductance through the heat shield has been modified in one simulation also).

In those simulations, it seems that the heat path between this heat shield and the telescope casing doesn't have a real impact on M1, but in the same time the temperature of the heat shield is increasing a lot. For instance, if the conductivity between the heat shield and satellite casing is below 50W/m2.K, the simulation can not be solved because the temperature on the heat shield diverge (more than 1.0E10 °C !!!).

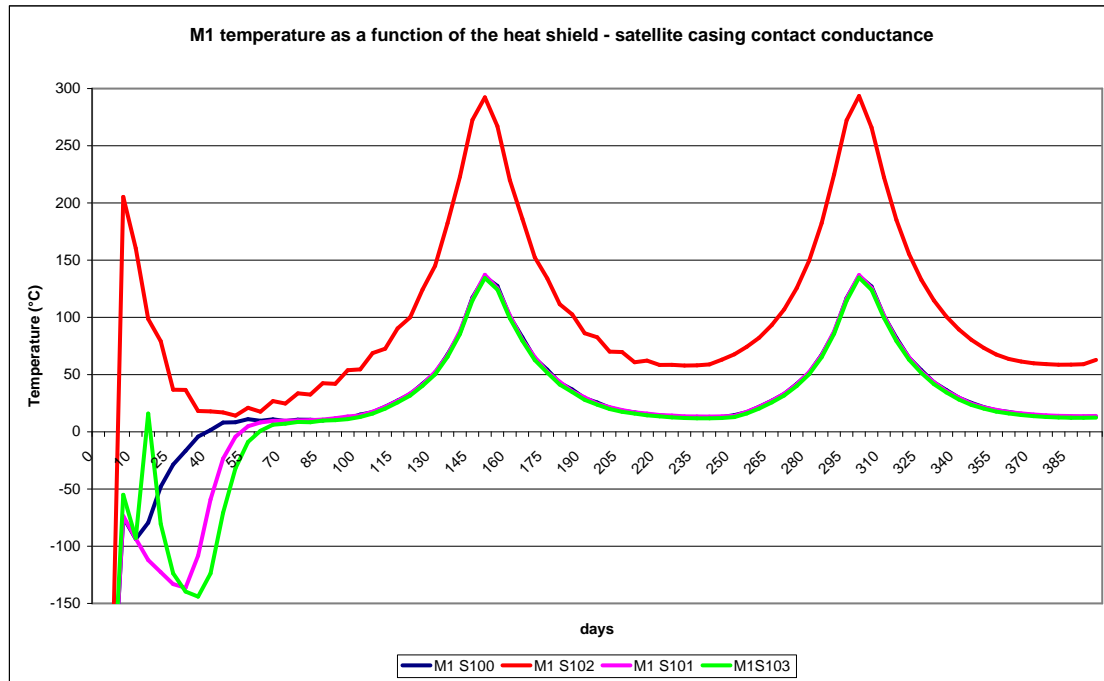


Figure 4-15 : M1 temperature variations with different values of the contact conductance between the heat shield and the satellite casing.

Once again, that means that the heat shield has to be carefully cooled.

4.4.3.3 Sensibility of the model to the conductance between the satellite casing and the telescope casing

Because the heat shield will use the satellite casing to cool its temperature (by putting radiator on its side for instance) it is also essential to limit any conductive heat path between this one and the telescope. A way to do so is to decrease (by putting a thermal blanket for instance) the conductance between the telescope casing and the satellite casing.

Figure 4-16 presents some of the results which have been obtained by modifying this conductance and also some other parameters.

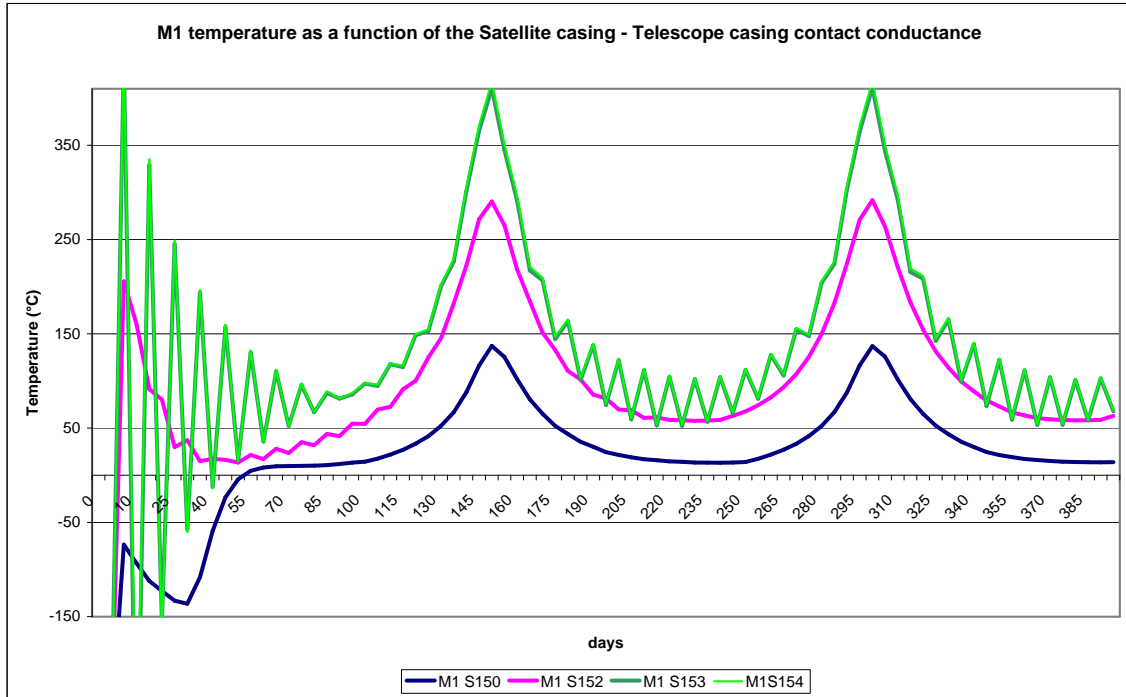


Figure 4-16 : M1 temperature variations with different values of the contact conductance between the telescope casing and the satellite casing.

Once again, because the heat shield is very hot, it is not possible to detach (on a thermal point of view) the satellite casing from the telescope casing while having a very low conductance through the thickness of the heat shield.

The only possibility is to link it to a radiator. This is what has been done in simulation 153 and 154. The heat shield is linked to the primary mirror radiator. Because the heat shield is too hot, the radiator is too small to evacuate the heat load which is coming both from the mirror and the heat shield and so the temperature of the mirror is very high. Oscillations that occur in simulation S154 are due to the very high temperature which are reached and make the simulation unstable for the ESATAN solver.

4.4.3.4 M1 temperature with specific radiators attached to the heat shield.

In those simulations, two radiators have been added to cool the heat shield. The total radiator area dedicated to the heat shield is 1.92 m^2 .

Figure 4-17 presents the temperature evolution of M1 with those two radiators linked to the heat shield. Different configurations have been tried to find the best strategy.

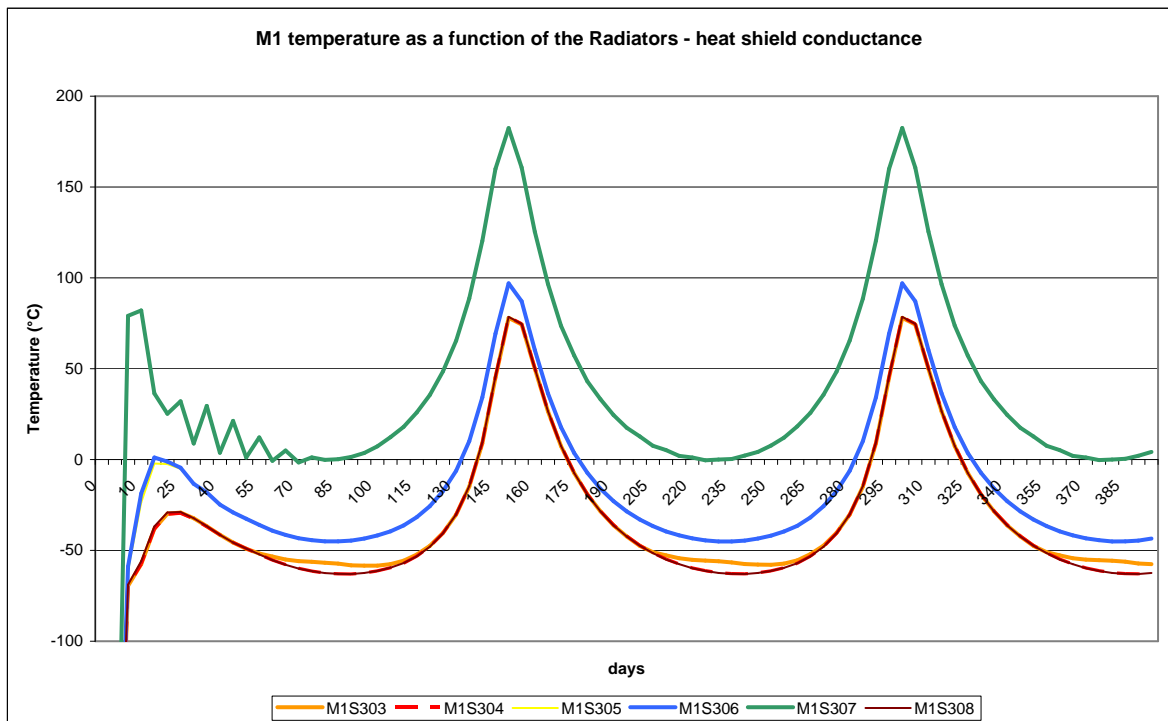


Figure 4-17 : M1 temperature variations with different values of the conductivity between the heat shield and its radiators.

As one can see there, this solution really improves the temperature on M1 (it also decreases the temperature on the heat shield to 200-300 °C instead of 1200°C or more !!)

In S303, S304, S305, S306 and S308 the conductivity through the heat shield is $0.5\text{W/m}^2\cdot\text{K}$. Modifying the other parameter has a relatively low impact on the temperature (S303, S304 and S308 gives the same value for M1 temperature).

If now, this conductivity is increased to $5\text{W/m}^2\cdot\text{K}$, this temperature obviously increase but is still “low” compare to the results obtained in the previous paragraphs.

4.4.3.5 Influence of M1 absorptivity

Three different values of absorptivity for M1 have been tried.

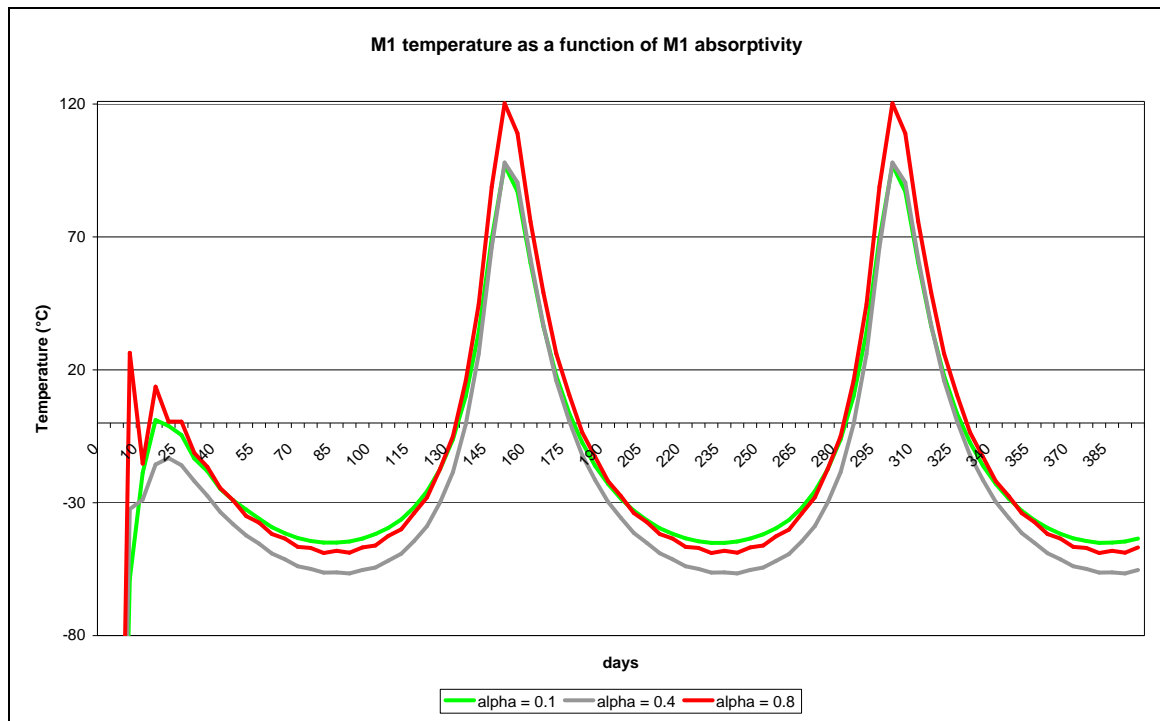


Figure 4-18 : Influence of M1 absorptivity on M1 temperature

As one can see in Figure 4-19, the temperature range is obviously different but in relatively small proportions (those results seem to validate those found with I-DEAS). When the absorptivity of M1 is increased, the temperature of the mirror is almost the same, but its range is slightly extended.

Table 4-11 gives the exact values of the maximum and minimum temperatures on M1 for each case.

M1 absorptivity	M1 Max temperature (°C)	M1 Min temperature (°C)
0.1	98	-45
0.4	92	-56.6
0.8	120.3	-48.8

Table 4-11 : M1 temperature extremums as a function of its absorptivity

The effect of increasing the absorptivity of M1 is to increase its thermal inertia and so make its temperature oscillating more. Moreover, if the absorptivity increases a lot ($\alpha = 0.8$), the maximum temperature will also be higher and so it will be more difficult to control it.

So the absorptivity of the multilayer coating applied on M1 has to be as much reflective as possible.

5. Conclusion

5.1 Further work

In order to continue the thermal design of the Solar Orbiter, several things need to be finished.

First of all, it is necessary to modify in the I-DEAS and ESARAD models the size of the entrance aperture on the heat shield and the telescope casing and also the size of the primary mirror. They were in this report respectively 120 mm and 100 mm diameters and they should be respectively 135 mm and 120 mm diameters. As it has been mentioned previously, those changes came at the end of the study and so could not have been updated on time. Even if the values of the different heat flows are different, this should not modify the general thermal control strategy.

Then it would be useful to make a feasibility study of some active control devices such as thermal switches, variable conductance heat pipes and louvers. The two last one already exist and have been used previously on satellite. Nevertheless, because of the very severe thermal environment SOLO will have to face, the reliability of such components has to be tested carefully.

Next point is to look at the temperature gradients on the mirror. In the example showed in the report the gradient is maximal because of the MLI which covers the telescope casing. It is necessary to do the same simulation with other coatings (the black paint for instance should minimise the radiative heat path between elements and so decrease the temperature gradient) and to check that this gradient does not create any deformation on the mirrors.

Last point is to make a parametric study of the mirror radiator area in order to optimise it. In this report, the radiator area is the one given by the preliminary thermal analysis, but this value is rough.

5.2 Conclusion

During this MSc research project, the detailed transient thermal analysis which has been done shows that the spectrometer and its components need a thermal control strategy to stay in the allowable temperature range. After several simulations, the off-axis design seems feasible from a thermal point of view provided that:

- the heat shield is conductively isolated and its conductance through its thickness is also minimised (by using Multi Layers Insulation for instance)
- the required thermo-optical properties (alpha and epsilon) are achieved on the heat shield at the elevated temperatures during all the life-time of the solar probe
- the required radiator area is accommodated
- the necessary thermal links are provided between the M1 mirror and its radiator

As it has been said before, there is still some analysis and design to do, especially for the thermal control devices selection and the radiator area optimization.

6. Bibliography

Larson W.J. and J.T. Wertz. *Space Mission Analysis and Design*. Microcosm Press. 3rd ed ElSegundo. CA. 1999

Gilmore D.G. *Satellite thermal Control Handbook*. The Aerospace Corporation Press. El Segundo. CA. 1994

Escudier B and Pouillard J-Y. *Mecanique Spatiale*. SupAero, Departement systeme spatiaux, 1998

Solar Orbiter Website.

<http://solarsystem.estec.esa.nl> (Projects/Under Development) (Accessed 21th August 2002)

K&K Associates, Thermal Connection.

<http://www.tak2000.com/data2.htm#surffin> (Accessed 21th August 2002)

Appendix A :
Thermo-Optical properties of some thermal
control coatings
(Courtesy of K&K Associates, Thermal Connection)

a= solar absorptivity

e= normal emittance

ESH=equivalent Sun Hours

Coating thickness is usually critical

NAME BLACK COATINGS	SOLAR a	NORMAL e	Ratio a/e
Anodize Black	0.88	0.88	1.00
Carbon Black Paint NS-7	0.96	0.88	1.09
Catalac Black Paint	0.96	0.88	1.09
Chemglaze Black Paint Z306	0.96	0.91	1.05
Delrin Black Plastic	0.96	0.87	1.10
Ebanol C Black	0.97	0.73	1.33
Ebanol C Black-384 ESH* UV	0.97	0.75	1.29
GSFC Black Silicate MS-94	0.96	0.89	1.08
GSFC Black Paint 313-1	0.96	0.86	1.12
Hughson Black Paint H322	0.96	0.86	1.12
Hughson Black Paint L-300	0.95	0.84	1.13
Martin Black Paint N-150-1	0.94	0.94	1.00
Martin Black Velvet Paint	0.91	0.94	0.97
3M Black Velvet Paint	0.97	0.91	1.07
Paladin Black Lacquer	0.95	0.75	1.27
Parsons Black Paint	0.98	0.91	1.08
Polyethylene Black Plastic	0.93	0.92	1.01
Pyramil Black on Beryllium Copper	0.92	0.72	1.28
Tedlar Black Plastic	0.94	0.90	1.04
Velesat Black Plastic	0.96	0.85	1.13

WHITE COATINGS	a	e	a/e
Barium Sulphate with Polyvinyl Alcohol	0.06	0.88	0.07
Biphenyl-White Solid	0.23	0.86	0.27
Catalac White Paint	0.24	0.90	0.27
Dupont Lucite Acrylic Lacquer	0.35	0.90	0.39
Dow Corning White Paint DC-007	0.19	0.88	0.22
GSFC White Paint NS43-C	0.20	0.92	0.22
GSFC White Paint NS44-B	0.34	0.91	0.37
GSFC White Paint NS-74	0.17	0.92	0.18
GSFC White Paint NS-37	0.36	0.91	0.40
Hughson White Paint A-276	0.26	0.88	0.30
Hughson White Paint A-276+1036 ESH UV	0.44	0.88	0.50
Hughson White Paint V-200	0.26	0.89	0.29
Hughson White Paint Z-202	0.25	0.87	0.29
Hughson White Paint Z-202+1000 ESH UV	0.40	0.87	0.46
Hughson White Paint Z-255	0.25	0.89	0.28
Mautz White House Paint	0.30	0.90	0.33
3M-401 White Paint	0.25	0.91	0.27
Magnesium Oxide White Paint	0.09	0.90	0.10
Magnesium Oxide Aluminium Oxide Paint	0.09	0.92	0.10

Opal Glass	0.28	0.87	0.32
OSO-H White Paint 63W	0.27	0.83	0.33
P764-1A White Paint	0.23	0.92	0.25
Potassiuml Fluorotitanate White Paint	0.15	0.88	0.17
Sherwin Williams White Paint (A8W11)	0.28	0.87	0.32
Sherwin Williams White Paint (F8WJ2030)	0.39	0.82	0.48
Sherwin Williams F8W2030 w Polasol V6V241	0.36	0.87	0.41
Sperex White Paint	0.34	0.85	0.40
Tedlar White Plastic	0.39	0.87	0.45
Titanium Oxide White Paint with Methyl Silicone	0.20	0.90	0.22
Titanium Oxide White Paint with Potassium Silicate	0.17	0.92	0.18
Zerlauts S-13G White Paint	0.20	0.90	0.22
Zerlauts Z-93 White Paint	0.17	0.92	0.18
Zinc Orthotitanate with Potassium Silicate	0.13	0.92	0.14
Zinc Oxide with Sodium Silicate	0.15	0.92	0.16
Zirconium Oxide with 650 Glass Resin	0.23	0.88	0.26

CONDUCTIVE PAINT

	a	e	a/e
Brilliant Aluminum Paint	0.30	0.31	0.97
Epoxy Aluminum Paint	0.77	0.81	0.95
Finch Aluminum Paint 643-1-1	0.22	0.23	0.96
Leafing Aluminum in Epon 828	0.37	0.36	1.03
Leafing Aluminum (80-U)	0.29	0.32	0.91
NRL Leafing Aluminum Paint	0.24	0.24	1.00
NRL Leafing Aluminum Paint	0.28	0.29	0.97
Silicone Aluminum Paint	0.29	0.30	0.97
Dupont Silver Paint 4817	0.43	0.49	0.88
Chromeric Silver Paint 586	0.30	0.30	1.00
GSFC Yellow NS-43-G	0.38	0.90	0.42
GSFC Green NS-53-B	0.52	0.87	0.60
GSFC Green NS-43-E	0.57	0.89	0.64
GSFC White NS-43-C	0.20	0.92	0.22
GSFC Green NS-55-F	0.57	0.91	0.63
GSFC Green NS-79	0.57	0.91	0.63

ANODIZED ALUMINUM SAMPLES

	a	e	a/e
Black	0.65	0.82	0.79
Black	0.86	0.86	1.00
Blue	0.67	0.87	0.77
Blue	0.53	0.82	0.65
Brown	0.73	0.86	0.85
Chromic	0.44	0.56	0.79
Clear	0.27	0.76	0.36
Clear	0.35	0.84	0.42
Green	0.66	0.88	0.75
Gold	0.48	0.82	0.59
Plain	0.26	0.04	6.50
Red	0.57	0.88	0.65

Sulphuric	0.42	0.87	0.48
Yellow	0.47	0.87	0.54
Blue Anodized Titanium 1 Foil	0.70	0.13	5.38

**METALS AND
CONVERSION COATINGS**

	a	e	a/e
<hr/>			
Alzac A-2	0.16	0.73	0.22
Alzac A-5	0.18	-	
Black Chrome	0.96	0.62	1.55
Black Copper	0.98	0.63	1.56
Black Irridite	0.62	0.17	3.65
Black Nickel	0.91	0.66	1.38
Buffed Aluminum	0.16	0.03	5.33
Buffed Copper	0.30	0.03	10.00
Constantan-Metal Strip	0.37	0.09	4.11
Copper Foil Tape			
Plain	0.32	0.02	16.00
Sanded	0.26	0.04	6.50
Tarnished	0.55	0.04	13.75
Dow 7 on Polished Magnesium	0.49	-	
Dow 7 on Sanded Magnesium	0.65	-	
Dow 9 on Magnesium	0.87	-	
Dow 23 on Magnesium	0.62	0.67	0.93
Ebanol C Black	0.97	0.77	1.26
Electroplated Gold	0.23	0.03	7.67
Electroless Nickel	0.39	0.07	5.57
Irridite Aluminum	-	0.11	
Inconel X Foil (1 mil)	0.52	0.10	5.20
Kannigen-Nickel Alloy	0.45	0.08	5.63
Plain Beryllium Copper	0.31	0.03	10.33
Platinum Foil	0.33	0.04	8.25
Stainless Steel			
Polished	0.42	0.11	3.82
Machined	0.47	0.14	3.36
Sandblasted	0.58	0.38	1.53
Machine Rolled	0.39	0.11	3.55
Boom-Polished	0.44	0.10	4.40
1-mil 304 Foil	0.40	0.05	8.00
Tantalum Foil	0.40	0.05	8.00
Tungsten Polished	0.44	0.03	14.67

VAPOR DEPOSITED COATINGS

	a	e	a/e
<hr/>			
Aluminum	0.08	0.02	4.00
Aluminum on Fiberglass	0.15	0.07	2.14
Aluminum on Stainless Steel	0.08	0.02	4.00
Chromium	0.56	0.17	3.29
Chromium on 5-mil Kapton	0.57	0.24	2.38
Germanium	0.52	0.09	5.78
Gold	0.19	0.02	9.50
Iron Oxide	0.85	0.56	1.52

Molybdenum	0.56	0.21	2.67
Nickel	0.38	0.04	9.50
Rhodium	0.18	0.03	6.00
Sliver	0.04	0.02	2.00
Titanium	0.52	0.12	4.33
Tungsten	0.60	0.27	2.22

Spacecraft Solar Arrays	a	e	a/e
AE	0.78	0.82	0.95
AMSAT	0.82	0.85	0.96
ATN Black	0.77	0.80	0.96
ATN Blue	0.86	0.85	1.01
ATSF	0.85	0.85	1.00
COMSAT	0.82	0.85	0.96
DE	0.77	0.81	0.95
ETS/GOES	0.82	0.80	1.02
GOES	0.91	0.81	1.12
GPS-Conductive Coating	0.81	0.80	1.01
HELIOS	0.80	0.82	0.98
IME-Conductive Coating	0.75	0.79	0.95
IMP-H	0.78	0.82	0.95
IMP-I	0.78	0.81	0.96
ISEE-Conductive Coating	0.91	0.79	1.15
IUE	0.86	0.84	1.02
OA0	0.85	0.81	1.05
PAC	0.77	0.81	0.95
SMS-B	0.81	0.80	1.01
Spanish INTASAT	0.86	0.86	1.00
SSS	0.79	0.82	0.96

MISC	a	e	a/e
Aluminum Oxide (Al ₂ O ₃)-(12/4) on Buffed Alum			
Initial	0.13	0.23	0.57
2560 ESH UV + P+	0.13	0.23	0.57
Aluminum Oxide(Al ₂ O ₃)(12/4) on Fused Silica	0.12	0.24	0.50
Silver Beryllium Copper (AgBeCu)	0.19	0.03	6.33
Kapton Overcoating	0.31	0.57	0.54
Parylene C Overcoating	0.22	0.34	0.65
Teflon Overcoating	0.12	0.38	0.32
GSFC DArk Mirror Coating-SiO-Cr-Al	0.86	0.04	21.50
GSFC Composite SiO _x -Al ₂ O ₃ -Ag	0.07	0.68	0.10
Helios Second Surface Mirror/Silver Backing			
Initial	0.07	0.79	0.09
24 Hours at 5 Suns	0.07	0.80	0.09
48 Hours at 11 Suns + P+	0.08	0.79	0.10
Inconel with Teflon Overcoating-1mil	0.55	0.46	1.20
Vespel Polyimide SP1	0.89	0.90	0.99
Aclar Film (Aluminum Backing)			
1 mil	0.12	0.45	0.27
2 mil	0.11	0.62	0.18

5 mil	0.11	0.73	0.15
Kapton Film (Aluminum Backing)			
0.08 mil	0.23	0.24	0.96
0.15 mil	0.25	0.34	0.74
0.25 mil	0.31	0.45	0.69
0.50 mil	0.34	0.55	0.62
1.0 mil	0.38	0.67	0.57
1.5 mil	0.40	0.71	0.56
2.0 mil	0.41	0.75	0.55
3.0 mil	0.45	0.82	0.55
5.0 mil	0.46	0.86	0.53
Kapton Film (Chromium-Silicon Oxide-Aluminum Backing (Green))			
1.0 mil	0.79	0.78	1.01
Kapton Film (Aluminum-Aluminum Oxide Overcoating)-1 mil			
Initial	0.12	0.20	0.60
1800 ESH UV	0.12	0.20	0.60
Kapton Film (Aluminum-Silicon Oxide Overcoating)-1 mil			
Initial	0.11	0.33	0.33
2400 ESH UV	0.22	0.33	0.67
Kapton Film (Silver-Aluminum Oxide Overcoating)-1 mil			
Initial	0.08	0.19	0.42
2400 ESH UV	0.08	0.21	0.38
Kapton Film (Aluminum-Silicon Oxide Overcoating)-0.5 mil			
Initial	0.12	0.18	0.67
4000 ESH UV	0.28	0.24	1.17
Kimfoil-Polycarbonate Film (Aluminum Backing)			
0.08 mil	0.19	0.23	0.83
0.20 mil	0.20	0.30	0.67
0.24 mil	0.17	0.28	0.61
Mylar Film			
Aluminum Backing			
0.15 mil	0.14	0.28	0.50
0.25 mil	0.15	0.34	0.44
3.0 mil	0.17	0.76	0.22
5.0 mil	0.19	0.77	0.25
Skylab Sail			
Initial	0.15	0.35	0.43
1900 ESH UV	0.19	0.36	0.53
Skylab Parasol Fabric (Orange)			
Initial	0.51	0.86	0.59
2400 ESH UV	0.65	0.86	0.76
Teflon (Gold Backing)			
0.5 mil	0.30	0.49	0.61
1.0 mil	0.26	0.58	0.45
Teflon Aluminum Backing			
2 mil	0.08	0.66	0.12
5 mil	0.13	0.81	0.16
10 mil	0.13	0.87	0.15
Gold Backing			
0.5 mil	0.24	0.43	0.56
1.0 mil	0.22	0.52	0.42
5.0 mil	0.22	0.81	0.27
10 mil	0.23	0.82	0.28

Silver Backing			
2 mil	0.08	0.68	0.12
5 mil	0.08	0.81	0.10
10 mil	0.09	0.88	0.10
Tefzel (Gold Backing)			
0.05 mil	0.29	0.47	0.62
1.0 mil	0.26	0.61	0.43

Tapes	a	e	a/e
-----	-----	-----	-----
235-3M Black	0.95	0.90	1.06
425-3M Aluminum Foil	0.20	0.03	6.67
850-3M Mylar-Aluminum Backing	0.15	0.59	0.25
7361-Mystic Alummized Kapton	0.09	0.03	3.00
7452- Mystic Aluminum Foil	0.14	0.03	4.67
7800-Mystic Aluminum Foil	0.21	0.03	7.00
Y9360-3M Aluminized Mylar	0.19	0.03	6.33

Appendix B :
Excel calculation spreadsheets and results
of the preliminary thermal analysis

Entrance area (cm ²)	12.25	Grazing Incidence Telescope preliminary thermal analysis (entrance aperture : 35 x 35 mm)	
Incident flux on the telescope (W)	41.34		
M1 incidence (°)	74.00		
M1 inclined area (cm ²)	44.26		
M1 effective area (cm ²)	12.20	M1 absorptivity	0.80
M2 incidence (°)	78.00	M2 absorptivity	0.80
M2 inclined area (cm ²)	30.00	rastering mirror absorptivity	0.20
M2 effective area (cm ²)	6.24	total heat absorption on M1 (W)	32.94
rastering mirror incidence (°)	81.00	total heat absorption on M2 (W)	6.26
rastering mirror inclined area (cm ²)	32.50	total heat absorption on rastering mirror (W)	0.03
rastering mirror effective area (cm ²)	5.08	heat load coming from the rastering mirror to the slit (W)	0.13
M1 reflectivity	0.200	M1 temperature without radiator (°C)	1242.19
M2 reflectivity	0.200	M2 temperature without radiator (°C)	969.88
rastering mirror reflectivity	0.800	Rastering mirror temperature without radiator (°C)	191.93
heat load on M1 (W)	41.18	M1 Radiator temperature (°C)	50
Flux density on M1 (W/cm ²)	0.93	M1 Temperature (°C)	61
absorbed flux density on M1 (W/cm ²)	0.74	M1 radiator absorptivity	0.1
heat load coming from M1 to M2 (W)	8.24	M1 radiator area if no absorption (m ²)	0.0590
% of flux received by M2	95	M1 radiator area if absorption (m ²)	0.1504
heat load on M2 (W)	7.82	M2 Radiator temperature (°C)	50
Flux density on M2 (W/cm ²)	0.26	M2 Temperature (°C)	61
absorbed flux density on M2 (W/cm ²)	0.21	M2 radiator absorptivity	0.1
heat load coming from M2 to rastering (W)	1.56	M2 radiator area if no absorption (m ²)	0.0111
% of flux received by the rastering	10	M2 radiator area if absorption (m ²)	0.0283
heat load on rastering mirror (W)	0.16	Rastering mirror Radiator temperature (°C)	50
Flux density on rastering mirror (W/cm ²)	0.00	Rastering mirror Temperature (°C)	61
absorbed flux density on rastering mirror	0.0010	Rastering mirror radiator absorptivity	0.1
M1 radiator emissivity	0.9	Rastering mirror radiator area if no absorption (m ²)	-0.0004604
M2 radiator emissivity	0.9	Rastering mirror radiator area if absorption (m ²)	-0.0011733
% of the M2 radiator seeing the sun	10.00	% of the radiator seeing the sun	10.00
Rastering mirror radiator emissivity	0.9	Total radiator area (m²)	0.0696
% of the rastering radiator seeing the sun	10.00	Total radiator area (m²) if absorption	0.1775

M1 coating	Silicon-Carbon 1	Silicon-Carbon 1	Silicon-Carbon 1	Silicon-Carbon 1	Gold	Gold
M2 coating	Silicon-Carbon 1	Gold	Platinum	Silicon-Carbon 2	Silicon-Carbon 1	Gold
M1 absorptivity	0.10	0.10	0.10	0.10	0.20	0.20
M2 absorptivity	0.10	0.20	0.40	0.80	0.10	0.20
rastering mirror absorptivity	0.20	0.20	0.20	0.20	0.20	0.20
total heat absorption on M1 (W)	4.12	4.12	4.12	4.12	8.24	8.24
total heat absorption on M2 (W)	3.52	7.04	14.08	28.16	3.13	6.26
total heat absorption on rastering mirror (W)	0.63	0.56	0.42	0.14	0.56	0.50
heat load coming from the rastering to the slit (W)	2.53	2.25	1.69	0.56	2.25	2.00
Total radiator area (m2)	0.0123	0.0186	0.0311	0.0563	0.0190	0.0246
Total radiator area (m2) if absorption	0.0313	0.0473	0.0794	0.1435	0.0484	0.0627
M1 coating	Gold	Gold	Platinum	Platinum	Platinum	Platinum
M2 coating	Platinum	Silicon-Carbon 2	Silicon-Carbon 1	Gold	Platinum	Gold
M1 absorptivity	0.20	0.20	0.40	0.40	0.40	0.40
M2 absorptivity	0.40	0.80	0.10	0.20	0.40	0.80
rastering mirror absorptivity	0.20	0.20	0.20	0.20	0.20	0.20
total heat absorption on M1 (W)	8.24	8.24	16.47	16.47	16.47	16.47
total heat absorption on M2 (W)	12.52	25.03	2.35	4.69	9.39	18.78
total heat absorption on rastering mirror (W)	0.38	0.13	0.42	0.38	0.28	0.09
heat load coming from the rastering to the slit	1.50	0.50	1.69	1.50	1.13	0.38
Total radiator area (m2)	0.0358	0.0582	0.0325	0.0367	0.0451	0.0620
Total radiator area (m2) if absorption	0.0913	0.1483	0.0828	0.0935	0.1150	0.1581
M1 coating	Silicon-Carbon 2	Silicon-Carbon 2	Silicon-Carbon 2	Silicon-Carbon 2		
M2 coating	Silicon-Carbon 1	Gold	Platinum	Silicon-Carbon 2		
M1 absorptivity	0.80	0.80	0.80	0.80		
M2 absorptivity	0.10	0.20	0.40	0.80		
rastering mirror absorptivity	0.20	0.20	0.20	0.20		
total heat absorption on M1 (W)	32.94	32.94	32.94	32.94		
total heat absorption on M2 (W)	0.78	1.56	3.13	6.26		
total heat absorption on rastering mirror (W)	0.14	0.13	0.09	0.03		
heat load coming from the rastering to the slit	0.56	0.50	0.38	0.13		
Total radiator area (m2)	0.0594	0.0609	0.0638	0.0696		
Total radiator area (m2) if absorption	0.1515	0.1552	0.1626	0.1775		

Entrance area (cm2) (13.5 cm diameter)	143.13	Two mirrors off-axis Telescope preliminary thermal analysis	
Incident flux on the telescope (W)	483.06		
M1 incidence (°)	7.50		
M1 inclined area (cm2)	113.40		
M1 effective area (cm2)	112.43		
M2 incidence (°)	8.50	M1 absorptivity	0.10
M2 inclined area (cm2)	3.14	heat stop absorptivity	0.20
M2 effective area (cm2)	3.11	heat stop transmissivity	0.05
Heat stop incidence	0.00	M2 absorptivity	0.20
heat stop inclined area (cm2)	132.00	total heat absorption on M1 (W)	37.95
heat stop effective area (cm2)	132.00	total heat absorption on heat stop (W)	68.30
		total heat absorption on M2 (W)	3.41506
M1 reflectivity	0.900	heat load coming from M2 to the slit (W)	13.66
M2 reflectivity	0.800	M1 temperature without radiator (°C)	507.12
heat stop reflectivity	0.750	Heat stop temperature without radiator (°C)	624.50
		M2 temperature without radiator (°C)	701.69
heat load on M1 (W)	379.45	M1 Radiator temperature (°C)	◀ ◻ ▶
Flux density on M1 (W/cm2)	3.35	M1 Temperature (°C)	◀ ◻ ▶
absorbed flux density on M1 (W/cm2)	0.33	M1 radiator absorptivity	0.1
heat load coming from M1 to heat stop (W)	341.51	M1 radiator area if no absorption (m2)	0.0555
% of flux received by heat stop	100	M1 radiator area if absorption (m2)	0.1413
heat load on heat stop (W)	341.51	Heat stop Radiator temperature (°C)	◀ ◻ ▶
absorbed heat on heat stop (W)	68.30	Heat stop Temperature (°C)	◀ ◻ ▶
rejected heat to space	256.13	Heat stop radiator absorptivity	0.1
heat load coming from heat stop to M2 (W)	17.08	Heat stop area if no absorption (m2)	0.1096
% of flux received by M2	100	Heat stop radiator area if absorption (m2)	0.2792
heat load on M2 (W)	17.08	M2 Radiator temperature (°C)	◀ ◻ ▶
Flux density on M2 (W/cm2)	5.44	M2 Temperature (°C)	◀ ◻ ▶
absorbed flux density on M2 (W/cm2)	1.0876	M2 radiator absorptivity	0.1
		M2 radiator area if no absorption (m2)	0.0058328
		M2 radiator area if absorption (m2)	0.0148655
M1 radiator emissivity	0.9		
heat stop radiator emissivity	0.9		
% of the heat stop radiator seeing the sun	10.00	% of the radiator seeing the sun	10.00
M2 radiator emissivity	0.9		
% of the M2 radiator seeing the sun	10.00		
		Total radiator area (m2)	0.1708
		Total radiator area (m2) if absorption	0.4354

M1 coating	Silicon-Carbon 1	Silicon-Carbon 1	Silicon-Carbon 1	Silicon-Carbon 1	Gold	Gold
M2 coating	Silicon-Carbon 1	Gold	Platinum	Silicon-Carbon 2	Silicon-Carbon 1	Gold
M1 absorptivity	0.10	0.10	0.10	0.10	0.20	0.20
heat stop absorptivity	0.20	0.20	0.20	0.20	0.20	0.20
heat stop transmissivity	0.05	0.05	0.05	0.05	0.05	0.05
M2 absorptivity	0.10	0.20	0.40	0.80	0.10	0.20
total heat absorption on M1 (W)	37.95	37.95	37.95	37.95	75.89	75.89
total heat absorption on heat stop (W)	68.30	68.30	68.30	68.30	60.71	60.71
total heat absorption on M2 (W)	1.70753	3.41506	6.83011	13.66023	1.51780	3.03561
heat load coming from M2 to the slit (W)	15.37	13.66	10.25	3.42	13.66	12.14
Total radiator area (m2)	0.1677	0.1708	0.1771	0.1895	0.2235	0.2262
Total radiator area (m2) if absorption	0.4232	0.4354	0.4598	0.5087	0.5653	0.5766
M1 coating	Gold	Gold	Platinum	Platinum	Platinum	Platinum
M2 coating	Platinum	Silicon-Carbon 2	Silicon-Carbon 1	Gold	Platinum	Silicon-Carbon 2
M1 absorptivity	0.20	0.20	0.40	0.40	0.40	0.40
heat stop absorptivity	0.20	0.20	0.20	0.20	0.20	0.20
heat stop transmissivity	0.05	0.05	0.05	0.05	0.05	0.05
M2 absorptivity	0.40	0.80	0.10	0.20	0.40	0.80
total heat absorption on M1 (W)	75.89	75.89	151.78	151.78	151.78	151.78
total heat absorption on heat stop (W)	60.71	60.71	45.53	45.53	45.53	45.53
total heat absorption on M2 (W)	6.07121	12.14242	1.13835	2.27670	4.55341	9.10682
heat load coming from M2 to the slit (W)	9.11	3.04	10.25	9.11	6.83	2.28
Total radiator area (m2)	0.2318	0.2429	0.3350	0.3370	0.3412	0.3496
Total radiator area (m2) if absorption	0.5993	0.6446	0.8494	0.8590	0.8782	0.9166
M1 coating	Silicon-Carbon 1	Silicon-Carbon 2	Silicon-Carbon 2	Silicon-Carbon 2		
M2 coating	Silicon-Carbon 2	Gold	Platinum	Silicon-Carbon 2		
M1 absorptivity	0.80	0.80	0.80	0.80		
heat stop absorptivity	0.20	0.20	0.20	0.20		
heat stop transmissivity	0.05	0.05	0.05	0.05		
M2 absorptivity	0.10	0.20	0.40	0.80		
total heat absorption on M1 (W)	303.56	303.56	303.56	303.56		
total heat absorption on heat stop (W)	15.18	15.18	15.18	15.18		
total heat absorption on M2 (W)	0.37945	0.75890	1.51780	3.03561		
heat load coming from M2 to the slit (W)	3.42	3.04	2.28	0.76		
Total radiator area (m2)	0.5579	0.5586	0.5601	0.5630		
Total radiator area (m2) if absorption	1.4176	1.4237	1.4360	1.4604		

Appendix C :
Maple program giving the Sun heat load as
a function of time

```
T := 12960000:                                     # period of the satellite
ecc := 0.578:                                       # eccentricity of the orbit
p := 0.475*150*10^6*(1-ecc^2):                     # parameter of the orbit

for i from 1 to 150 do
  t_jours := i:
  t_secondes := t_jours*86400:
  t := t_secondes:
  kepler := x - ecc * sin(x) - (2*Pi/T)*t:          # definition of the Kepler
equation
  E := solve( kepler, x):
  gauss := tan(E/2) - sqrt((1-ecc)/(1+ecc))*tan(x/2): # definition of the Gauss
equation
  teta := solve( gauss, x):
  radius := p/(1+ecc*cos(teta)):
  radius_AU := radius/(150*10^6):
  heat(i) := 1367/(radius_AU^2);
end do:

for i from 1 to 150 do
  "heat"(i);
  print (heat(i));
end do;
```

Appendix D : ESARAD program

```
/* Esarad version 5.1.3, run date 00:20 Wed 22 Aug 2002 */
BEGIN_MODEL solo5

OPTICAL Alu_brillant;
Alu_brillant = [0.26, 0.69, 0.05, 0.8, 0.15, 0.05, 0.0, 0.0];

OPTICAL Ml_coating;
Ml_coating = [0.8, 0.2, 0.0, 0.1, 0.9, 0.0, 0.0, 0.0];

OPTICAL MLI;
MLI = [0.012, 0.0, 0.0, 0.2, 0.0, 0.0, 0.988, 0.8];

/* OPTICAL MLI;
MLI = [0.8, 0.0, 0.0, 0.2, 0.0, 0.0, 0.2, 0.8]; */

OPTICAL black_paint;
black_paint = [0.874, 0.126, 0.0, 0.975, 0.025, 0.0, 0.0, 0.0];

OPTICAL gold_coating;
gold_coating = [0.02, 0.98, 0.0, 0.19, 0.81, 0.0, 0.0, 0.0];

OPTICAL heat_shield_coating;
heat_shield_coating = [0.012, 0.988, 0.0, 0.2, 0.8, 0.0, 0.0, 0.0];

OPTICAL white_paint;
white_paint = [0.89, 0.11, 0.0, 0.19, 0.81, 0.0, 0.0, 0.0];

OPTICAL Teflon_coating;
Teflon_coating = [0.88, 0.0, 0.0, 0.09, 0.0, 0.0, 0.12, 0.91];

SHELL rectangle2_heat_shield;
rectangle2_heat_shield = SHELL_SCS_RECTANGLE(xmax = 1.2,
                                              ymax = 0.6,
                                              height = 0.0,
                                              xmin = 0.0,
                                              ymin = 0.0,
                                              colour1 = "GREEN",
                                              colour2 = "GREEN",
                                              nodes1 = 1,
                                              nodes2 = 1,
                                              nbase1 = 100,
                                              ndelta1 = 1,
                                              nbase2 = 150,
                                              ndelta2 = 1,
                                              opt1 =
heat_shield_coating,
                                              opt2 =
heat_shield_coating);
```

```
SHELL aperture2_heat_shield;
aperture2_heat_shield = SHELL_SCS_CYLINDER(radius = 0.06,
                                             hmax = 1.0,
                                             hmin = 0.0,
                                             angmin = 0.0,
                                             angmax = 360.0,
                                             sense = -1,
                                             nodes1 = 1,
                                             nodes2 = 1,
                                             nbase1 = 0,
                                             ndelta1 = 1,
                                             nbase2 = 0,
                                             ndelta2 = 1
                                             );

aperture2_heat_shield = TRANSLATE(
    object_name = aperture2_heat_shield,
    x_dist = 0.31);
aperture2_heat_shield = TRANSLATE(
    object_name = aperture2_heat_shield,
    y_dist = 0.3);
aperture2_heat_shield = TRANSLATE(
    object_name = aperture2_heat_shield,
    z_dist = -0.5);

SHELL heat_shield;
heat_shield = rectangle2_heat_shield - aperture2_heat_shield;

heat_shield = TRANSLATE(
    object_name = heat_shield,
    z_dist = -0.01);

SHELL radiator_M1;
radiator_M1 = SHELL_SCS_RECTANGLE(xmax = 0.433,
                                    ymax = 0.9,
                                    height = 0.0,
                                    xmin = 0.0,
                                    ymin = 0.0,
                                    colour1 = "YELLOW",
                                    colour2 = "YELLOW",
                                    nodes1 = 1,
                                    nodes2 = 1,
                                    nbase1 = 1200,
                                    ndelta1 = 1,
                                    nbase2 = 1250,
                                    ndelta2 = 1,
                                    sidel = "INACTIVE",
                                    opt2 = Teflon_coating,
                                    opt1 = black_paint);
```

```

radiator_M1 = ROTATE(
    object_name = radiator_M1,
    x_ang = 90.0);
radiator_M1 = TRANSLATE(
    object_name = radiator_M1,
    x_dist = 0.22);
radiator_M1 = TRANSLATE(
    object_name = radiator_M1,
    y_dist = 0.41);
radiator_M1 = TRANSLATE(
    object_name = radiator_M1,
    z_dist = 0.27);

SHELL radiator_M1_inside;
radiator_M1_inside = SHELL_SCS_RECTANGLE(xmax = 0.433,
                                           ymax = 0.90,
                                           height = 0.0,
                                           xmin = 0.0,
                                           ymin = 0.0,
                                           colour1 = "YELLOW",
                                           colour2 = "YELLOW",
                                           nodes1 = 1,
                                           nodes2 = 1,
                                           nbase1 = 1200,
                                           ndelta1 = 1,
                                           nbase2 = 1250,
                                           ndelta2 = 1,
                                           side2 = "INACTIVE",
                                           opt2 = Teflon_coating,
                                           opt1 = black_paint);

radiator_M1_inside = ROTATE(
    object_name = radiator_M1_inside,
    x_ang = 90.0);
radiator_M1_inside = TRANSLATE(
    object_name = radiator_M1_inside,
    x_dist = 0.22);
radiator_M1_inside = TRANSLATE(
    object_name = radiator_M1_inside,
    y_dist = 0.395);
radiator_M1_inside = TRANSLATE(
    object_name = radiator_M1_inside,
    z_dist = 0.27);

SHELL radiator_heat_stop;
radiator_heat_stop = SHELL_SCS_RECTANGLE(xmax = 0.4,
                                           ymax = 0.025,
                                           height = 0.0,
                                           xmin = 0.0,
                                           ymin = 0.0,
                                           colour1 = "METAL_GREY",

```

```

colour2 = "METAL_GREY",
nodes1 = 1,
nodes2 = 1,
nbase1 = 1100,
ndelta1 = 1,
nbase2 = 1150,
ndelta2 = 1,
side1 = "INACTIVE",
opt2 = Teflon_coating,
opt1 = black_paint);

radiator_heat_stop = ROTATE(
    object_name = radiator_heat_stop,
    x_ang = 90.0);
radiator_heat_stop = TRANSLATE(
    object_name = radiator_heat_stop,
    x_dist = 0.25);
radiator_heat_stop = TRANSLATE(
    object_name = radiator_heat_stop,
    y_dist = 0.41);
radiator_heat_stop = TRANSLATE(
    object_name = radiator_heat_stop,
    z_dist = 0.22);

SHELL radiator_heat_stop_inside;
radiator_heat_stop_inside = SHELL_SCS_RECTANGLE(xmax = 0.4,
    ymax = 0.025,
    height = 0.0,
    xmin = 0.0,
    ymin = 0.0,
    colour1 = "METAL_GREY",
    colour2 = "METAL_GREY",
    nodes1 = 1,
    nodes2 = 1,
    nbase1 = 1100,
    ndelta1 = 1,
    nbase2 = 1150,
    ndelta2 = 1,
    side2 = "INACTIVE",
    opt2 = Teflon_coating,
    opt1 = black_paint);

radiator_heat_stop_inside = ROTATE(
    object_name = radiator_heat_stop_inside,
    x_ang = 90.0);
radiator_heat_stop_inside = TRANSLATE(
    object_name = radiator_heat_stop_inside,
    x_dist = 0.25);
radiator_heat_stop_inside = TRANSLATE(
    object_name = radiator_heat_stop_inside,
    y_dist = 0.395);
radiator_heat_stop_inside = TRANSLATE(
    object_name = radiator_heat_stop_inside,

```

```

    z_dist = 0.22);

SHELL heat_shield_radiator_1;
heat_shield_radiator_1= SHELL_SCS_RECTANGLE(xmax = 1.2,
                                              ymax = 0.08,
                                              height = 0.0,
                                              xmin = 0.0,
                                              ymin = 0.0,
                                              colour1 = "METAL_GREY",
                                              colour2 = "METAL_GREY",
                                              nodes1 = 1,
                                              nodes2 = 1,
                                              nbase1 = 1500,
                                              ndelta1 = 1,
                                              nbase2 = 1550,
                                              ndelta2 = 1,
                                              opt2 = Teflon_coating,
                                              opt1 = black_paint);

heat_shield_radiator_1 = ROTATE(
    object_name = heat_shield_radiator_1 ,
    y_ang = 90.0);
heat_shield_radiator_1 = TRANSLATE(
    object_name = heat_shield_radiator_1 ,
    x_dist = -0.01);
heat_shield_radiator_1 = TRANSLATE(
    object_name = heat_shield_radiator_1 ,
    y_dist = 0.1);
heat_shield_radiator_1 = TRANSLATE(
    object_name =heat_shield_radiator_1 ,
    z_dist = 1.3);

SHELL heat_shield_radiator_2;
heat_shield_radiator_2 = SHELL_SCS_RECTANGLE(xmax = 1.2,
                                              ymax = 0.08,
                                              height = 0.0,
                                              xmin = 0.0,
                                              ymin = 0.0,
                                              colour1 = "METAL_GREY",
                                              colour2 = "METAL_GREY",
                                              nodes1 = 1,
                                              nodes2 = 1,
                                              nbase1 = 1600,
                                              ndelta1 = 1,
                                              nbase2 = 1650,
                                              ndelta2 = 1,
                                              opt1 = Teflon_coating,
                                              opt2 = black_paint);

heat_shield_radiator_2 = ROTATE(
    object_name = heat_shield_radiator_2 ,
    y_ang = 90.0);
heat_shield_radiator_2 = TRANSLATE(

```

```

        object_name = heat_shield_radiator_2 ,
        x_dist = 1.21);
heat_shield_radiator_2 = TRANSLATE(
    object_name = heat_shield_radiator_2 ,
    y_dist = 0.1);
heat_shield_radiator_2 = TRANSLATE(
    object_name = heat_shield_radiator_2 ,
    z_dist = 1.4);

SHELL radiator;
radiator = radiator_heat_stop + radiator_M1 + radiator_M1_inside +
radiator_heat_stop_inside + heat_shield_radiator_2 +
heat_shield_radiator_1 ;

SHELL satellite_casing;
satellite_casing = SHELL_SCS_BOX(height = 1.5,
                                xmax = 1.2,
                                ymax = 0.1,
                                xmin = 0.0,
                                ymin = 0.0,
                                colour1 = "BLUE",
                                colour2 = "BLUE",
                                nodes1 = 1,
                                nodes2 = 1,
                                nodes3 = 1,
                                nbase1 = 200,
                                ndelta1 = 1,
                                side2 = "INACTIVE",
                                opt1 = MLI
                                );
satellite_casing = TRANSLATE(
    object_name = satellite_casing,
    y_dist = 0.09);

SHELL M1;
M1 = SHELL_SCS_DISC(rmax = 0.05,
                    rmin = 0.0,
                    height = 0.0,
                    angmin = 0.0,
                    angmax = 360.0,
                    colour1 = "YELLOW",
                    colour2 = "YELLOW",
                    nodes1 = 1,
                    nodes2 = 1,
                    nbase1 = 1300,
                    ndelta1 = 1,

                    nbase2 = 1350,
                    ndelta2 = 1,
                    opt1 = M1_coating,
                    opt2 = M1_coating);

```

```

M1 = ROTATE(
    object_name = M1,
    y_ang = -8.0);
M1 = TRANSLATE(
    object_name = M1,
    x_dist = 0.31);
M1 = TRANSLATE(
    object_name = M1,
    y_dist = 0.3);
M1 = TRANSLATE(
    object_name = M1,
    z_dist = 0.65);

SHELL heat_stop;
heat_stop = SHELL_SCS_RECTANGLE(xmax = 0.45,
                                ymax = 0.190,
                                height = 0.0,
                                xmin = 0.0,
                                ymin = 0.0,
                                colour1 = "METAL_GREY",
                                colour2 = "METAL_GREY",
                                nodes1 = 1,
                                nodes2 = 1,
                                nbase1 = 1400,
                                ndelta1 = 1,
                                nbase2 = 1450,
                                ndelta2 = 1,
                                opt1 = Alu_brillant,
                                opt2 = Alu_brillant);

heat_stop = ROTATE(
    object_name = heat_stop,
    y_ang = -90.0);
heat_stop = TRANSLATE(
    object_name = heat_stop,
    x_dist = 0.4);
heat_stop = TRANSLATE(
    object_name = heat_stop,
    y_dist = 0.202);
heat_stop = TRANSLATE(
    object_name = heat_stop,
    z_dist = 0.21);

SHELL telescope;
telescope = M1 + heat_stop;

SHELL telescope_casing_front_2;
telescope_casing_front_2 = SHELL_SCS_RECTANGLE(xmax = 0.3,
                                                ymax = 0.2,
                                                height = 0.0,
                                                xmin = 0.0,
                                                ymin = 0.0,

```

```

colour1 = "RED",
colour2 = "RED",
nodes1 = 1,
nodes2 = 1,
nbase1 = 800,
ndelta1 = 1,
nbase2 = 850,
ndelta2 = 1,
opt2 = MLI,
opt1 = black_paint);

telescope_casing_front_2 = TRANSLATE(
    object_name = telescope_casing_front_2,
    x_dist = 0.4);
telescope_casing_front_2 = TRANSLATE(
    object_name = telescope_casing_front_2,
    y_dist = 0.2);
telescope_casing_front_2 = TRANSLATE(
    object_name = telescope_casing_front_2,
    z_dist = 0.2);

SHELL telescope_casing_front;
telescope_casing_front = SHELL_SCS_RECTANGLE(xmax = 0.2,
    ymax = 0.2,
    height = 0.0,
    xmin = 0.0,
    ymin = 0.0,
    colour1 = "RED",
    colour2 = "RED",
    nodes1 = 1,
    nodes2 = 1,
    nbase1 = 800,
    ndelta1 = 1,
    nbase2 = 850,
    ndelta2 = 1,
    opt2 = MLI,
    opt1 = black_paint);

telescope_casing_front = TRANSLATE(
    object_name = telescope_casing_front,
    x_dist = 0.2);
telescope_casing_front = TRANSLATE(
    object_name = telescope_casing_front,
    y_dist = 0.2);
telescope_casing_front = TRANSLATE(
    object_name = telescope_casing_front,
    z_dist = 0.2);

SHELL telescope_box_front;
telescope_box_front = telescope_casing_front +
telescope_casing_front_2;

SHELL aperture_telescope_box_front;

```

```

aperture_telescope_box_front = SHELL_SCS_CYLINDER(radius = 0.06,
                                                    hmax = 1.0,
                                                    hmin = 0.0,
                                                    angmin = 0.0,
                                                    angmax = 360.0,
                                                    sense = -1,
                                                    nodes1 = 1,
                                                    nodes2 = 1,
                                                    nbase1 = 0,
                                                    ndelta1 = 1,
                                                    nbase2 = 0,
                                                    ndelta2 = 1,
                                                    opt1 =
heat_shield_coating,
                                                    opt2 =
heat_shield_coating);

aperture_telescope_box_front = TRANSLATE(
    object_name = aperture_telescope_box_front,
    x_dist = 0.31);
aperture_telescope_box_front = TRANSLATE(
    object_name = aperture_telescope_box_front,
    y_dist = 0.3);
aperture_telescope_box_front = TRANSLATE(
    object_name = aperture_telescope_box_front,
    z_dist = -0.5);

SHELL telescope_front_shield;
telescope_front_shield = telescope_box_front -
aperture_telescope_box_front;

SHELL telescope_back_shield;
telescope_back_shield = SHELL_SCS_RECTANGLE(xmax = 0.5,
                                              ymax = 0.2,
                                              height = 0.0,
                                              xmin = 0.0,
                                              ymin = 0.0,
                                              nodes1 = 1,
                                              nodes2 = 1,
                                              nbase1 = 1000,
                                              ndelta1 = 1,
                                              nbase2 = 1050,
                                              ndelta2 = 1,
                                              opt1 = MLI,
                                              opt2 = black_paint);

telescope_back_shield = TRANSLATE(
    object_name = telescope_back_shield,
    x_dist = 0.2);
telescope_back_shield = TRANSLATE(
    object_name = telescope_back_shield,
    y_dist = 0.2);
telescope_back_shield = TRANSLATE(
    object_name = telescope_back_shield,

```

```

    z_dist = 1.2);

SHELL telescope_top1_shield;
telescope_top1_shield = SHELL_SCS_RECTANGLE(xmax = 0.5,
                                              ymax = 1.0,
                                              height = 0.0,
                                              xmin = 0.0,
                                              ymin = 0.0,
                                              nodes1 = 1,
                                              nodes2 = 1,
                                              nbase1 = 600,
                                              ndelta1 = 1,
                                              nbase2 = 650,
                                              ndelta2 = 1,
                                              opt2 = MLI,
                                              opt1 = black_paint);

telescope_top1_shield = ROTATE(
    object_name = telescope_top1_shield,
    x_ang = 90.0);
telescope_top1_shield = TRANSLATE(
    object_name = telescope_top1_shield,
    x_dist = 0.2);
telescope_top1_shield = TRANSLATE(
    object_name = telescope_top1_shield,
    y_dist = 0.4);
telescope_top1_shield = TRANSLATE(
    object_name = telescope_top1_shield,
    z_dist = 0.2);

SHELL telescope_bottom1_shield;
telescope_bottom1_shield = SHELL_SCS_RECTANGLE(xmax = 0.5,
                                                  ymax = 1.0,
                                                  height = 0.0,
                                                  xmin = 0.0,
                                                  ymin = 0.0,
                                                  nodes1 = 1,
                                                  nodes2 = 1,
                                                  nbase1 = 700,
                                                  ndelta1 = 1,
                                                  nbase2 = 750,
                                                  ndelta2 = 1,
                                                  opt1 = MLI,
                                                  opt2 = black_paint);

telescope_bottom1_shield = ROTATE(
    object_name = telescope_bottom1_shield,
    x_ang = 90.0);
telescope_bottom1_shield = TRANSLATE(
    object_name = telescope_bottom1_shield,
    x_dist = 0.2);
telescope_bottom1_shield = TRANSLATE(
    object_name = telescope_bottom1_shield,

```

```
    y_dist = 0.2);
telescope_bottom1_shield = TRANSLATE(
    object_name = telescope_bottom1_shield,
    z_dist = 0.2);

SHELL telescope_edge_shield_1;
telescope_edge_shield_1 = SHELL_SCS_RECTANGLE(xmax = 1.0,
                                                ymax = 0.2,
                                                height = 0.0,
                                                xmin = 0.0,
                                                ymin = 0.0,
                                                nodes1 = 1,
                                                nodes2 = 1,
                                                nbase1 = 500,
                                                ndelta1 = 1,
                                                nbase2 = 550,
                                                ndelta2 = 1,
                                                opt2 = MLI,
                                                opt1 = black_paint);

telescope_edge_shield_1 = ROTATE(
    object_name = telescope_edge_shield_1,
    y_ang = 90.0);
telescope_edge_shield_1 = TRANSLATE(
    object_name = telescope_edge_shield_1,
    x_dist = 0.2);
telescope_edge_shield_1 = TRANSLATE(
    object_name = telescope_edge_shield_1,
    y_dist = 0.2);
telescope_edge_shield_1 = TRANSLATE(
    object_name = telescope_edge_shield_1,
    z_dist = 1.2);

SHELL telescope_edge_shield_2;
telescope_edge_shield_2 = SHELL_SCS_RECTANGLE(xmax = 1.0,
                                                ymax = 0.2,
                                                height = 0.0,
                                                xmin = 0.0,
                                                ymin = 0.0,
                                                nodes1 = 1,
                                                nodes2 = 1,
                                                nbase1 = 400,
                                                ndelta1 = 1,
                                                nbase2 = 450,
                                                ndelta2 = 1,
                                                opt1 = MLI,
                                                opt2 = black_paint);

telescope_edge_shield_2 = ROTATE(
    object_name = telescope_edge_shield_2,
    y_ang = 90.0);
```

```
telescope_edge_shield_2 = TRANSLATE(  
    object_name = telescope_edge_shield_2,  
    x_dist = 0.7);  
telescope_edge_shield_2 = TRANSLATE(  
    object_name = telescope_edge_shield_2,  
    y_dist = 0.2);  
telescope_edge_shield_2 = TRANSLATE(  
    object_name = telescope_edge_shield_2,  
    z_dist = 1.2);  
  
SHELL telescope_casing;  
telescope_casing = telescope_edge_shield_2 + telescope_edge_shield_1 +  
telescope_top1_shield + telescope_bottom1_shield +  
telescope_front_shield + telescope_back_shield;  
  
solo5 = satellite_casing + heat_shield + telescope_casing + radiator +  
telescope;  
  
PURGE_MODEL();  
  
END_MODEL
```

Appendix E : ESATAN program

```

# Esarad version 5.1.3, run date 0:28 Thu 22 Aug 2002
# Model name: solo5           Analysis case: model5
# template file: Template.tpl
# Esarad version 5.1.3, run date 0:28 Thu 22 Aug 2002
# Model name: solo5           Analysis case: model5

$MODEL solo5_model5
$LOCALS
$NODES
  D100 = 'heat shield internal side' , T = 0.000000,
    A = 0.708838, ALP = 0.200000, EPS = 0.012000;

  D150 = 'heat shield sun facing side', T = 0.000000,
    A = 0.708838, ALP = 0.200000, EPS = 0.012000;

  D200 = ' satellite casing rear', T = 0.000000,
    A = 0.120000, ALP = 0.200000, EPS = 0.012000;

  D201 = ' satellite casing bottom', T = 0.000000,
    A = 1.800000, ALP = 0.200000, EPS = 0.012000;

  D202 = ' satellite casing right edge', T = 0.000000,
    A = 0.150000, ALP = 0.200000, EPS = 0.012000;

  D203 = ' satellite casing top', T = 0.000000,
    A = 1.800000, ALP = 0.200000, EPS = 0.012000;

  D204 = ' satellite casing left edge', T = 0.000000,
    A = 0.150000, ALP = 0.200000, EPS = 0.012000;

  D205 = ' satellite casing front', T = 0.000000,
    A = 0.120000, ALP = 0.200000, EPS = 0.012000;

  D400 = ' telescope casing right edge external side ' , T =
0.000000,
    A = 0.200000, ALP = 0.200000, EPS = 0.012000;

  D450 = ' telescope casing right edge internal side', T = 0.000000,
    A = 0.200000, ALP = 0.975000, EPS = 0.874000;

  D500 = ' telescope casing left edge internal side ' , T =
0.000000,
    A = 0.200000, ALP = 0.975000, EPS = 0.874000;

  D550 = ' telescope casing left edge external side ' , T =
0.000000,
    A = 0.200000, ALP = 0.200000, EPS = 0.012000;

  D600 = ' telescope casing top internal', T = 0.000000,
    A = 0.500000, ALP = 0.975000, EPS = 0.874000;

  D650 = ' telescope casing top external', T = 0.000000,
    A = 0.500000, ALP = 0.200000, EPS = 0.012000;

```

```
D700 = ' telescope casing bottom external' , T = 0.000000,  
      A = 0.500000, ALP = 0.200000, EPS = 0.012000;  
  
D750 = ' telescope casing bottom internal', T = 0.000000,  
      A = 0.500000, ALP = 0.975000, EPS = 0.874000;  
  
D800 = ' telescope casing front internal' , T = 0.000000,  
      A = 0.088701, ALP = 0.975000, EPS = 0.874000;  
  
D850 = ' telescope casing front external', T = 0.000000,  
      A = 0.088701, ALP = 0.200000, EPS = 0.012000;  
  
D1000 = ' telescope casing rear external', T = 0.000000,  
      A = 0.100000, ALP = 0.200000, EPS = 0.012000;  
  
D1050 = ' telescope casing rear internal', T = 0.000000,  
      A = 0.100000, ALP = 0.975000, EPS = 0.874000;  
  
D1100 = ' heat stop radiator internal', T = 0.000000,  
      A = 0.010000, ALP = 0.975000, EPS = 0.874000;  
  
D1150 = ' heat stop radiator external', T = 0.000000,  
      A = 0.010000, ALP = 0.090000, EPS = 0.880000;  
  
D1200 = ' M1 radiator internal' , T = 0.000000,  
      A = 0.389700, ALP = 0.975000, EPS = 0.874000;  
  
D1250 = ' M1 radiator external', T = 0.000000,  
      A = 0.389700, ALP = 0.090000, EPS = 0.880000;  
  
D1300 = ' M1 rear face', T = 0.000000,  
      A = 0.007854, ALP = 0.100000, EPS = 0.800000;  
  
D1350 = ' M1 sun facing side', T = 0.000000,  
      A = 0.007854, ALP = 0.100000, EPS = 0.800000;  
  
D1400 = ' Heat stop M1 facing', T = 0.000000,  
      A = 0.085500, ALP = 0.800000, EPS = 0.260000;  
  
D1450 = ' Heat Stop side 2', T = 0.000000,  
      A = 0.085500, ALP = 0.800000, EPS = 0.260000;  
  
D1500 = ' left radiator heat shield internal', T = 0.000000,  
      A = 0.096000, ALP = 0.975000, EPS = 0.874000;  
  
D1550 = ' left radiator heat shield external', T = 0.000000,  
      A = 0.096000, ALP = 0.090000, EPS = 0.880000;  
  
D1600 = ' right radiator heat shield external', T = 0.000000,  
      A = 0.096000, ALP = 0.090000, EPS = 0.880000;  
  
D1650 = ' right radiator heat shield internal', T = 0.000000,  
      A = 0.096000, ALP = 0.975000, EPS = 0.874000;
```

```

B99999 = 'DEEP_SPACE_NODE', T = -270.000000,
A = 1.000000E+020, ALP = 1.000000, EPS = 1.000000;

X99998 = 'INACTIVE_NODE', T = 0.000000,
A = 0.000000, ALP = 0.000000, EPS = 0.000000;

$CONDUCTORS
# linear

# Conductive link between two faces of a same element
#GL = K x AREA / LENGTH
GL(100,150) = kHeatShield * 7200.0 /10000.0 ; # CFRP thickness 5
mm
GL(400,450) = kCfrp * 0.2 / (5.0/1000.0) ; # CFRP thickness 5 mm
GL(500,550) = kCfrp * 0.2 / (5.0/1000.0) ; # CFRP thickness 5 mm
GL(600,650) = kCfrp * 0.5 / (5.0/1000.0) ; # CFRP thickness 5 mm
GL(700,750) = kCfrp * 0.5 / (5.0/1000.0) ; # CFRP thickness 5 mm
GL(800,850) = kCfrp * 0.0886 / (5.0/1000.0) ; # CFRP thickness 5
mm
GL(1000,1050) = kCfrp * 0.01 / (5.0/1000.0) ; # CFRP thickness 5
mm
GL(1100,1150) = kRad1 * 0.075 / (3.0/1000.0) ; # Heat Stop
Radiator thickness 3 mm
GL(1200,1250) = kRad1 * 0.1 / (3.0/1000.0) ; # M1 Radiator
thickness 3 mm
GL(1300,1350) = kMir * 0.0079 / (10.0/1000.0) ; # M1 thickness 10
mm
GL(1400,1450) = kHstop * 0.09 / (2.0/1000.0) ; # Heat Stop
thickness 2 mm
GL(1500,1550) = kRad1 * 0.12 / (3.0/1000.0) ; # Heat Shield
radiator 1 thickness 3 mm
GL(1600,1650) = kRad1 * 0.12 / (3.0/1000.0) ; # Heat Shield
radiator 1 thickness 3 mm

#Contact between each side of the satellite casing
#GL = K x LENGTH
GL(205,204) = kContact1 * 10.0 /10000.0; # satellite casing CFRP
thickness 10 mm
GL(205,202) = kContact1 * 10.0 /10000.0; # satellite casing CFRP
thickness 10 mm
GL(205,203) = kContact1 * 120.0 /10000.0; # satellite casing CFRP
thickness 10 mm
GL(205,201) = kContact1 * 120.0 /10000.0; # satellite casing CFRP
thickness 10 mm
GL(200,204) = kContact1 * 10.0 /10000.0; # satellite casing CFRP
thickness 10 mm
GL(200,202) = kContact1 * 10.0 /10000.0; # satellite casing CFRP
thickness 10 mm
GL(200,203) = kContact1 * 120.0 /10000.0; # satellite casing CFRP
thickness 10 mm
GL(200,201) = kContact1 * 120.0 /10000.0; # satellite casing CFRP
thickness 10 mm

```

```

    GL(204,203) = kContact1 * 150.0 /10000.0; # satellite casing CFRP
thickness 10 mm
    GL(204,201) = kContact1 * 150.0 /10000.0; # satellite casing CFRP
thickness 10 mm
    GL(202,203) = kContact1 * 150.0 /10000.0; # satellite casing CFRP
thickness 10 mm
    GL(202,201) = kContact1 * 150.0 /10000.0; # satellite casing CFRP
thickness 10 mm

# Conductive link between element

#Satellite casing - telescope casing bottom
    GL(203,700) = (kContact2/10000.0) * 5000.0 / 10000.0 ;

#Heat shield - satellite casing
    GL(100,205) = (kContact2/10.0) * 2400.0 / 10000.0 ;

#Heat Shield - M1 radiator
    #GL(150,1250) = kRad2;

#Telescope casing edge2 - telescope casing bottom
    GL(400,700) = kContact1 * 50.0 / 10000.0 ;
#Telescope casing edge2 - telescope casing front
    GL(400,850) = kContact1 * 10.0 / 10000.0 ;
#Telescope casing edge2 - telescope casing back
    GL(400,1000) = kContact1 * 10.0 / 10000.0 ;
#Telescope casing edge2 - telescope casing top
    GL(400,650) = kContact1 * 50.0 / 10000.0 ;
#Telescope casing edge1 - telescope casing front
    GL(550,850) = kContact1 * 10.0 / 10000.0 ;
#Telescope casing edge1 - telescope casing back
    GL(550,1000) = kContact1 * 10.0 / 10000.0 ;
#Telescope casing edge1 - telescope casing bottom
    GL(550,700) = kContact1 * 50.0 / 10000.0 ;
#Telescope casing edge1 - telescope casing top
    GL(550,650) = kContact1 * 50.0 / 10000.0 ;
#Telescope casing top - telescope casing front
    GL(650,850) = kContact1 * 25.0 / 10000.0 ;
#Telescope casing top - telescope casing back
    GL(650,1000) = kContact1 * 25.0 / 10000.0 ;
#Telescope casing bottom - telescope casing front
    GL(700,850) = kContact1 * 25.0 / 10000.0 ;
#Telescope casing bottom - telescope casing back
    GL(700,1000) = kContact1 * 25.0 / 10000.0 ;

#Heat stop radiator - heat stop
    # GL(1150,1400) = kRad2 / 0.2 ;
    GL(1150,1450) = kRad2 / 0.2 ;
#M1 radiator - M1
    # GL(1250,1300) = kRad3 / 0.2 ;
    GL(1250,1350) = kRad3 / 0.2 ;

```

```
#Heat Shield - radiator1
  GL (150, 1600) = kRad4 ;
#Heat Shield - radiator2
  GL (150, 1550) = kRad4 ;

#Heat stop - Telescope casing bottom
  GL(1400,700) = kContact2 * 9.0 / 10000.0 ;
```

```
#Radiative
```

```
GR(200, 99999) = 0.00144000;
GR(201, 203) = 1.24990E-008;
GR(201, 204) = 2.60204E-010;
GR(201, 205) = 1.10661E-006;
GR(201, 100) = 6.75389E-006;
GR(201, 400) = 2.65897E-009;
GR(201, 500) = 2.19426E-009;
GR(201, 600) = 2.90539E-007;
GR(201, 700) = 7.39642E-009;
GR(201, 850) = 1.28218E-008;
GR(201, 1100) = 1.00129E-008;
GR(201, 1500) = 9.89065E-008;
GR(201, 1350) = 8.82096E-010;
GR(201, 1400) = 3.01624E-009;
GR(201, 99999) = 0.0215890;
GR(202, 203) = 3.29021E-010;
GR(202, 100) = 1.46505E-009;
GR(202, 400) = 1.96829E-010;
GR(202, 850) = 1.03564E-010;
GR(202, 1650) = 0.00105925;
GR(202, 99999) = 0.000739184;
GR(203, 204) = 4.96131E-009;
GR(203, 205) = 2.05553E-006;
GR(203, 100) = 3.41480E-005;
GR(203, 400) = 1.21460E-005;
GR(203, 450) = 1.46073E-007;
GR(203, 500) = 2.57845E-005;
GR(203, 550) = 8.25572E-006;
GR(203, 600) = 1.40849E-005;
GR(203, 650) = 5.47449E-007;
GR(203, 700) = 0.00101727;
GR(203, 750) = 9.45136E-006;
GR(203, 800) = 2.25336E-006;
GR(203, 850) = 9.29630E-006;
GR(203, 1000) = 4.71575E-006;
GR(203, 1050) = 6.55556E-008;
GR(203, 1150) = 2.70178E-006;
GR(203, 1250) = 2.50199E-005;
GR(203, 1200) = 2.06107E-005;
GR(203, 1100) = 5.29073E-006;
GR(203, 1650) = 7.27941E-007;
GR(203, 1500) = 1.23892E-007;
```

```
GR(203, 1300) = 5.66134E-009;  
GR(203, 1350) = 5.76798E-007;  
GR(203, 1400) = 6.07951E-006;  
GR(203, 1450) = 8.01875E-009;  
GR(203, 99999) = 0.0193302;  
GR(203, 99998) = 1.98535E-005;  
GR(204, 100) = 2.31714E-009;  
GR(204, 550) = 2.45380E-010;  
GR(204, 700) = 4.04533E-009;  
GR(204, 800) = 2.89438E-009;  
GR(204, 850) = 2.70905E-010;  
GR(204, 1500) = 0.00106738;  
GR(204, 99999) = 0.000727324;  
GR(205, 100) = 0.000105705;  
GR(205, 400) = 1.85011E-007;  
GR(205, 450) = 7.36937E-008;  
GR(205, 500) = 5.26900E-006;  
GR(205, 550) = 5.86211E-008;  
GR(205, 600) = 1.81437E-006;  
GR(205, 650) = 1.87049E-008;  
GR(205, 700) = 3.95382E-007;  
GR(205, 750) = 9.50793E-007;  
GR(205, 800) = 1.35361E-007;  
GR(205, 850) = 1.54707E-006;  
GR(205, 1050) = 7.57263E-009;  
GR(205, 1150) = 2.49262E-007;  
GR(205, 1250) = 8.18626E-007;  
GR(205, 1200) = 5.82457E-006;  
GR(205, 1100) = 1.78485E-008;  
GR(205, 1300) = 2.80274E-009;  
GR(205, 1350) = 1.46848E-007;  
GR(205, 1400) = 1.04000E-006;  
GR(205, 1450) = 4.06741E-009;  
GR(205, 99999) = 0.00122288;  
GR(205, 99998) = 9.94027E-007;  
GR(100, 400) = 2.49937E-006;  
GR(100, 450) = 5.78314E-007;  
GR(100, 500) = 5.24707E-005;  
GR(100, 550) = 8.49602E-007;  
GR(100, 600) = 1.38206E-005;  
GR(100, 650) = 8.12723E-007;  
GR(100, 700) = 9.39578E-006;  
GR(100, 750) = 2.76385E-005;  
GR(100, 800) = 3.25760E-006;  
GR(100, 850) = 1.44055E-005;  
GR(100, 1050) = 7.76152E-007;  
GR(100, 1150) = 1.22096E-005;  
GR(100, 1250) = 8.91754E-005;  
GR(100, 1200) = 3.36922E-005;  
GR(100, 1100) = 3.13283E-006;  
GR(100, 1650) = 1.44794E-006;  
GR(100, 1500) = 1.37776E-006;  
GR(100, 1300) = 1.74584E-008;  
GR(100, 1350) = 1.43966E-006;
```

```
GR(100, 1400) = 9.32779E-006;  
GR(100, 1450) = 1.74858E-008;  
GR(100, 99999) = 0.00790936;  
GR(100, 99998) = 4.63477E-005;  
GR(150, 99999) = 0.00850605;  
GR(400, 500) = 3.39090E-007;  
GR(400, 550) = 4.03519E-009;  
GR(400, 650) = 9.57252E-009;  
GR(400, 700) = 1.55456E-007;  
GR(400, 750) = 1.10926E-008;  
GR(400, 800) = 1.50768E-008;  
GR(400, 850) = 1.23274E-007;  
GR(400, 1150) = 9.41053E-008;  
GR(400, 1250) = 8.48979E-007;  
GR(400, 1200) = 1.21767E-008;  
GR(400, 1100) = 1.30009E-009;  
GR(400, 1650) = 2.56727E-007;  
GR(400, 1350) = 8.56192E-009;  
GR(400, 1400) = 1.89653E-008;  
GR(400, 99999) = 0.00238236;  
GR(400, 99998) = 6.88968E-007;  
GR(450, 500) = 0.0123167;  
GR(450, 600) = 0.0201579;  
GR(450, 750) = 0.0622146;  
GR(450, 800) = 0.0115224;  
GR(450, 850) = 4.90304E-008;  
GR(450, 1050) = 0.0127940;  
GR(450, 1200) = 0.0418723;  
GR(450, 1100) = 0.000767739;  
GR(450, 1300) = 0.000280995;  
GR(450, 1350) = 3.82518E-005;  
GR(450, 1400) = 4.81878E-005;  
GR(450, 1450) = 0.00528866;  
GR(450, 99999) = 5.37378E-005;  
GR(450, 99998) = 0.000408809;  
GR(500, 550) = 1.95518E-007;  
GR(500, 600) = 0.0128763;  
GR(500, 650) = 2.58669E-007;  
GR(500, 700) = 2.64238E-006;  
GR(500, 750) = 0.0596335;  
GR(500, 800) = 0.00748501;  
GR(500, 850) = 1.23317E-005;  
GR(500, 1050) = 0.0123543;  
GR(500, 1150) = 3.33978E-006;  
GR(500, 1250) = 4.02292E-005;  
GR(500, 1200) = 0.0456237;  
GR(500, 1100) = 0.000641872;  
GR(500, 1500) = 5.96639E-006;  
GR(500, 1300) = 0.00159390;  
GR(500, 1350) = 0.00150281;  
GR(500, 1400) = 0.00712578;  
GR(500, 1450) = 5.97784E-005;  
GR(500, 99999) = 0.00299800;  
GR(500, 99998) = 0.000705457;
```

GR(550, 650) = 6.91781E-009;
GR(550, 700) = 1.82720E-008;
GR(550, 750) = 1.51449E-009;
GR(550, 800) = 1.34253E-007;
GR(550, 850) = 7.06776E-008;
GR(550, 1050) = 8.23252E-011;
GR(550, 1150) = 2.94844E-008;
GR(550, 1250) = 3.39182E-007;
GR(550, 1200) = 3.72239E-007;
GR(550, 1100) = 3.54975E-008;
GR(550, 1500) = 9.26149E-008;
GR(550, 1300) = 6.75625E-010;
GR(550, 1350) = 3.14417E-009;
GR(550, 1400) = 2.84384E-007;
GR(550, 99999) = 0.00238884;
GR(550, 99998) = 2.34275E-007;
GR(600, 700) = 4.08453E-006;
GR(600, 750) = 0.0298296;
GR(600, 800) = 0.00926031;
GR(600, 850) = 2.13512E-006;
GR(600, 1050) = 0.00820685;
GR(600, 1150) = 1.24199E-006;
GR(600, 1250) = 2.72359E-006;
GR(600, 1200) = 0.00309918;
GR(600, 1100) = 0.000184133;
GR(600, 1300) = 0.000102359;
GR(600, 1350) = 0.000104167;
GR(600, 1400) = 0.000589780;
GR(600, 1450) = 0.000806138;
GR(600, 99999) = 0.000490505;
GR(600, 99998) = 0.350680;
GR(650, 700) = 2.52690E-007;
GR(650, 750) = 4.49160E-009;
GR(650, 800) = 4.12692E-009;
GR(650, 850) = 9.36925E-008;
GR(650, 1150) = 3.14655E-007;
GR(650, 1250) = 2.78264E-006;
GR(650, 1200) = 1.48185E-007;
GR(650, 1100) = 2.25376E-009;
GR(650, 1500) = 9.23123E-008;
GR(650, 1350) = 7.89838E-009;
GR(650, 1400) = 1.19047E-008;
GR(650, 99999) = 0.00122819;
GR(650, 99998) = 0.00476516;
GR(700, 750) = 1.78143E-006;
GR(700, 800) = 3.52149E-007;
GR(700, 850) = 1.81312E-006;
GR(700, 1050) = 3.87520E-009;
GR(700, 1150) = 4.13703E-007;
GR(700, 1250) = 7.86215E-006;
GR(700, 1200) = 1.41433E-006;
GR(700, 1100) = 4.44767E-008;
GR(700, 1500) = 8.45227E-009;
GR(700, 1300) = 2.65287E-010;

```
GR(700, 1350) = 1.28826E-007;  
GR(700, 1400) = 1.81133E-006;  
GR(700, 99999) = 0.00399518;  
GR(700, 99998) = 5.70738E-006;  
GR(750, 800) = 0.0244733;  
GR(750, 850) = 5.96959E-006;  
GR(750, 1050) = 0.0286718;  
GR(750, 1150) = 9.91878E-006;  
GR(750, 1250) = 6.63655E-005;  
GR(750, 1200) = 0.176098;  
GR(750, 1100) = 0.00284737;  
GR(750, 1300) = 0.00193504;  
GR(750, 1350) = 0.00180049;  
GR(750, 1400) = 0.00611160;  
GR(750, 1450) = 0.00703182;  
GR(750, 99999) = 0.00262913;  
GR(750, 99998) = 0.000355668;  
GR(800, 850) = 6.17961E-007;  
GR(800, 1050) = 0.00163565;  
GR(800, 1150) = 3.03770E-007;  
GR(800, 1250) = 1.88015E-006;  
GR(800, 1200) = 0.0118835;  
GR(800, 1100) = 0.00289333;  
GR(800, 1500) = 1.60542E-006;  
GR(800, 1300) = 6.13298E-006;  
GR(800, 1350) = 0.000282074;  
GR(800, 1400) = 0.00141370;  
GR(800, 1450) = 0.00251121;  
GR(800, 99999) = 0.000339375;  
GR(800, 99998) = 0.000367281;  
GR(850, 1050) = 2.50216E-007;  
GR(850, 1150) = 1.46865E-006;  
GR(850, 1250) = 9.60037E-006;  
GR(850, 1200) = 6.87462E-006;  
  
GR(850, 1100) = 6.73309E-007;  
GR(850, 1650) = 7.62073E-008;  
GR(850, 1500) = 1.62834E-007;  
GR(850, 1300) = 2.58580E-009;  
GR(850, 1350) = 4.04183E-007;  
GR(850, 1400) = 1.34789E-006;  
GR(850, 1450) = 2.39628E-009;  
GR(850, 99999) = 0.000986667;  
GR(850, 99998) = 5.60090E-006;  
GR(1000, 99999) = 0.00119529;  
GR(1050, 1200) = 0.0203745;  
GR(1050, 1100) = 2.77557E-005;  
GR(1050, 1300) = 0.000511818;  
GR(1050, 1350) = 1.33046E-005;  
GR(1050, 1400) = 7.18645E-005;  
GR(1050, 1450) = 0.000168107;  
GR(1050, 99999) = 8.46197E-005;  
GR(1050, 99998) = 0.000236199;  
GR(1150, 1250) = 4.55646E-005;
```

```

GR(1150, 1200) = 2.63293E-006;
GR(1150, 1100) = 4.24129E-007;
GR(1150, 1350) = 3.04314E-009;
GR(1150, 1400) = 1.03407E-006;
GR(1150, 99999) = 0.00869048;
GR(1150, 99998) = 1.88994E-005;
GR(1250, 1200) = 3.57392E-006;
GR(1250, 1100) = 3.08928E-006;
GR(1250, 1500) = 7.47006E-006;
GR(1250, 1300) = 8.60346E-009;
GR(1250, 1350) = 7.91295E-008;
GR(1250, 1400) = 4.34082E-006;
GR(1250, 99999) = 0.342090;
GR(1250, 99998) = 0.000100426;
GR(1200, 1100) = 0.000374267;
GR(1200, 1500) = 9.08329E-007;
GR(1200, 1300) = 0.00181445;
GR(1200, 1350) = 0.00177367;
GR(1200, 1400) = 0.00516051;
GR(1200, 1450) = 0.00594509;
GR(1200, 99999) = 0.00179441;
GR(1200, 99998) = 5.22679E-005;
GR(1100, 1300) = 2.26202E-007;
GR(1100, 1350) = 1.24943E-005;
GR(1100, 1400) = 0.000219153;
GR(1100, 1450) = 0.000264026;
GR(1100, 99999) = 0.000383618;
GR(1100, 99998) = 4.87860E-006;
GR(1600, 99999) = 0.0844800;
GR(1650, 99999) = 0.0214771;
GR(1500, 1400) = 1.43128E-009;
GR(1500, 99999) = 0.0212674;
GR(1500, 99998) = 9.22221E-006;
GR(1550, 99999) = 0.0844800;
GR(1300, 1350) = 1.20358E-006;
GR(1300, 1400) = 8.52518E-006;
GR(1300, 1450) = 1.27187E-006;
GR(1300, 99999) = 1.37023E-006;
GR(1300, 99998) = 9.54939E-007;
GR(1350, 1400) = 0.000536211;
GR(1350, 1450) = 1.27904E-006;
GR(1350, 99999) = 0.000120255;
GR(1350, 99998) = 2.00538E-006;
GR(1400, 1450) = 7.13958E-007;
GR(1400, 99999) = 0.000768266;
GR(1400, 99998) = 1.46768E-005;
GR(1450, 99999) = 1.56618E-006;
GR(1450, 99998) = 1.22619E-005;

```

\$CONSTANTS

\$REAL

PERIOD = 1.296E+007;

kHeatShield = 0.5; #W/(m.K) cf MLI Austrian aerospace

kCfrp = 50.0; # W/(m.K)

```

kRad1 = 20.0; # W/(m.K)
kRad2 = 50.0; #(W/K) or (W/m.K)
kRad3 = 50.0; #(W/K) or (W/m.K)
kRad4 = 50.0; #(W/K) or (W/m.K)
kMir = 190.0; # W/(m.K)
kHstop = 190.0; # W/(m.K)
kContact1 = 10000.0; # W/(m2.K)
kContact2 = 5000.0; # W/(m2.K)
solfac = 0.0; # factor required to correct solar flux
HSfac = 1.0; # correction view factor for the heat stop radiator
Mlfac = 1.0;# correction view factor for the M1 radiator

$ARRAYS
# this array gives the value of the solar flux (in kiloWatts)
# with respect to the time (in seconds) on 1 whole orbit (150 days)
$REAL
FACSOL(2,151)=
0.0,33.56959,
86400.0, 32.291942,
172800.0, 30.392455,
259200.0, 28.12498,
345600.0, 25.722453,
432000.0, 23.358164,
518400.0, 21.139527,
604800.0, 19.120163,
691200.0, 17.316958,
777600.0, 15.724946,
864000.0, 14.32792,
950400.0, 13.10510,
1036800.0, 12.03493,
1123200.0, 11.09704,
1209600.0, 10.27309,
1296000.0, 9.547047,
1382400.0, 8.905097,
1468800.0, 8.335471,
1555200.0, 7.828186,
1641600.0, 7.374788,
1728000.0, 6.968123,
1814400.0, 6.602130,
1900800.0, 6.271661,
1987200.0, 5.972335,
2073600.0, 5.700412,
2160000.0, 5.452686,
2246400.0, 5.226405,
2332800.0, 5.019194,
2419200.0, 4.828998,
2505600.0, 4.654034,
2592000.0, 4.492749,
2678400.0, 4.343784,
2764800.0, 4.20595,
2851200.0, 4.07819,
2937600.0, 3.95961,

```

3024000.0, 3.849366,
3110400.0, 3.746743,
3196800.0, 3.651098,
3283200.0, 3.561857,
3369600.0, 3.478509,
3456000.0, 3.400593,
3542400.0, 3.327700,
3628800.0, 3.259458,
3715200.0, 3.195534,
3801600.0, 3.135627,
3888000.0, 3.079465,
3974400.0, 3.026802,
4060800.0, 2.977415,
4147200.0, 2.9311002,
4233600.0, 2.8876737,
4320000.0, 2.8469679,
4406400.0, 2.8088302,
4492800.0, 2.7731212,
4579200.0, 2.7397143,
4665600.0, 2.7084935,
4752000.0, 2.6793535,
4838400.0, 2.6521978,
4924800.0, 2.6269388,
5011200.0, 2.6034964,
5097600.0, 2.5817979,
5184000.0, 2.5617771,
5270400.0, 2.5433741,
5356800.0, 2.5265347,
5443200.0, 2.5112099,
5529600.0, 2.4973559,
5616000.0, 2.4849335,
5702400.0, 2.473908,
5788800.0, 2.4642489,
5875200.0, 2.4559297,
5961600.0, 2.4489279,
6048000.0, 2.4432245,
6134400.0, 2.4388042,
6220800.0, 2.4356552,
6307200.0, 2.4337692,
6393600.0, 2.4331411,
6480000.0, 2.4337692,
6566400.0, 2.4356552,
6652800.0, 2.4388042,
6739200.0, 2.4432245,
6825600.0, 2.4489279,
6912000.0, 2.4559297,
6998400.0, 2.4642489,
7084800.0, 2.473908,
7171200.0, 2.4849335,
7257600.0, 2.4973559,
7344000.0, 2.5112099,
7430400.0, 2.5265347,
7516800.0, 2.5433741,
7603200.0, 2.5617771,

7689600.0, 2.5817979,
7776000.0, 2.6034964,
7862400.0, 2.6269388,
7948800.0, 2.6521978,
8035200.0, 2.6793535,
8121600.0, 2.7084935,
8208000.0, 2.7397143,
8294400.0, 2.7731212,
8380800.0, 2.8088302,
8467200.0, 2.8469679,
8553600.0, 2.887673,
8640000.0, 2.9311,
8726400.0, 2.977415,
8812800.0, 3.026802,
8899200.0, 3.079465,
8985600.0, 3.135627,
9072000.0, 3.195534,
9158400.0, 3.259458,
9244800.0, 3.3277,
9331200.0, 3.400593,
9417600.0, 3.478509,
9504000.0, 3.561857,
9590400.0, 3.651098,
9676800.0, 3.746743,
9763200.0, 3.849366,
9849600.0, 3.95961,
9936000.0, 4.078199,
10022400.0, 4.20595,
10108800.0, 4.34378,
10195200.0, 4.492749,
10281600.0, 4.654034,
10368000.0, 4.828998,
10454400.0, 5.019194,
10540800.0, 5.226405,
10627200.0, 5.452686,
10713600.0, 5.700412,
10800000.0, 5.972335,
10886400.0, 6.271661,
10972800.0, 6.60213,
11059200.0, 6.968123,
11145600.0, 7.374788,
11232000.0, 7.828186,

11318400.0, 8.335471,
11404800.0, 8.905097,
11491200.0, 9.547047,
11577600.0, 10.27309,
11664000.0, 11.09704,
11750400.0, 12.03493,
11836800.0, 13.1051,
11923200.0, 14.3279,
12009600.0, 15.72494,
12096000.0, 17.31695,
12182400.0, 19.12016,

```

12268800.0,21.13952,
12355200.0,23.35816,
12441600.0,25.72245,
12528000.0,28.12498,
12614400.0,30.39245,
12700800.0,32.29194,
12787200.0,33.56959,
12873600.0,34.02172,
12960000.0,33.56959;

```

\$SUBROUTINES

```

# gives the value of the absorbed heat load on each node ( QSxxx)
# the first number corresponds to the absorbed heat load for an
incident load of 1000W
# solfac correspond to the multiplying factor necessary to obtain the
real value of the
# sun heat load.

```

```

SUBROUTINE QCYCLC LANG = MORTRAN
    solfac = INTCY1 (TIMEM,FACSOL,1,PERIOD,0.0)

```

```

QS100 = 0.017035 * solfac
QS150 = 141.767578 * solfac
QS200 = 0.000000 * solfac

```

```

QS201 = 0.000000 * solfac
QS202 = 0.000000 * solfac
QS203 = 0.003828 * solfac
QS204 = 0.000000 * solfac
QS205 = 0.000191 * solfac
QS400 = 2.799917E-006 * solfac
QS450 = 0.039180 * solfac
QS500 = 1.329593 * solfac
QS550 = 1.433558E-006 * solfac
QS600 = 0.093486 * solfac
QS650 = 2.799917E-006 * solfac
QS700 = 0.000222 * solfac
QS750 = 1.772367 * solfac
QS800 = 0.306731 * solfac
QS850 = 0.003271 * solfac
QS1000 = 0.000000 * solfac
QS1050 = 3.785072 * solfac
QS1100 = 0.009473 * solfac * HSfac
QS1150 = 0.000000 * solfac * HSfac
QS1200 = 1.740279 * solfac * M1fac
QS1250 = 0.000053 * solfac * M1fac
QS1300 = 0.000054 * solfac
QS1350 = 0.780363 * solfac
QS1400 = 1.674063 * solfac
QS1450 = 0.000791 * solfac

```

```

RETURN

```

```

END

```

```

SUBROUTINE QAVERG LANG = MORTRAN
  QS100 = 0.017035 * solfac
  QS150 = 141.767578 * solfac
  QS200 = 0.000000 * solfac
  QS201 = 0.000000 * solfac
  QS202 = 0.000000 * solfac
  QS203 = 0.003828 * solfac
  QS204 = 0.000000 * solfac
  QS205 = 0.000191 * solfac
  QS400 = 2.799917E-006 * solfac
  QS450 = 0.039180 * solfac
  QS500 = 1.329593 * solfac
  QS550 = 1.433558E-006 * solfac
  QS600 = 0.093486 * solfac
  QS650 = 2.799917E-006 * solfac
  QS700 = 0.000222 * solfac
  QS750 = 1.772367 * solfac
  QS800 = 0.306731 * solfac
  QS850 = 0.003271 * solfac
  QS1000 = 0.000000 * solfac
  QS1050 = 3.785072 * solfac
  QS1100 = 0.009473 * solfac
  QS1150 = 0.000000 * solfac
  QS1200 = 1.740279 * solfac
  QS1250 = 0.000053 * solfac
  QS1300 = 0.000054 * solfac
  QS1350 = 0.780363 * solfac
  QS1400 = 1.674063 * solfac
  QS1450 = 0.000791 * solfac

  RETURN
END
SUBROUTINE RCYCLC LANG = MORTRAN
  RETURN
END

```

```

$INITIAL
# heat capacity of each node
# because there is one node per face, the heat capacity has been
# equally distributed among the two face ( that is the reason of the /
2.0 ...)

```

```

  C100 = 2.84 * 1000.0 / 2.0
  C150 = 2.84 * 1000.0 / 2.0
  C200 = 0.48 * 1000.0
  C201 = 7.2 * 1000.0
  C202 = 0.6 * 1000.0
  C203 = 7.2 * 1000.0
  C204 = 0.6 * 1000.0
  C205 = 0.48 * 1000.0
  C400 = 0.8 * 1000.0 / 2.0
  C450 = 0.8 * 1000.0 / 2.0
  C500 = 0.8 * 1000.0 / 2.0
  C550 = 0.8 * 1000.0 / 2.0
  C600 = 2.0 * 1000.0 / 2.0

```

```

      C650 = 2.0 * 1000.0 / 2.0
      C700 = 2.0 * 1000.0 / 2.0
      C750 = 2.0 * 1000.0 / 2.0
      C800 = 0.355 * 1000.0 / 2.0
      C850 = 0.355 * 1000.0 / 2.0
      C1000 = 0.4 * 1000.0 / 2.0
      C1050 = 0.4 * 1000.0 / 2.0
      C1100 = 0.09 * 667.0 / 2.0      # carbon-carbon radiator 3g/cm3
and thickness 3 mm
      C1150 = 0.09 * 667.0 / 2.0      # carbon-carbon radiator 3g/cm3
and thickness 3 mm
      C1200 = 3.375 * 667.0 / 2.0      # carbon-carbon radiator 3g/cm3
and thickness 3 mm
      C1250 = 3.375 * 667.0 / 2.0      # carbon-carbon radiator 3g/cm3
and thickness 3 mm
      C1300 = 0.25 * 700.0 / 2.0
      C1350 = 0.25 * 700.0 / 2.0
      C1400 = 0.491 * 900.0 / 2.0
      C1450 = 0.8 * 900.0 / 2.0
      C1500 = 0.108 * 667.0 / 2.0      # carbon-carbon radiator 3g/cm3
and thickness 3 mm
      C1550 = 0.108 * 667.0 / 2.0      # carbon-carbon radiator 3g/cm3
and thickness 3 mm
      C1600 = 0.108 * 667.0 / 2.0      # carbon-carbon radiator 3g/cm3
and thickness 3 mm
      C1650 = 0.108 * 667.0 / 2.0      # carbon-carbon radiator 3g/cm3
and thickness 3 mm

      # C99999 = NOT CALCULATED      # DEEP_SPACE_NODE
      # C99998 = NOT CALCULATED      # INACTIVE_NODE

$VARIABLES1
      IF (SOLVER(:2) .EQ. 'SS') THEN
        CALL QAVERG
      ELSE
        CALL QCYCLC
        CALL RCYCLC
      END IF
$VARIABLES2

$EXECUTION

      OPEN(UNIT=81,FILE='SOLO.DAT',STATUS='UNKNOWN')
      NLOOP=100
      RELXCA=0.01
      CALL SOLVFM

      NLOOP=1000
      RELXCA=0.001
      TIMEO=0.0
      TIMEND=PERIOD*5
      OUTINT=432000.0
      DTIMEI=86400.0

```

```
CALL SLFWBK
CLOSE(81)

$OUTPUTS
# INTEGER I
# WRITE(81,1001) TIMEN,(T(26)),(T(I),I=2,8)
WRITE(81,1001) ,(T(26))
1001 FORMAT (F12.1,30F8.2)
CALL PRQBAL(' ',CURRENT)
CALL PRTUC(CURRENT)
CALL PRNDTB(' ','L,T,QS,C',CURRENT)
CALL PRQNOD(' ',CURRENT)
CALL QRATES(' ',CURRENT)
CALL DMPGFF(' ',CURRENT)

$ENDMODEL #solo5_model5
```

This document was created with Win2PDF available at <http://www.daneprairie.com>.
The unregistered version of Win2PDF is for evaluation or non-commercial use only.